جمهورية العراق
وزارة التعليم العالي
والبحث العلمي
جامعة بابل


# التحليل الديناميكي للمتربات المصنوعة من المواد المركبة المقوّاة بالألياف تحت تأثير الأحمال الصدمية

رسالة

مقدمة إلى كلية الهندسة في جامعة بابل

كجزء من متطلبات نيل درجة ماجستير علوم

في الهندسة الميكانيكية

(ميكانيك تطبيقي)

أعدت من قبل

سلوى عبير وجيه

بكالوريوس هندسة ميكانيك

٢٠٠٥

## خلاصة البحث:

يتناول هذا البحث موضوعين أساسيين: في الموضوع الأول, تم اقتراح طريقة عددية عامة اعتمدت على طريقة العناصر المحددة (Finite elements) وطريقة حساب التغايرات (Calculus of Variations) لبحث التصميم الأمثل لرقيقه مقواة بالألياف و مؤلفه من طبقات متعددة من المواد المركبة تحت تأثير حمل معين. استخدمت المواد المركبة المقواة بالألياف لإنشاء رقائق متعددة الطبقات بغية استخدامها في بعض الهياكل التركيبية.

تتألف الطريقة المقترحة بدورها من جزئين: في الجزء الأول، تم استخراج المقادير المثلى لزوايا وضع الألياف في كل طبقة على أساس إنها المقادير المناظرة لأعلى ترددات طبيعية للهيكل المتكون من تلك الطبقة. أما في الجزء الثاني، فقد تم حساب القيم المثلى لترتيب الألياف خلال المادة المركبة ( زوايا التدوير), أفضل سمك للطبقة, وترتيب الطبقات على مقطع الرقيقة المركبة طبقا لتصرفها الستاتيكي تحت تأثير الأحمال المؤثرة عليها. طبقت الطريقة المقترحة لحالة دراسية تضمنت جناح طائرة مسّيرة مسيطر عليها عن بعد لإيجاد التصميم الامثل بغية تحليله ديناميكيا تحت شروط معينه لحمل صدمي. اعتبرت الطريقة كل من الشكل الايروديناميكي (Aerodynamic shape ) لهيكل الجناح والأحمال التصميمية التي يتعرض لها كقيم ثابتة, بينما اعتبرت كل من زوايا وضع الألياف, سمك الطبقة, تعاقب الطبقات, وطريقة ترتيب الطبقات على مقطع الرقيقة كمتغيرات بغية البحث عن مقاديرها المثلى. للتحقق من نتائج الطريقة, تم بناء سبعة نماذج للجناح تكون زوايا وضع الألياف مثلى في الأربعة الأولى وعشوائية في الثلاثة المتبقية لأغراض المقارنة. وقد أظهرت نتائج المقارنة فاعلية الطريقة وأفضلية التصميم الامثل.

أما الموضوع الثاني فقد تضمن التحليل الديناميكي لبعض نماذج الجناح التي بنيت سابقا لدراسة استجابتها الديناميكية. تم استخدام طريقة نيومارك (Newmark) للتكامل العددي لحل معادلة التوازن الديناميكي و إخماد رايلي (Rayleigh damping) للتعبيرعن خواص الإخماد. بالإضافة إلى ذلك استخدمت طريقة التكرار المعكوس (Inverse iteration) لحساب الترددات الطبيعية للرقائق. تمت كتابة برنامج عددي يتضمن كل الخواص المذكورة سابقا بلغة APDL (Ansys Parametric Design Language) تمت إضافته إلى بيئة أل-Ansys كخاصية جديدة تعمل على إيجاد التصميم الامثل للمواد المركبة بالإضافة إلى التحليل الديناميكي لها.

من النتائج المستحصلة, وجد انه أقصى معامل فشل يحدث عند مسافة تتراوح بين (١٠%-٠ ) من طول الجناح من منطقة الجذر(wing root) ويقل باتجاه النهاية الحرة. DLF للمواد المركبة يتراوح بين ١.٤٥ و١.٧٥ في الوضع الأمن. يعتمد التخميد بشكل كبير على زاوية تدوير الألياف ويعمل على تقليل الزمن اللازم للوصول إلى الحالة المستقرة في الوقت نفسه. يتغير التردد الطبيعي للمواد المركبة بتغير زاوية تدوير الألياف والتي تعتمد بدورها على الشكل الهندسي و الشروط الحدودية.

بسم الله الرحمن الرحيم

" وأنزل عليك الكتاب والحكمة

وعلمك ما لم تكن تعلم وكان

فضل الله عليك عظيما "

صدق الله العلّي العظيم

النساء – الايه (١١٣)

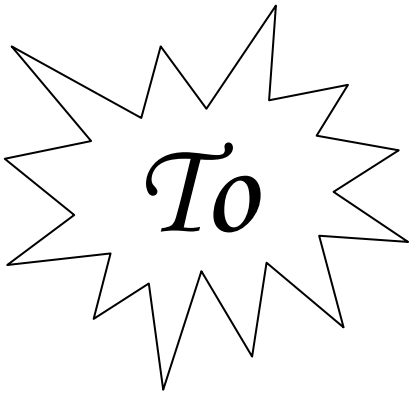


My Family

My Supervisors

My Teachers

My Friend

With Love

# Abstract

This research deals with two aspects, In the first a general numerical technique based on finite elements and calculus of variation was suggested to investigate the optimum design of multi-layered fiber-reinforced composite stiffened shell under certain design load.

The technique consists of two parts: in the first, the optimum orientation angles are estimated according to that values corresponding to the maximum lamina natural frequencies. In the second part, optimum layer thickness, their arrangement through shell section, and optimum stacking sequence were recognized according to their static behavior under applied loads. The suggested technique was executed to a case study which included wing structure of remotely guided aircraft to obtain the optimum design to be analyzed dynamically under certain impulsive load conditions. The technique assumed both of the aerodynamic shape and the design load (maximum load condition) as real constants, while lamina types, arrangement, layer sequence, layer thickness, and orientation angles were considered as variables to obtain their optimum configurations. In order to verify the obtained optimum configuration of design variables, seven models of composite wing structure were created when the fiber orientations are optimum in the first four models and arbitrary in the last three. The comparison between them showed the reliability of the technique and priority of the optimized design.

The second aspect was concerned with the dynamic analysis for some of wing structures that were created previously in order to study their dynamic responses. Newmark integration method was used to solve the dynamic equilibrium equation. Damping property was considered using Rayleigh type which is linearly related to the mass and stiffness matrices. Systems natural frequencies were obtained by solving the eigenvalue problem by inverse iteration method. The Numerical program which includes all the above features and written in APDL (Ansys Parametric Design Language) which was achieved and added to the ANSYS milieu as a new feature to obtain the optimum design of composite materials in addition to their dynamic analysis.

From the results obtained, it is found that the maximum failure index occurs at a distance from ٠-١٠٪ from the wing root and decreases in the direction of the free end. DLF (Dynamic Load Factor) for the composite materials is arranged between ١.٤٥ and ١.٧٥ in the safe case. Damping properties largely depend on the fiber orientation and reduces the time required to reach to the steady state response. Natural frequency of composite material varies with the variation of fiber orientation which depends itself on the structural configuration and boundary conditions.

## *ACKNOWLEDGMENTS*

**"Praise be to ALLAH, Lord of the whole creations"**

**I would like to sincerely and wholeheartedly thank Dr. Hatem H. Al-Taee and Dr. Alaa M. Husain for their guidance, kindness, and their patience as advisors, boundless energy while teaching, promptness while reviewing all my writing and passion for research in this work. I am indebted to them for helping me to achieve the research and thus opening a new exciting world for me.**

**Most importantly, I would like to thank my parents, for their unconditional support, love, and affection. Their encouragement and never ending kindness made everything easier to achieve.**

**Thanks to the mechanical department and college of engineering of Babylon University.**

**Finally, I apologize for all those whom I forget to mention their names.**

**Salwan Obeed Waheed**

**٢٠٠٥**

# APPENDIX-A

## *A. ١ Stress- Strain Matrix*

The transformation matrix $[T_m]$ for rotation by angle $\theta$ of plane coordinate is denoted by:

$$[T_m]=\begin{bmatrix} c^2 & s^2 & 0 & sc & 0 & 0 \\ s^2 & c^2 & 0 & -sc & 0 & 0 \\ 0 & 0 & 1 & 0 & 0 & 0 \\ -2sc & 2sc & 0 & c^2-s^2 & 0 & 0 \\ 0 & 0 & 0 & 0 & c & -s \\ 0 & 0 & 0 & 0 & s & c \end{bmatrix} \qquad \ldots (A.\ ١)$$

Where, $c=\cos\theta$ *and* $s=\sin\theta$.

The elements of $[Q_{ij}]$ matrix are defined as:

$Q_{١j}$ = - (E)/ (B)* $F_{١j}$ + (C)/ (B)* $F_{٢j}$ -sc/ (D)* $F_{٤j}$ ( j =١, ٢, ٤)

$Q_{٢j}$ = - (E)/ (B)* $F_{٢j}$ + (C)/ (B)* $F_{١j}$ + sc/ (D)* $F_{٤j}$ ( j =١, ٢, ٤)

$Q_{٣٣}$ = $F_{٣٣}$

$Q_{٤j}$ = ٢*sc/ (D)* $F_{١j}$ - ٢*sc/ (D)*$F_{٢j}$ -(s^٢-c^٢)/(D)* $F_{٤j}$ ( j =١, ٢, ٤)

$Q_{٥j}$ = c/(s^٢+c^٢)* $F_{٥j}$ + s/(s^٢+c^٢)* $F_{٦j}$ ( j =٥, ٦)

$Q_{٦j}$ = - s/(s^٢+c^٢)* $F_{٥j}$ + c/(s^٢+c^٢)* $F_{٦j}$ ( j =٢, ٦)

Where,

$F_{١١} = C_{١١}\, c^{٢} + C_{١٢}\, s^{٢}$ $F_{١٢} = C_{١١}\, s^{٢} + C_{١٢}\, c^{٢}$

$F_{١٤} = sc\,(C_{١١} - C_{١٢})$ $F_{٢١} = C_{١٢}\, c^{٢} + C_{٢٢}\, s^{٢}$

$F_{٢٢} = C_{١٢}\, s^{٢} + C_{٢٢}\, c^{٢}$ $F_{٢٤} = sc\,(C_{١٢} - C_{٢٢})$

$F_{٣٣} = C_{٣٣}$ $F_{٤١} = -٢sc\, C_{٤٤}$

$F_{٤٢} = ٢sc\, C_{٤٤}$ $F_{٤٤} = C_{٤٤}\,(c^{٢} - s^{٢})$

$F_{٥٥} = cf\, C_{٥٥}$ $F_{٥٦} = -sf\, C_{٥٥}$

$F_{٦٥} = sf\, C_{٦٦}$ $F_{٦٦} = cf\, C_{٦٦}$

B=c^٦-s^٢*c^٤+٤*c^٢*sc^٢-c^٢*s^٤+s^٦+٤*sc^٢*s^٢
C=s^٤-c^٢*s^٢+٢*sc^٢
D=s^٤-٢*c^٢*s^٢+c^٤+٤*sc^٢
E=c^٢*s^٢-c^٤-٢*sc^٢

## *A.٢ Shear Correction Factor*

In ***Timshenko's*** deep beam theory, the transverse shearing stress is assumed constant. Actually, the transverse shear stress is zero at the top and bottom sides of the section and maximum at the neutral axis (usually parabola for rectangular sections).

To attain the parabolic shear stress distribution, the equality concept of the strain energy in both constant and parabolic distributions is used. The shearing strain energy for an element (dx dy dz ), shown in Figure (A.١), under shearing stress is:

$$\Omega = \int_{Vol} \frac{1}{2}\,\tau\,\gamma\, d(Vol) = \int_{Vol} \frac{\tau^2}{2G}\, d(Vol) \qquad \textbf{…(A. ٢)}$$

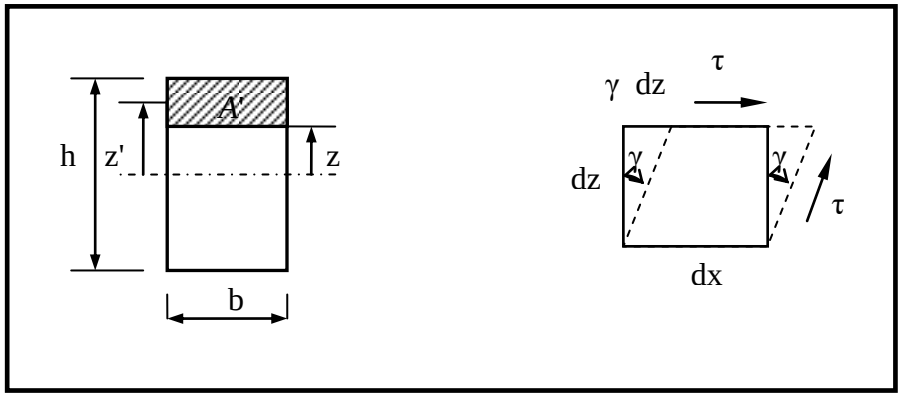


**Figure (A.١):** Beam element undergoing shear deformation.

For a constant shearing stress distribution, the strain energy is equal to:

$$\Omega_1 = \int_{Vol} \frac{\tau^2}{2KG}\, d(Vol) \qquad \textbf{…(A. ٣)}$$

where $K$ is the shear correction factor.

Now by assuming a piece of beam of unit length with rectangular cross section, equation (A.٣) will reduce to:

$$\Omega_1 = \frac{Q^2}{2KGA^2}\ (A.١) = \frac{Q^2}{2KGbh} \qquad \textbf{… (A. ٤)}$$

For the parabolic shearing stress, the following relations are used:

$$\tau = \frac{QA'z'}{Ib} \qquad \text{… (A. ٥)}$$

$$A' = b\,(\frac{h}{2} - z) \qquad \text{… (A. ٦)}$$

$$z' = \frac{1}{2}(\frac{h}{2} + z) \qquad \text{… (A. ٧)}$$

Substituting Equations (A.٦) and (A.٧) in Equation (A.٥) to find that,

$$\tau = \frac{6Q(\frac{h^2}{4} - z^2)}{bh^3} \qquad \text{… (A. ٨)}$$

then

$$\Omega_2 = \int_{Vol} \frac{\tau^2}{2G}\, d(Vol) = \frac{36Q^2}{2Gb^2h^2}(\frac{h^2}{4} - z^2)(1.b.dz)$$

$$= \frac{18Q^2}{bh^6G}\{\ ٢ * \int_0^{h/2} (\frac{h^2}{4} - z^2)\ dz\}$$

$$= \frac{3}{5}(\frac{Q^2}{bhG}) \qquad \text{… (A. ٩)}$$

Put $\Omega_2 = \Omega_1$

$$\frac{3}{5}(\frac{Q^2}{bhG}) = \frac{Q^2}{2KGbh} \quad \Longrightarrow \quad K = \frac{5}{6} = ١/\,f \text{ (}\textbf{\textit{Nawras, ٢٠٠٥}}\text{)}^{(٤٩)}.$$

## ***A. ٣ Shape Functions***

For quadrilateral Serendipity element, the shape functions are (***Bathe, ١٩٩٦***)$^{(٥٩)}$:

$$N_I(s,t) = -\frac{1}{4}(1-s)(1-t)(1+s+t) \qquad N_J(s,t) = -\frac{1}{4}(1+s)(1-t)(1-s+t)$$

$$N_K(s,t) = -\frac{1}{4}(1+s)(1+t)(1-s-t) \qquad N_L(s,t) = -\frac{1}{4}(1-s)(1+t)(1+s-t)$$

$$N_M(s,t) = \frac{1}{2}(1-s^2)(1-t) \qquad N_N(s,t) = \frac{1}{2}(1+s)(1-t^2)$$

$$N_O(s,t) = \frac{1}{2}(1-s^2)(1+t) \qquad N_P(s,t) = \frac{1}{2}(1-s)(1-t^2)$$

For triangular elements, (***Bathe, ١٩٩٦***) [٥٩]:

$$N_I(s,t) = s(2s-1) \qquad N_J(s,t) = t(2t-1)$$

$$N_K(s,t) = (1-s-t)(1+2s-2t) \qquad N_L(s,t) = 4st$$

$$N_M(s,t) = 4t(1-s-t) \qquad N_N(s,t) = 4s(1-s-t)$$

## ***A.٤ Applied Load***

Load will be applied on nodes (as nodal forces) on the lower surface of the wing structure. Nodal force that corresponds to each node is illustrated in Table (A.١).

**Table (A.١):** Nodal forces and corresponding nodes numbers.

| Node number | Force (N) | Node number | Force (N) | Node number | Force (N) | Node number | Force (N) |
|---|---|---|---|---|---|---|---|
| ٢٤ | ١٧٥.٦٧ | ٢٨ | ٥٥٨.١٤ | ٣٢ | ٤٥٤.٨١ | ٣٦ | ٢٥٧.٣٤ |
| ٣٣٦ | ٥٢٠.٤ | ٣٣٢ | ٦١٠.٢٥ | ٣٢٨ | ٤٩٧.٥٢ | ٣٢٤ | ٢٨١.٩٣ |
| ٣٥٨ | ٥٠٢.٣٥ | ٣٥٤ | ٥٨٩.٥٤ | ٣٥٠ | ٤٨٠.٢٥ | ٣٤٦ | ٢٢٤.٧٢ |
| ٣٨٠ | ٤٤٨.٤٩ | ٣٧٦ | ٥٢٦.٢٤ | ٣٧٢ | ٤٢٨.٧٨ | ٣٦٨ | ٢٤٢.٦٨ |
| ٤٠٢ | ٤٠٣.٩٥ | ٣٩٨ | ٤٧٣.٩٨ | ٣٩٤ | ٣٨٦.٢٧ | ٣٩٠ | ٢١٨.٦٥ |
| ٤٢٤ | ٣١٤.٣٤ | ٤٢٠ | ٣٦٧.٤٣ | ٤١٦ | ٣٠٠.٤٧ | ٤١٢ | ١٦٩.٣٦ |
| ٤٤٦ | ٢٢٤.٤٦ | ٤٤٢ | ٢٦٣.٢٧ | ٤٣٨ | ٢١٤.٦٢ | ٤٣٤ | ١٢١.٥٦ |
| ٤٦٨ | ١٦٦.٦٣ | ٤٦٤ | ١٣٦.٥٢ | ٤٦٠ | ١١١.٦٢ | ٤٥٦ | ٦٣.١٤ |
| ٤٩٨ | ٢.٧٥ | ٤٨٦ | ٣.١٦ | ٤٨٢ | ٢.٦٤١ | ٤٧٨ | ١.٨٩ |
| ٥١٢ | ٨٩.٤٥ | ٥٠٨ | ١٠٥.٢٦ | ٥٠٤ | ٨٥.٦٩ | ٥٠٠ | ٤٨.٤٥ |
| ٥٩ | ١٠٧.١٧ | ٦٣ | ١٢٦.٨٣ | ٦٧ | ١٠٢.٦٩ | ٧١ | ٥٨.٦٢ |
| ٢٦ | ٥٢٩.٢٥ | ٣٠ | ٥١٥.٠٢ | ٣٤ | ٣٨٦.٣٢ | ٢ | ٨٦.٧١ |
| ٣٣٤ | ٥٧٨.٠٥ | ٣٣٠ | ٥٦٣.٢٥ | ٣٢٦ | ٤٢٢.٨٢ | ٢٧٩ | ٧٥.٢١ |
| ٣٥٦ | ٥٥٨.٦٢ | ٣٥٢ | ٥٤٤.٨٧ | ٣٤٨ | ٤٠٨.٤١ | ٢٨١ | ٧٢.٥٦ |
| ٣٧٨ | ٤٩٨.٥٢ | ٣٧٤ | ٤٨٥.٦٢ | ٣٧٠ | ٣٦٤.٣٥ | ٢٨٣ | ٦٤.٧٤ |
| ٤٠٠ | ٤٤٩.٦٩ | ٣٩٠ | ٤٣٧.٦٢ | ٣٩٢ | ٣٢٨.١٣ | ٢٨٥ | ٥٨.٢٦ |
| ٤٢٢ | ٣٤٩.٦٥ | ٤١٨ | ٣٣٧.٦٩ | ٤١٤ | ٢٥٥.١٢٧ | ٢٨٧ | ٤٥.٩٨ |
| ٤٤٤ | ٢٤٩.٣٢ | ٤٤٠ | ٢٤٢.٩٢ | ٤٣٦ | ١٨٢.٣٤ | ٢٨٩ | ٣٣.٠٣ |
| ٤٦٦ | ١٢٩.٩٨ | ٤٦٢ | ١٢٦.٥٤ | ٤٥٨ | ٩٤.٨ | ٣٩١ | ١٦.٠٨ |
| ٤٨٨ | ٣.٠٦ | ٤٨٤ | ٢.٧٩ | ٤٨٠ | ٢.٢٢ | ٢٩٣ | ٠.٩٩ |
| ٥١٠ | ٩٩.٨٥ | ٥٠٦ | ٩٦.٩٧ | ٥٠٢ | ٧٢.٨٩ | ٢٩٥ | ١٢.٩٩ |
| ٦١ | ١١٩.٦٣ | ٦٥ | ١١٦.٤٩ | ٦٩ | ٨٧.٤٢ | ٧٣ | ١٥.٢٣ |

# Appendix-B

The derivation of strain-displacement and mass matrices is illustrated.

## *B. ١ Strain-Displacement Matrix*

١. for *[B.]*,

$$\begin{Bmatrix} B_{1,i} \\ B_{1,j} \\ B_{1,k} \end{Bmatrix} = J^{-1}_{13,A}\ t_l N_l \begin{Bmatrix} a_l^u \\ b_l^u \\ c_l^u \end{Bmatrix} \qquad \textbf{…(B. ١)}$$

$$\begin{Bmatrix} B_{2,i} \\ B_{2,j} \\ B_{2,k} \end{Bmatrix} = J^{-1}_{23,A}\ t_l N_l \begin{Bmatrix} a_l^v \\ b_l^v \\ c_l^v \end{Bmatrix} \qquad \textbf{…(B. ٢)}$$

$$\begin{Bmatrix} B_{3,i} \\ B_{3,j} \\ B_{3,k} \end{Bmatrix} = J^{-1}_{33,A}\ t_l N_l \begin{Bmatrix} a_l^w \\ b_l^w \\ c_l^w \end{Bmatrix} \qquad \textbf{…(B. ٣)}$$

$$\begin{Bmatrix} B_{4,i} \\ B_{4,j} \\ B_{4,k} \end{Bmatrix} = J^{-1}_{13,A}\ t_l N_l \begin{Bmatrix} a_l^v \\ b_l^v \\ c_l^v \end{Bmatrix} + J^{-1}_{23,A}\ t_l N_l + \begin{Bmatrix} a_l^u \\ b_l^u \\ c_l^u \end{Bmatrix} \qquad \textbf{…(B. ٤)}$$

$$\begin{Bmatrix} B_{5,i} \\ B_{5,j} \\ B_{5,k} \end{Bmatrix} = J^{-1}_{33,A}\ t_l N_l \begin{Bmatrix} a_l^v \\ b_l^v \\ c_l^v \end{Bmatrix} + J^{-1}_{23,A}\ t_l N_l + \begin{Bmatrix} a_l^w \\ b_l^w \\ c_l^w \end{Bmatrix} \qquad \textbf{…(B. ٥)}$$

$$\begin{Bmatrix} B_{6,i} \\ B_{6,j} \\ B_{6,k} \end{Bmatrix} = J^{-1}_{33,A}\ t_l N_l \begin{Bmatrix} a_l^w \\ b_l^w \\ c_l^w \end{Bmatrix} + J^{-1}_{13,A}\ t_l N_l + \begin{Bmatrix} a_l^u \\ b_l^u \\ c_l^u \end{Bmatrix} \qquad \textbf{…(B. ٦)}$$

٢. For the strain-displacement matrix, *[B ,]*, the elements can be defined as:

$B_{m,n}=R_{m,n}+F_{m,n}$ *(m= ١ to ٦, and n= ١ to ٤٨ step ١)* ***...(B. ٧)***

where,

$$\begin{Bmatrix} R_{4,i} \\ R_{4,j} \\ R_{4,k} \end{Bmatrix} = J_{12,A}^{-1}\ t_l \frac{\partial N_l}{\partial s}\left(\begin{Bmatrix} a_l^u \\ b_l^u \\ c_l^u \end{Bmatrix} + \begin{Bmatrix} a_l^v \\ b_l^v \\ c_l^v \end{Bmatrix}\right) + J_{22,A}^{-1}\ t_l \frac{\partial N_l}{\partial t}\left(\begin{Bmatrix} a_l^u \\ b_l^u \\ c_l^u \end{Bmatrix} + \begin{Bmatrix} a_l^v \\ b_l^v \\ c_l^v \end{Bmatrix}\right)$$

***…(B.٨)***

$$\begin{Bmatrix} R_{5,i} \\ R_{5,j} \\ R_{5,k} \end{Bmatrix} = J_{21,A}^{-1}\ t_l \frac{\partial N_l}{\partial s}\begin{Bmatrix} a_l^w \\ b_l^w \\ c_l^w \end{Bmatrix} + J_{22,A}^{-1}\ t_l \frac{\partial N_l}{\partial t}\begin{Bmatrix} a_l^w \\ b_l^w \\ c_l^w \end{Bmatrix}$$

***…(B.٩)***

$$\begin{Bmatrix} R_{6,i} \\ R_{6,j} \\ R_{6,k} \end{Bmatrix} = J_{11,A}^{-1}\ t_l \frac{\partial N_l}{\partial s}\begin{Bmatrix} a_l^w \\ b_l^w \\ c_l^w \end{Bmatrix} + J_{12,A}^{-1}\ t_l \frac{\partial N_l}{\partial t}\begin{Bmatrix} a_l^w \\ b_l^w \\ c_l^w \end{Bmatrix}$$

***…(B.١٠)***

$$\begin{Bmatrix} F_{1,i} \\ F_{1,j} \\ F_{1,k} \end{Bmatrix} = J_{13,V}^{-1}\ t_l N_l \begin{Bmatrix} a_l^u \\ b_l^u \\ c_l^u \end{Bmatrix}$$

***…(B.١١)***

$$\begin{Bmatrix} F_{2,i} \\ F_{2,j} \\ F_{2,k} \end{Bmatrix} = J_{23,V}^{-1}\ t_l N_l \begin{Bmatrix} a_l^v \\ b_l^v \\ c_l^v \end{Bmatrix}$$

***…(B.١٢)***

$$\begin{Bmatrix} F_{3,i} \\ F_{3,j} \\ F_{3,k} \end{Bmatrix} = J_{33,V}^{-1}\ t_l N_l \begin{Bmatrix} a_l^w \\ b_l^w \\ c_l^w \end{Bmatrix}$$

***…(B.١٣)***

$$\begin{Bmatrix} F_{4,i} \\ F_{4,j} \\ F_{4,k} \end{Bmatrix} = J_{13,V}^{-1}\ t_l N_l \begin{Bmatrix} a_l^v \\ b_l^v \\ c_l^v \end{Bmatrix} + J_{23,V}^{-1}\ t_l N_l + \begin{Bmatrix} a_l^u \\ b_l^u \\ c_l^u \end{Bmatrix}$$

***…(B.١٤)*** $$\begin{Bmatrix} F_{5,i} \\ F_{5,j} \\ F_{5,k} \end{Bmatrix} = J_{33,V}^{-1}\ t_l N_l \begin{Bmatrix} a_l^v \\ b_l^v \\ c_l^v \end{Bmatrix} + J_{23,V}^{-1}\ t_l N_l + \begin{Bmatrix} a_l^w \\ b_l^w \\ c_l^w \end{Bmatrix}$$

***…(B.١٥)***

$$\begin{Bmatrix} F_{6,i} \\ F_{6,j} \\ F_{6,k} \end{Bmatrix} = J^{-1}_{33,V}\ t_l N_l \begin{Bmatrix} a_l^w \\ b_l^w \\ c_l^w \end{Bmatrix} + J^{-1}_{13,V}\ t_l N_l + \begin{Bmatrix} a_l^u \\ b_l^u \\ c_l^u \end{Bmatrix}$$

***…(B. ١٦)***

٣. For strain displacement matrix,[$B_٣$],

$$\begin{Bmatrix} B_{4,i} \\ B_{4,j} \\ B_{4,k} \end{Bmatrix} = J^{-1}_{12,V}\ t_l \frac{\partial N_l}{\partial s}\left(\begin{Bmatrix} a_l^u \\ b_l^u \\ c_l^u \end{Bmatrix} + \begin{Bmatrix} a_l^v \\ b_l^v \\ c_l^v \end{Bmatrix}\right) + J^{-1}_{22,V}\ t_l \frac{\partial N_l}{\partial t}\left(\begin{Bmatrix} a_l^u \\ b_l^u \\ c_l^u \end{Bmatrix} + \begin{Bmatrix} a_l^v \\ b_l^v \\ c_l^v \end{Bmatrix}\right)$$

B-٢

***…(B. ١٧)***

$$\begin{Bmatrix} B_{5,i} \\ B_{5,j} \\ B_{5,k} \end{Bmatrix} = J^{-1}_{21,V}\ t_l \frac{\partial N_l}{\partial s} \begin{Bmatrix} a_l^w \\ b_l^w \\ c_l^w \end{Bmatrix} + J^{-1}_{22,V}\ t_l \frac{\partial N_l}{\partial t} \begin{Bmatrix} a_l^w \\ b_l^w \\ c_l^w \end{Bmatrix}$$

***…(B. ١٨)***

$$\begin{Bmatrix} B_{6,i} \\ B_{6,j} \\ B_{6,k} \end{Bmatrix} = J^{-1}_{11,V}\ t_l \frac{\partial N_l}{\partial s} \begin{Bmatrix} a_l^w \\ b_l^w \\ c_l^w \end{Bmatrix} + J^{-1}_{12,V}\ t_l \frac{\partial N_l}{\partial t} \begin{Bmatrix} a_l^w \\ b_l^w \\ c_l^w \end{Bmatrix}$$

***…(B. ١٩)***

in which,

$$[J^{-1}_{op,V}\ ] = 0.5\ \left([J^{-1}_{op}]\big|_{r=1.0} - [J^{-1}_{op}]\big|_{r=-1.0}\right)$$

***…(B. ٢٠)***

$$[J^{-1}_{op,A}\ ] = 0.5\ \left([J^{-1}_{op}]\big|_{r=1.0} + [J^{-1}_{op}]\big|_{r=-1.0}\right)$$

***…(B. ٢١)***

For all illustrated equations, the values of *i, j, k, and l* are given by:

*(i = ٢٥, j = ٢٦, k = ٢٧, and l = ١), (i = ٢٨, j = ٢٩, k = ٣٠, and l = ٢).*

*(i = ٣١, j = ٣٢, k = ٣٣, and l = ٣), (i = ٣٤, j = ٣٥, k = ٣٦, and l = ٤).*

*(i = ٣٧, j = ٣٨, k = ٣٩, and l = ٥), (i = ٤٠, j = ٤١, k = ٤٢, and l = ٦).*

*(i = ٤٣, j = ٤٤, k = ٤٥, and l = ٧), (i = ٤٦, j = ٤٧, k = ٤٨, and l = ٨).*

All the other values are equal to zero.

***B. ٢Mass Matrix.***

Elements of mass matrix are derived below so that;

mass matrix equation is,

$$[M_1] = diag[[M_0] \quad [M_0] \quad [M_0] \quad [0]]$$

***…(B. ٢٢)***

where,

$$[M_0] = \rho_a \int_{-1}^{1}\int_{-1}^{1} \Delta_a^2 \; [M_{a,b}] \; ds \; dt \qquad \textbf{…(B. ٢٣)}$$

in which,

$$[M_{a,b}] = \begin{bmatrix} N_{11} & N_{12} & N_{13} & N_{14} & N_{15} & N_{16} & N_{17} & N_{18} \\ N_{21} & N_{22} & N_{23} & N_{24} & N_{25} & N_{26} & N_{27} & N_{28} \\ N_{31} & N_{32} & N_{33} & N_{34} & N_{35} & N_{36} & N_{37} & N_{38} \\ N_{41} & N_{42} & N_{43} & N_{44} & N_{45} & N_{46} & N_{47} & N_{48} \\ N_{51} & N_{52} & N_{53} & N_{54} & N_{55} & N_{56} & N_{57} & N_{58} \\ N_{61} & N_{62} & N_{63} & N_{64} & N_{65} & N_{66} & N_{67} & N_{68} \\ N_{71} & N_{72} & N_{73} & N_{74} & N_{75} & N_{76} & N_{77} & N_{78} \\ N_{81} & N_{82} & N_{83} & N_{84} & N_{85} & N_{86} & N_{87} & N_{88} \end{bmatrix}$$



***…(B. ٢٤)***

$N_{yh}=N_y\,N_h$ *for y,h=١ to ٨ step ١*. As example, $N_{١,٢}=N_١\,N_٢$ and so on.

Finally, elements of *[M١]* are:

$$M_{m,n} = \rho_a \int_{-1}^{1}\int_{-1}^{1} \Delta_a^2 \; [M_{a,b}] \; ds \; dt \qquad \text{(m and n =١ to ٨, step ١)}$$

(a and b =١ to ٨ step ١)

$$M_{o,p} = \rho_a \int_{-1}^{1}\int_{-1}^{1} \Delta_a^2 \; [M_{a,b}] \; ds \; dt \qquad \text{(o and p =٩ to ١٦ step ١)}$$

(a and b =١ to ٨ step ١)

$$M_{q,r} = \rho_a \int_{-1}^{1}\int_{-1}^{1} \Delta_a^2 \; [M_{a,b}] \; ds \; dt \qquad \text{(q and r =١٧ to ٢٤ step ١)}$$

(a and b = ١ to ٨ step ١)

and the rest value equal to zero.

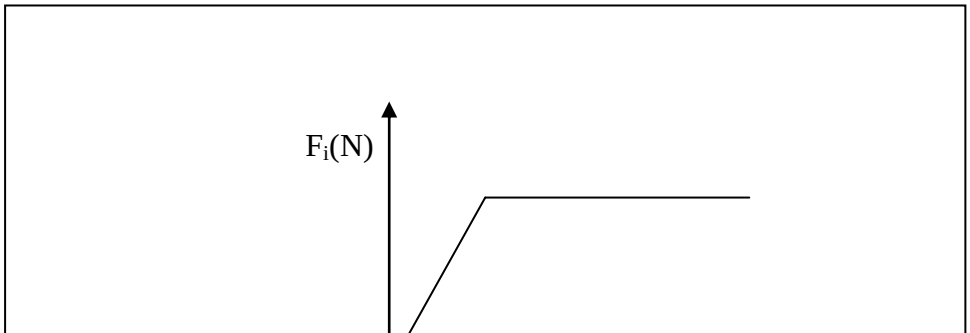

**Fig.(B.١):** Dynamic characteristics of the terminated dynamic impulsive excitation.

# APPENDIX-C

## *C.١ Tsai-Wu Theory*

Tsai and Wu postulated that a failure surface in stress space exists in the form, ***(Abdul-Raheem, ٢٠٠٠)*** [٧]***:***

$$F_i\ \sigma_i + F_{ij}\ \sigma_i\sigma_j \geq 1 \qquad i,j = ١, ٢, \ldots, ٦ \qquad \ldots \textbf{(C.١)}$$

where,

$$F_1 = \frac{1}{X_T} - \frac{1}{X_C} \qquad F_{11} = \frac{1}{X_T X_C}$$

$$F_2 = \frac{1}{Y_T} - \frac{1}{Y_C} \qquad F_{22} = \frac{1}{Y_T Y_C}$$

$$F_3 = \frac{1}{Z_T} - \frac{1}{Z_C} \qquad F_{33} = \frac{1}{Z_T Z_C}$$

$$F_{44} = \left(\frac{1}{R^2}\right),\ F_{55} = \left(\frac{1}{S^2}\right),\ F_{66} = \left(\frac{1}{T^2}\right)$$

$$F_{12} = -\frac{1}{2}\left[\frac{1}{X_T.X_C.Y_T.Y_C}\right]^{0.5}$$

$$F_{13} = -\frac{1}{2}\left[\frac{1}{X_T.X_C.Z_T.Z_C}\right]^{0.5}$$

$$F_{23} = -\frac{1}{2}\left[\frac{1}{Y_T.Y_C.Z_T.Z_C}\right]^{0.5}$$

The coefficients $F_{١}$, $F_{٢}$, and $F_{٣}$ correspond to the linear stress terms and $F_{١١}$, $F_{٢٢}$, $F_{٣٣}$, $F_{٤٤}$, $F_{٥٥}$, and $F_{٦٦}$ correspond to the quadratic stress terms. $F_{١٢}$, $F_{١٢}$, and $F_{١٢}$ are the coefficients, which take into account the interaction effect of various normal stress components. This criterion is the most general polynomial failure criterion for composite materials. It doesn't say any thing about the mode of failure (fiber breakage, matrix cracking, delaminating, etc.)

In this work, first play prediction based on Tsai-Wu failure criteria is presented tacking into account the same shear strengths in all direction (i.e. T=S=R) because there is no available experimental data about inter-laminar shear strengths of unidirectional composite lamina.

## *C.٢ Calculus of Variations*

The calculus of variations is mainly concerned with the stationary or extreme values of certain definite integrals called functionals. These integrals involve functions, which are unknown at the beginning of the analysis and the purpose of the calculus of variations is to determine what conditions are imposed on them. In this work, for each natural frequency that corresponds to the m$^{th}$ normal mode of the modal analysis, it is required to estimate the magnitude of the lamina orientation angle that raises the natural frequency to its maximum possible value, *RAYLEIGH-RITZ* method can be applied herein to perform that object. *RAYLEIGH-RITZ* method has included three steps, which are:

- Deriving mathematical relationships, called the objective functions, relating the functionals (natural frequencies) with the dependent variables (orientation angles of lamina).
- Specifying the domain interval of the dependent variables, to define the so-called constraint equations.
- First and second order derivative functions are derived from the objective functions. The first order derivative function is solved to estimate their roots, to be substituted in the second order derivative function to recognize the value of this function at each substituted root if it is less or greater than zero. The roots that make the second derivative function to be less than zero are examined in the objective function to specify that which maximize the objective function. The first step can be applied to predict the objective equations that relate each of the m$^{th}$ natural frequency with the orientation angles for unidirectional fibers laminas, using numerical regression ***( Hate, ٢٠٠٠)***$^{(\circ\circ)}$ as follows:

$$f_m(\theta) = N_1(\theta)\cdot f_m(0) + N_2(\theta)\cdot f_m(10) + \ldots + N_{10}(\theta)\cdot f_m(90) \qquad \ldots \textbf{(C.٢)}$$

where *m* is any integer, representing the m$^{th}$ normal mode of the structural analysis

The shape functions $\{N_1(\theta), N_2(\theta), \ldots N_{10}(\theta)\}$ can be derived according to the Lagrange numerical regression as following:

$$N_1 = \frac{(\theta-10).(\theta-20).(\theta-30).(\theta-40).(\theta-50).(\theta-60).(\theta-70).(\theta-80).(\theta-90)}{(0-10).(0-20).(0-30).(0-40).(0-50).(0-60).(0-70).(0-80).(0-90)} \quad \textbf{..(C. ٣)}$$

$$N_1 = \frac{(\theta-10).(\theta-20).(\theta-30).(\theta-40).(\theta-50).(\theta-60).(\theta-70).(\theta-80).(\theta-90)}{-3.6288 * 10^{14}}$$

Noting that, $N_1(0) = 1$, but $N_1(10) = N_1(20) = 0. \ . \ .N_1(90) = 0$.

then using the same procedure, all other functions can be derived as:

$$N_2 = \frac{(\theta).(\theta-20).(\theta-30).(\theta-40).(\theta-50).(\theta-60).(\theta-70).(\theta-80).(\theta-90)}{4.032 * 10^{12}}$$

$$N_3 = \frac{(\theta-10).(\theta).(\theta-30).(\theta-40).(\theta-50).(\theta-60).(\theta-70).(\theta-80).(\theta-90)}{-1.008 * 10^{13}}$$

$$N_4 = \frac{(\theta-10).(\theta-20).(\theta).(\theta-40).(\theta-50).(\theta-60).(\theta-70).(\theta-80).(\theta-90)}{4.32 * 10^{12}}$$

$$N_5 = \frac{(\theta-10).(\theta-20).(\theta-30).(\theta).(\theta-50).(\theta-60).(\theta-70).(\theta-80).(\theta-90)}{-2.88 * 10^{12}}$$

$$N_6 = \frac{(\theta-10).(\theta-20).(\theta-30).(\theta-40).(\theta).(\theta-60).(\theta-70).(\theta-80).(\theta-90)}{2.88 * 10^{12}}$$

$$N_7 = \frac{(\theta-10).(\theta-20).(\theta-30).(\theta-40).(\theta-50).(\theta).(\theta-70).(\theta-80).(\theta-90)}{-4.32 * 10^{12}}$$

$$N_8 = \frac{(\theta-10).(\theta-20).(\theta-30).(\theta-40).(\theta-50).(\theta-60).(\theta).(\theta-80).(\theta-90)}{1.008 * 10^{13}}$$

$$N_9 = \frac{(\theta-10).(\theta-20).(\theta-30).(\theta-40).(\theta-50).(\theta-60).(\theta-70).(\theta).(\theta-90)}{-4.032 * 10^{13}}$$

$$N_{10} = \frac{(\theta-10).(\theta-20).(\theta-30).(\theta-40).(\theta-50).(\theta-60).(\theta).(\theta-80).(\theta)}{3.6288 * 10^{14}}$$

This step would be executed using the results of the modal analysis of the wing finite element models.

# Main Flow-chart of the Suggested Technique



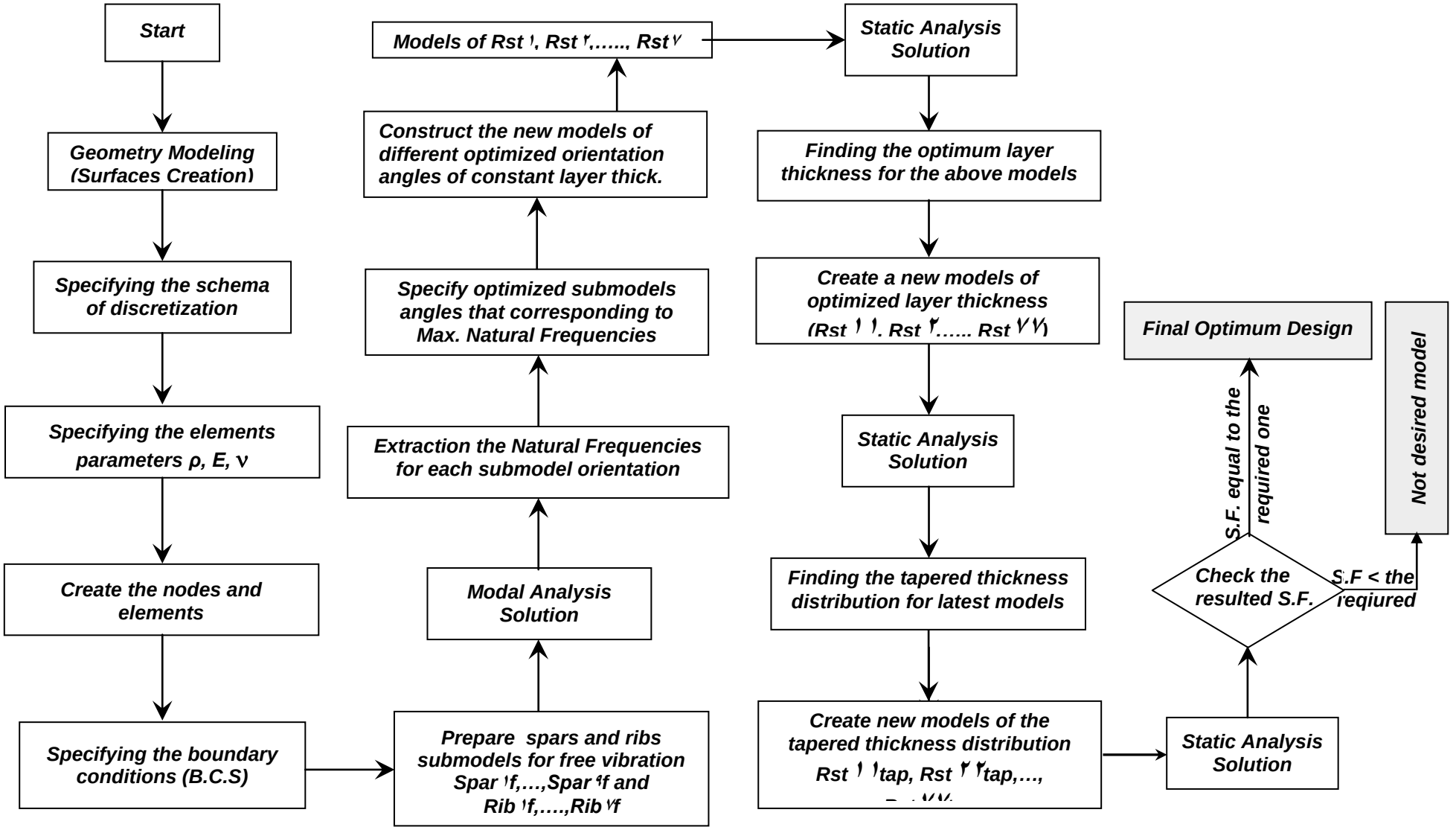

# *CHAPTER ONE*

# *INTRODUCTION*

## ١.١ General Comments

The engineering of modern composite materials has a significant impact on the technology of structural design and construction. The high-quality composite materials are being lighter, stiffer and stronger than most other structural material used in construction. Composite materials are ideal for structural applications where high stiffness per unit weight and potentially low unit cost are required. Aircrafts, spacecrafts, and vehicles are typical weight–sensitive structures in which composite materials are cost–effective.

A composite material can be defined as a material that is composed of two or more distinct phases, usually a reinforcing material (filament) supported in compatible matrix, assembled in prescribed amounts to achieve specific physical and chemical properties ( ***Stegmann*** and ***Lund,*** ٢٠٠١) [١].

Composite materials have many characteristics that are different from many conventional engineering materials. Most common engineering materials are homogeneous and isotropic while the composite materials are often heterogeneous and anisotropic. Such materials have physical properties varying with respect to the position and orientation (***Lekhnitskii,*** ١٩٨١) [٢].

A basic ply or lamina of a fiber-reinforced composite material can be considered from macro-mechanical point of view as an orthotropic material with two principal material directions or natural axes parallel and perpendicular to the direction of the filaments. By bonding these laminas together, a multi-laminas

composite called laminate is formed. The stiffness and strength properties of laminate are depending upon several parameters such as: fiber orientation in each lamina, properties and volume fractions of constituent materials, and the number of bonded laminas, thus the properties of such materials is directional. In the design of structures that are fabricated from such materials, the changing in the directional properties due to the changing in orientations of the various laminas and the number of laminas must be taken into consideration. Thus, the design may be optimized with the optimum properties of the material that nearly matches the directional loading requirements at the considered point of the structure. Unlike bulk metals which must be sized by the design maximum load and its direction (and hence are over designed when considering the smaller loads in other directions), composite materials can be made to fit the requirements. The result gives more efficient utilization and also reduces weight if the strength-to-weight ratio of the composite material is comparable with that of the metal. Since the strength-to-weight ratios of composites are actually greater than those of the commonly used structural metals, the effect of designing with composites are cascading.

Composite polymeric materials are commonly classified into the following:

A. ***Fibrous composite materials*** that consist of fibers in a matrix, e.g.

- Orthotropic aligned reinforced materials: stiffeners, wires, and fibers in matrix.

B. ***Laminated composite materials*** that consist of layers of various materials, e.g.

- Laminated glass, plywood and clad metals.

C. ***Particulate composite materials*** that consist of particles in a matrix, e.g.

- Quasi-isotropic random reinforced materials: Powder or particles in a matrix like ceramics.

D. ***Combination of some or all of the above three types***, e.g.

- Laminated fiber-reinforced materials: Orthotropic lamina bonded together to form an anisotropic material.
- Sandwich constructions: face sheets bonded to a light weight core.

Fiber–reinforced laminates have increasingly found applications in many engineering structures because of their anisotropic material properties that can be tailored through variation of the fiber orientation and stacking sequence of lamina which gives the designer an added degree of flexibility.

Laminated composites can be pro-classified according to the configuration of fibers in laminate into the following types:

*** *Symmetric lamination***

This type of lamination is symmetric in both geometry and material properties about the middle surface of laminated composite. The symmetric lamination includes two configurations as follows:

**١-Cross-ply lamination**

($٠^{o}/٩٠^{o}/٠^{o}$) cross ply lamination is an example for this type. Symmetric cross-ply lamination consists of an odd or even number of orthotropic layers that have principal material directions aligned with the axes of lamina and laminated symmetrically about the middle surface, ***(Jones, ١٩٧٥)*** [٣].

**٢. Angle-ply lamination**

Symmetric angle-ply laminas include an odd or even number of orthotropic layers that are symmetrically disposed about the middle surface of the laminated composite. For example ($٣٠^{o}/٧٥^{o}/٣٠^{o}$), the principal material directions are not aligned with the lamina axes, ***(Jones, ١٩٧٥)*** [٣].

**** *Antisymmetric lamination***

This type of lamination is very effectively used in practical applications of laminated plates and shells. Material properties of the individual layers are not symmetric about its middle surface. The antisymmetric lamination has bending-extension coupling and bend-twist coupling.

The bending-extension coupling effects are illustrated as an example by antisymmetric laminated plates after curing. The laminate is flat before curing

but thermally induced residual stresses cause the laminate to become highly curved, as shown in Figure (١.١)***, (Stegmann*** and ***Lund, ٢٠٠١)*** [١].

**Figure (١.١):** An antisymmetric laminate after curing [١].

The effect of bend-twist coupling on plate bending can be shown in Figure (١.٢). Utilization from this coupling in advanced design can be illustrated in the design of forward-swept wings subjected to aerodynamic loads which tend to twist the wing about an axis that is along the wing and off perpendicular to the fuselage. The wings are designed using composite laminates at various angles to the wing axis which result in bend-twist coupling that cause the wing to twist in the opposite sense of the aerodynamic wing-twisting effect, as shown in Figure (١.٣), ***(Stegmann*** and ***Lund, ٢٠٠١)*** [١].

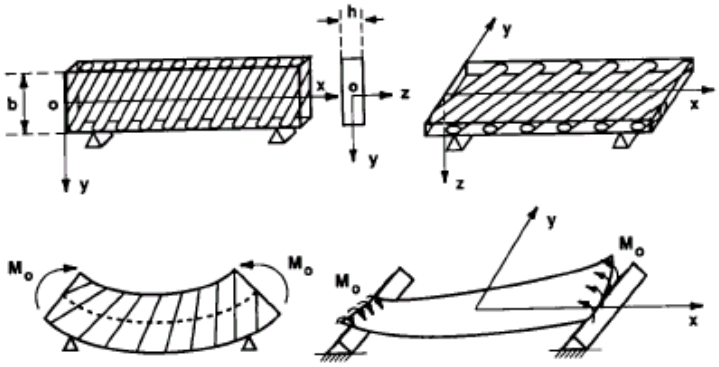


**Figure (١.٢):** Effect of bending-twist coupling on plate [١].

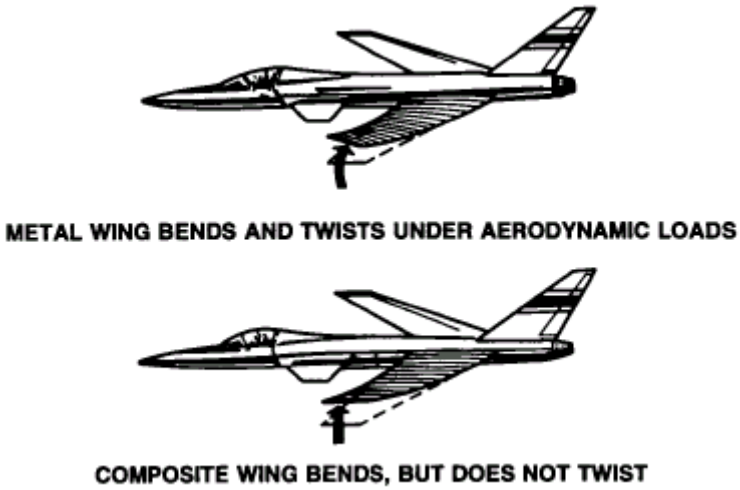


**Figure (١.٣):** Aerodynamic response of metal and composite wings [١].

Similarly to symmetric lamination, antisymmetric lamination includes two configurations as follows:

**١. Cross-ply lamination**

Antisymmetric cross-ply laminate consists of an even number of orthotropic layers laid on each other with principal material directions alternating at $٠^{o}$ and $٩٠^{o}$ to lamina axes. ($٠^{o}/٩٠^{o}/٠^{o}/٩٠^{o}$) is an example, ***(Jones, ١٩٧٥)*** [٣].

**٢. Angle-ply lamination**

This is the most general configuration type of laminate. It contains even number of orthotropic layers laid on each other with principal material directions not aligned with lamina axes. ($٦٠^{o}/٣٠^{o}/٦٠^{o}/٣٠^{o}$) is an example, ***(Jones, ١٩٧٥)*** [٣].

## ١.٢ Applications of Composite Materials

In this section, generally the properties of composite materials are considered and their application is based on the answers of the following questions:

**I-** What are the properties of the composite materials?

**II-** According to these properties, what are the suitable applications?

Composite materials which have uniquely properties make them applicable and more effective in comparison with the other materials. Some of these properties are:-

١-Directional materials properties; fiber reinforcement properties dominate the mechanical behavior of the composite in the direction of reinforcement.

٢- High strength and stiffness to weight ratios.

٣- Static mechanical properties of fiber-reinforce composite are affected by the hardener system and the curing conditions ***(Raj, et al. ١٩٨٢)*** [٥].

٤- Economic considerations of low unit and maintenance costs.

Composite materials have a long history of usage. Their beginnings are unknown, but all recorded history contains reference to some forms of composite materials. For example, plywood was used by the ancient Egyptians when they realized that wood could be rearranged to achieve superior strength and resistance to thermal expansion as well as to swelling in the presence of moisture, medieval swords and armor were constructed with layers of different materials ***(Jones, ١٩٧٥)*** [٣].

The procession road in ancient Babylon, one of the most wonders of the ancient world, was made of bitumen reinforced with straw. Straw and horsehair have been used to reinforce mud bricks for at least ٥٠٠٠ years, (***Ashby*** and ***Jones, ١٩٨٨***) [٦].

Preliminary feasibility investigations have revealed that incorporation of high strength, high modulus, and low-density glass or boron filaments in a low strength and low modulus epoxy matrix material can result in a composite material that offers the potential of a major breakthrough in air and space vehicle design. Weight saving over conventional metallic structures of as much as (٤٠ to ٥٠٪) has been predicted for some structural components and these studies have been indicated that the total structural weight of a typical aircraft could be reduced by more than (٣٥٪). For re-entry vehicles, the substitution of an integrated thermal shield and substructure of advanced composite materials for the conventional shield and structure will result in a predicted weight saving of (٢٥ to ٣٥ %), depending upon the vehicle type, size and the mission environment. The usage of advanced composite materials has also affected

propulsion systems. A weight reduction of as much as (٣٣ %) is considered possible in air-breathing engines. In addition, composites including both fiber-reinforced and dispersion-strengthened materials could make possible an increase in turbine inlet temperatures of several hundred degrees centigrade, also the application of these materials combinations may eventually double the attainable thrust-weight ratios in turbo fan engines.

The composite materials industry however is new. It has grown rapidly in the past fifty years with development of fibrous composites; to begin with glass fiber-reinforced polymers and more recently carbon fiber-reinforced polymers. Fiber reinforced polymer composite with high strength to weight and high stiffness to weight ratios have become more important in light weight applications such as aircraft, aerospace, sports and boats application….etc. Their use in such systems is a revolution in materials usage, which is still accelerating. Some of composite materials applications today are listed in Table (١.١).

**Table (١.١):** Applications of Composite Materials in Some Industries [٧].

| Application | *Parts* |
|---|---|
| **Marine** | **Boats, fairings, deck houses, tanks, deep submergence objects, vehicles, etc.** |
| **Aircraft** | **Rudder, fuselage, landing – gear, fairings.** |
| **Automobile** | **Tires, drive shaft, window glass.** |
| **Chemical Industries** | **Pipes, pressure vessels, and tanks.** |
| **Sport** | **Tennis rackets and sports equipments.** |
| **Medical** | **Dental materials, joints in human bodies, and denture bases.** |
| **Effective Passive Control System** | **Slider crank mechanism, and peaucellier [١٧].** |

## ١.٣ Analysis Development of Composite Laminas

A laminate composite is a series of laminate bonded together to act as an integral structural element. Thus, a laminate is a structural element with essential features of both material properties and geometry.

Figure (١.٤) shows the individual layers with arbitrary orientations

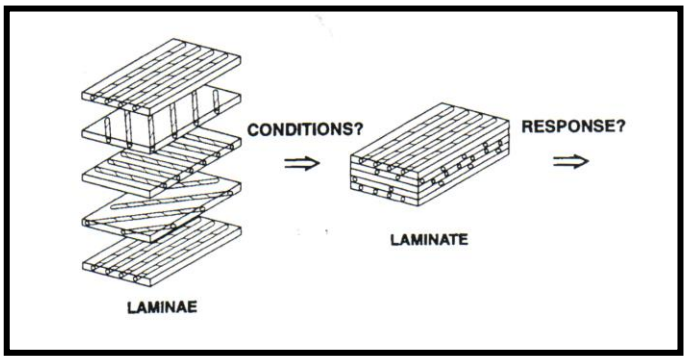


**Figure (١.٤):** Laminated composite with several lamina orientations [١].

In the analysis of laminated plates and shells, there are two categories of theories, equivalent single layer and three-dimensional elasticity theories. In the first category, the material properties of the constituent layers are smeared to form a hypothetical single layer whose properties are equivalent through thickness integrated sum of its constituents, and this category contains classical lamination theory, first order theory and higher order theory as subclasses. In the classical laminated theory [also called ‘‘classical lamination theory (CLT) ’’], which is based on Kirchhoff-Love hypothesis for plates and shells as shown in Figure (١.٥). One of its assumptions is that the normal to the midsurface before deformation remains straight and normal to the midsurface after deformation; through-thickness shear deformation effects are negligible.

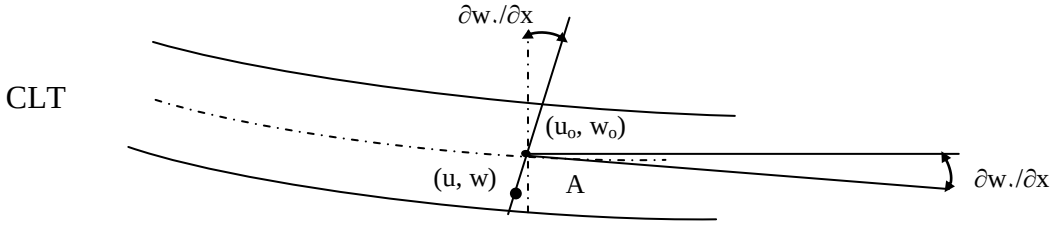


**Fig.(١.٥):** Classical Lamination Theory in After Deformation.

However, due to the low transverse shear modulus relative to the inplane Young's modulus of each lamina, the transverse shear deformation effects are more pronounced in composite than in isotropic laminate. Hence, several types of shear deformation theories have been introduced. Timoshenko beam theory, which includes transverse shear deformation and rotary inertia effects, has been extended to isotropic plates by Reissner and Mindlin**,** and to laminate anisotropic by Yang, Norris and Stavsky. The theory also called "First order shear deformation theory (FSDT)" takes into account the effect of transverse shear deformation and assumes it constant through the laminate thickness. Thus a shear correction factor is used.

The assumptions of a higher order lamination theory can also be used within equivalent single layer formulation ***(Stegmann*** and ***Lund, ٢٠٠١)*** [١]**:**

١. The lamina may be moderately thick.

٢. The in plane displacement u (x, y, z, t) and v (x, y, z, t) are cubic functions of z.

٣. The transverse shear stresses $\tau_{xz}$, $\tau_{yz}$ are parabolic in z.

٤. The in plane stresses $\sigma_x$, $\sigma_y$ and $\tau_{xy}$ are cubic functions of z.

٥. The normals to the mid-surface before deformation are straight, but not necessarily remaining normal to the mid-surface after deformation.

٦. The transverse normal strain $\varepsilon_z$ is negligible.

## ١.٤ Objective and Scope

In this thesis the focus will be on hybrid class, namely ***laminated fiber-reinforced composite materials*** *and* ***sandwich construction*** as they are the basic building element for composite shell structures. The mechanical properties and the response due to the environment loads of such materials are dependent upon: the fiber orientation, the number of layers, stacking sequence, and fiber orientation angle, in addition to the thickness of each lamina. Thus, the objective of the present work will be distributed in the following steps:

١-Suggest a general numerical technique based on the finite element method and calculus of variation to use the fiber-reinforced composite materials in the construction of complex structure. The technique takes into consideration the investigation of the optimum design such as optimum fiber orientation, optimum stacking sequence, optimum layer thickness, and optimum thickness distribution across the global structure.

٢-Apply the suggested technique on a case study of a remotely guided aircraft wing structure to obtain its optimum design, in addition to create an optimized and arbitrary wing models to present the validity of the technique.

٣-Analyzing the created models dynamically under the action of specific environment load to study their dynamic behavior and effect of some parameters such as fiber orientation, dynamic load factor (DLF), and damping properties on the dynamic response.

## ١.٥ Thesis Layout

This thesis is organized in five chapters:

***Chapter One*:** presents some of the basic definitions concerned with the fiber-reinforced composite materials, their importance, and usage of them. The objectives and the aim of the current work are also presented.

***Chapter Two*:** contains a brief review of previous studies on the subject under consideration.

***Chapter Three*:** presents the details of the theoretical consideration of the suggested technique and how to be executed to obtain the optimum design, in addition to structural consideration concerned with the static, free vibration, and dynamic analyses.

***Chapter Four:*** presents the results of the suggested technique to study the effect of the optimum orientation, layer thickness, and thickness. Failure indices and the dynamic responses for each configuration are also presented.

***Chapter Five:*** gives a summary of the conclusions which can be drawn from this study and the suggestions for future related works.

# *CHAPTER TWO*

# *REVIEW OF LITERATURE*

## ٢.١ Introduction

Laminated fiber-reinforced composite shells have continuous increasing usage in primary and secondary aerospace and aircraft structures owing to their superior mechanical properties as mentioned previously. One form of these materials, being used in current design studies, is the unidirectional fiber-reinforced lamina. In addition, anisotropy, non-homogeneity and larger ratio of longitudinal to transverse modulus of these materials supply an improvement in the existing analytical tools. As a result, the analysis of laminated composite shells has attracted many research workers and has been considerably improved to achieve realistic results.

The present review covers two aspects: The first includes the static analysis of laminated fiber-reinforced composite shell structures and the second aspect is concerned with the developments in the dynamic analysis of such shells under the action of dynamic loads.

## ٢.٢ Static Analysis

***Paul*** [٨] **(١٩٦٣)** developed the linear bending theory of laminated elastic cylindrical shells under axisymmetric loading from first principles. It was shown that a spontaneous "beam column" type of deformation may be developed even in the absence of end loads. Generally, however, this effect was shown to be small for metallic cylinders, in which case, the laminated shell deforms in the same manner as a homogeneous shell, where the effective flexural rigidity and effective extensional rigidity were both shown to have a simple dependence upon the elasticity distribution pressurized throughout the wall thickness. The

influence of edge loads on a semi-infinite shell are determined and applied to the stresses in a titanium shell with a steel-reinforcing band.

***Hsu*** [٩] **(١٩٧٠)** developed a general linear theory and the derivations of equations of motion for the analysis of laminated cylindrical shells consisting of layers of orthotropic lamina. The classical Kirshoff hypothesis of non-deformable normal commonly used for isotropic shells was banded so that compatible shear stresses and deformation between layers can be maintained. The transverse coordinate Z, when compared to the radius of midsurface of each layered cylinder, was generally small, however; was not neglected in the general derivation. The general procedure in the derivation was similar to that presented by Amburtsumian for orthotropic plates. However, the resulting governing differential equations were substantially more complicated than those for orthotropic plate.

***Ahmed*** and ***Zienkiewiez*** [١٠] **(١٩٧١)** presented a general formulation for curved arbitrary shape of thick and thin shell finite elements with a simplified form of axisymmetric situation. Several examples were illustrated ranging from thin to thick shell applications were given to demonstrate the formulation validity and the accuracy of the solution. At last, from the comparison, the accuracy of the formulation was in an excellent form.

***Govil***, ***et al*** [١١] **(١٩٧٩)** applied an iterative method for optimal design of large scale wing-type structure that incorporates the concept of substructuring to demonstrate its generality, effectiveness and efficiency. Optimum design for several wing-type structures were obtained and compared with available results. It was shown that considerable efficiencies have been achieved by integration of the substructuring concept into a structural optimization algorithm.

***Venkatesh*** and ***Rao*** [١٢] **(١٩٨٠)** developed the stiffness matrix for a doubly curved quadrilateral element suited for static and dynamic analysis of laminated anisotropic thin shells of revolution. By expressing an assumed displacement

state over the middle surface of the shell as products of one-dimensional first order Hermite polynomials, it is possible to ensure that the displacement state for the assembled set of such element is geometrically admissible. Systematic evaluation of performance of the element is conducted, and considering various examples for which analytical or other solutions are available.

***Panda*** and ***Nataragan*** [١٣] **(١٩٨١)** described a doubly curved super parametric quadrilateral shell element as a model for the static analysis of practical, non-classical structural configuration constructed of fiber-reinforced laminated composite. The coupling phenomenon between flexural bending deflection and in plane stretching and the effect of shear deformation were accounted in the formulation. Some examples were examined and compared with other available examples. The comparison resulted in good agreement.

***Reddy*** [١٤] **(١٩٨٤)** presented an extension of the Sander's shell theory for doubly curved shell to a shell deformation theory of laminated shells. The theory accounts for transverse shear strain and rotation about the normal of the shell mid surface. Exact solution of the equations were presented for simply supported, doubly curved, cross ply laminated shells, under sinusoidal, uniformly distributed, and concentrated point load at the center. Fundamental frequencies of cross ply laminated shells were also presented.

***Ramana*** [١٥] **(١٩٨٥)** presented the static small deflection analysis of composite shells by forty-eight degrees of freedom doubly curved quadrilateral shell finite element. All three displacements of shell element reference surface were expressed as a product of one-dimensional first order Hermite interpolation polynomials. The constitutive relationship for bi-modulus composite was assumed to be depending on the fiber direction strain experienced by each orthotropic layer. Consequently the state of stress /strain is obtained by specifying a maximum error in the locations.

***Seide*** and ***Chaudhuri*** [١٦] **(١٩٨٦)** presented a development of a general curved triangular element based on an assumed displacement potential energy

approach for static and dynamic analysis of arbitrarily laminated thick shells. The associated laminated shell theory assumes transverse inextensibility and layerwise constant shear angle. To demonstrate the accuracy and efficiency of the presented element, examples of two laminated shell problem were examined.

***Reddy*** and ***Pandy*** [١٧] **(١٩٨٧)** developed a finite element computational procedure for the first ply failure analysis of laminated composite. The procedure was based on shear deformation theory and tensor failure criteria that contain the maximum stress, maximum strain, Tsi-Wu and Hoffman failure as special cases. A number of problems were presented to evaluate those failure criteria when applied to laminates subjected to in plane and/or bending load.

***Yeom*** and ***Lee*** [١٨] **(١٩٨٩)** developed a nine node finite element model for the analysis of geometrically non-linear laminated composite shells. The formulation was based on the degenerated solid shell concept and utilizing a set of assumed strain fields as well as assumed displacement. The formulation assumes strain and the determinant of the Jacobian matrix to be linear in the thickness direction. This allows analytical integration in the thickness direction regardless of ply layups. The results of numerical tests demonstrated the validity and the effectiveness of the present approach.

***Kant*** and ***Menon*** [١٩] **(١٩٨٩)** presented a higher order displacement model for behavior of symmetrical and unsymmetrical laminated composites and sandwich cylindrical shells based on $C^o$ finite element discretization. Two theories, namely (١) geometrically thin shell theory based on assumption that the ratio of the shell thickness to radius (h/R) being less than unity and (٢) geometrically thick shell theory, in which $(h/R)^2 << ١$ were developed. These theories incorporate more realistic non-linear variation of longitudinal displacement–through the shell thickness and thus eliminate the use of correction coefficients. The influence of (h/R) for a thick shell was studied and the results were compared with those of geometrically thin shells and other available results.

***Yunus*** and ***Khonke*** [٢٠] **(١٩٨٩)** presented an efficient numerical integration scheme for evaluating the matrices (stiffness, mass, stress stiffness, and thermal load) for doubly curved, multilayered composite, quadrilateral shells. Finite element formulation was based on three dimensional continuum mechanics theory and used to analyze a thin and moderately thick composite shell. Numerical data were presented to demonstrate that the presented formulation is an order of magnitude economical compared to a conventional scheme.

***Liao*** and ***Reddy*** [٢١] **(١٩٩٠)** formulated the fundamental equations of motions based on the principle of virtual displacements of continuous medium using the total Lagrangian description. A degenerated shell element with the general shell element as a stiffness was developed for geometric nonlinear analysis of laminated, anisotropic, stiffened shells. An iteration solution procedure of Newton-Raphson method was employed to trace the nonlinear equilibrium path. Variety of numerical examples was presented to demonstrate the validity and efficiency of the stiffened shell element.

***Surana*** and ***Sorem*** [٢٢] **(١٩٩٠)** presented a new curved shell finite element formulation for linear static analysis of laminated composite plates and shells. An additional nodal variable in the element displacement approximation corresponding to the Lagrange interpolation polynomials in the element thickness direction was added. The element formulation was providing $C^o$ continuity or smoothness of displacement across the element boundary. The element properties (stiffness matrix and equivalent load vector ) were derived by principle of virtual work and the hierarchical approximation element extended for generally orthotropic behavior where the material directions are not necessarily parallel to the global axes. Several examples were examined and the accuracy was in good agreement.

***Mallikarjuna*** and ***Kant*** [٢٣] **(١٩٩٢)** developed a refined shell theory for the analysis of isotropic, orthotropic, and anisotropic fiber-reinforced laminated composite and sandwich shells. This theory was based on a higher-order displacement model and the three-dimensional Hooke's law for shell material, giving rise to a more realistic representation of the cross-sectional deformation. In addition, a higher-order shear deformation shell theory and a first-order shear deformation shell theory, following Reissner-Mindlin plate formulation was developed and the results were compared with the closed-form solution. The parametric effects of the finite element mesh, radius-to-arc length ratio, and length-to-thickness ratio, lamination scheme, Gaussian integration rule and material anisotropy on the response of the laminated composite shells were investigated. The results obtained were tabulated to provide an easy means for future comparisons by other investigators.

***Lee*** and ***Liu*** [٢٤] **(١٩٩٢)** presented a layer reduction technique for composite laminated analysis to decrease the number of degrees of freedom by combining a multi layer approach with a single layer approach. They concluded that the layer reduction technique increases computational efficiency in composite materials by reducing (n-layer) laminate to a four layer laminate, but retaining the easiness and accuracy in calculating the transverse stresses from constitutive equations directly. The feasibility of this technique was demonstrated by numerical examples of composite laminates under both directional bending and cylindrical bending.

***Kalamkarov*** and ***Kolpakov*** [٢٥] **(١٩٩٦)** obtained closed-form solutions based on general homogenization shell model for the effective stiffness module of the high-stiffness fiber-reinforced angle-ply composite shell. The design problem for the fiber-reinforced shell having the required set of effective stiffness was formulated and solved. The set of prescribed stiffness for which the problem is solvable was described, and the effective method of the design parameter calculation based on convex analysis was developed. The minimum

number of reinforcing layers required for the design of the fiber-reinforced angle-ply shell with the prescribed stiffness was determined. The solution of design problem was a generalized account of minimization of the fiber volume content.

***Mohan*** [٢٦] **(١٩٩٧)** presented a finite element analysis of thin laminated shells using a three-noded flat triangular shell element. The first shell element was obtained by combining the Discrete Kirchhoff (DkT) plate bending element and a membrane element similar to the Allman element, but derived from the Linear Strain Triangular (LST) element. The element is first thoroughly tested for the linear static analysis of laminated plate and shells and was extended for free vibration, thermal, and geometrically nonlinear analysis. Several numerical examples were solved to demonstrate the accuracy of the formulation. The results were compared with those obtained using the commercial finite element package ABAQUS and were found to be in good agreement. The researcher concluded that the element can be used to obtain the static and nonlinear responses of the complex structure under wind and snow loads.

***Masud*** and ***Panahadeh*** [٢٧] **(١٩٩٩)** presented multilayered/multidirector and shear deformable finite element formulation of shells for the analysis of composite laminates. The displacement field was assumed continuous across the finite element layers through the composite thickness. The rotation field, however, layerwise continuous were assumed discontinuous across these layers. This kinematics hypothesis results were resulted in independent shear deformation of the director associated with each individual layer and thus allowed the warping of the composite cross section. The resultant through-thickness strain field was therefore discontinuous across the element material sets. Numerical results were presented to show the performance of the method.

***Davila, et al*** [٢٨] **(١٩٩٩)** developed a progressive failure analysis method based on shell element for computation of damage initiation and growth in stiffened thick-skin stitched graphite-epoxy panels loaded in axial compression.

The analysis involved a step-by-step simulation of material degradation based on ply-level failure mechanics. High computational efficiency was derived from the use of superposed layers of shell elements to model each ply orientation in the laminate. The analysis results were compared with experimental results and the comparison was in good agreement with the experimental values.

***Wu*** and ***Lo*** [٢٩] **(٢٠٠٠)** presented an asymptotic theory for the analysis of laminated annular spherical shells by the perturbation method. A set of governing equations for the bending analysis through the thickness direction of an annular spherical shell were obtained. The method of differential quadrature was adopted for solving the problems of various orders. Illustrative examples were given to demonstrate the performance of the presented asymptotic theory.

***Kessler*** and ***Spearing*** [٣٠] (٢٠٠٢) focused on the design and analysis of a high-g composite fuselage structure. The aft section was not only subjected to high impulsive inertial load, but its weight had a substantial effect on the controllability of the structure; therefore, it was manufactured by advance composite materials to save the weight without incurring a strength penalty. Lay-up test specimens were produced to optimize the design. These specimens were tested statically as well as in a dynamic environment. The researches discovered that composite materials were better to manufacture light space vehicle.

***Langley*** [٣١] (٢٠٠٢) presented a method for creating a finite element model of tow-placed variable stiffness fiber-reinforced composite. The method provided a representation of the overlap regions and an accurate model of fiber orientation angle change through the laminate. The GENSIS finite element analysis and design package was used to solve for the static response of the modeled created. The results of the analysis compared favorably with the results from another search and showed some insight into the tow interaction of the thickness and fiber-orientation.

***Yu*** and ***Hodges*** [٣٢] (٢٠٠٤) developed a geometrically nonlinear shear deformation theory for elastic shells to accommodate a constitutive model suitable for composite shells when modeled as a two-dimensional continuum. A complete set of kinematical and intrinsic equilibrium equations were derived for shells undergoing large displacements and rotations but with small, two dimensional, generalized strains. The large rotations were represented by the general finite rotation of a frame that emended in the unrdeformed configuration, of which one axis was along the normal line. The unit vector along the normal line of the undeformed reference surface was not in general normal to the deformed reference surface because of the transverse shear.

## ٢.٣ Dynamic Analysis

***Stavsky*** and ***Loewy*** [٣٣] **(١٩٧٤)** established a refined Love-type theory of motion for orthotropic composite cylindrical shells. An extended version of the theory was formulated to account for dynamic stability problems involving time-dependent and non-conservative forces. The frequency spectra of free natural vibrations were investigated for numerous layered shells, using Love-and Donnell type theories. Heterogeneity was found to considerably affect the results for the natural frequencies; for certain shells produced of a fixed amount of materials, differing only in their arrangement, a suitable composition raises the lowest frequency by a factor of (١.٥٠). For length-to-radius ratios of about (٥) the resulting first lowest frequency may be higher by a factor of (١.١٠) than the one given by the present Love-type theory. It was noted that higher errors, strongly depending on shell heterogeneity, were noted as the length-to-radius ratios increase beyond (٥).

***Patnaik*** and ***Sankaran*** [٣٤] **(١٩٧٦)** presented the optimum design of stiffened cylindrical panels with weight as the objective function and constraints on the frequencies in the presence of initial stresses, using unconstrained minimization techniques of non-linear mathematical programming problem. The

interaction between the buckling constraints and the frequency constraints in the presence of initial stresses were included in the formulation. Loss of load carrying capacity due to imperfection and due to suddenly applied loads was included in the analyses. Results for cylindrical shell were obtained by setting the panel angle to (٣٦٠) degrees. The relationship between the weight of the cylinder and the panel (a segment of the cylinder) was also examined.

***Rao*** and ***Raju*** [٣٥] **(١٩٧٧)** considered the vibration of a laminated cross-ply circular cylindrical shell. It was shown that, the anti-symmetric lamination about the shell middle surface cause coupling between bending and extension of the laminate and that this coupling effect dies out rapidly as the number of layers increases.

***Reddy*** [٣٦] **(١٩٨١)** presented a finite-element analysis of the transient behavior of fiber-reinforced, single-layer and two-layer cross-ply rectangular plates and shells of bimodular materials. To validate the finite element results, a closed-form solution was also presented for a rectangular plate with all edges simply supported without in-plane restraints (along the edge) and tangential rotation and subjected to a suddenly applied sinusoidal distributed normal pressure. The time behavior of the transverse loading is arbitrary (e.g., steps loading, impulse loading, etc.). Numerical results for transverse deflection as functions of time were presented for two bimodular materials. The finite element solutions agree very closely with the closed-form solutions.

***Greenberg*** and ***Stavsky*** [٣٧] **(١٩٨١)** presented the equations of motion derived from a Love-type theory for laminated filament-wound cylindrical shells in which each layer was permitted an arbitrary fixed fiber orientation. A general method of solution was established, based upon the use of a complex finite Fourier transform. The frequency spectra of free natural vibrations were investigated for numerous single, big and tri-layered clamped or simply supported generally orthotropic shells. The effect of fiber orientation on the frequency response was found to be quite considerable in certain composite

shells, for some shells the frequency was increased by a fraction of (٣:١) by simply choosing an optimal combination of fiber winding angles. Similar important effects were noted due to the combined action of shell heterogeneity and fiber winding angle.

***Raj, et al.*** [٥] (١٩٨٢) presented the impact properties of the various glass fiber-reinforced composites and their fracture mode under dynamic load. The results of dynamic loads were compared with those corresponding to static state. They concluded that the impact strength of the most of composite material (as glass fiber reinforced composite) depends on its ability to absorb the energy, resist the dynamic load, hardened system, and curing conditions (such as the time); impact strength goes to the maximum value at a certain curing time and decreases after and before this time. In the other hand, they concluded that the composite materials sustain higher impact loads and show excellent impact strength.

***Rao*** [٣٨] **(١٩٨٣)** explained the effects of transverse shear and rotatory inertia in the case of an anti-symmetrically laminated cross-ply circular cylindrical shell. Representative results were given for the case of graphite/epoxy shells of varying length-to-radius and radius-to thickness ratios. It was shown that the effects under consideration have predominant influence on the frequencies even at higher radius-to-thickness ratios.

***Shapana*** [٣٩] **(١٩٨٦)** presented a finite element scheme for studying the effect of using composite on the dynamic response of multi body systems. The formulation was exemplified by using fiber-reinforced composite laminates. Two numerical examples of a slider crank mechanism and a peaucellier mechanism were presented in order to demonstrate the effect of use of composite material in the dynamic response of multi body system. Numerical results showed that the use of composite materials represents an effective passive control strategy.

***Mustafa*** and ***Ali*** [٤٠] **(١٩٨٧)** described the structural symmetry techniques to the free vibration analysis of cylindrical and conical shells for the prediction of natural frequencies and mode shapes. Appropriate boundary conditions have been developed for the analysis of only a part of the shell and have been shown to yield results comparable to the full shell analysis. Half and quarter models of the shell have been developed and analyzed using semi-loof and facet shell finite elements. Unstiffened and stiffened circular cylindrical shells and stiffened conical shells have been considered. It was concluded that the maximum magnitudes of the natural frequencies are corresponding to the maximum structural stiffness.

***Kumar*** and ***Rao*** [٤١] **(١٩٨٨)** presented free vibration characteristics of a multi layered graphite epoxy circular cylindrical shell using an eight-node isoparametric quadrilateral shell element. The effects of rotary inertia were considered in the formulation of the mass matrix. Variations of length to radius and radius to thickness ratios of the shell, and different fiber orientations such as (٠°/٩٠°), (٠°/٩٠°/٠°/٩٠°), (٠°/٩٠°), and (٠°/٩٠°/٠°/٩٠°), with respect to the frequency parameter were studied. Comparison of numerical results with other literature showed good agreement.

***Malhotra*** [٤٢] **(١٩٨٨)** studied the effect of fiber orientation on the natural frequency of the orthotropic shells having variable thickness. The effect of fiber orientation and boundary conditions on natural frequency was studied for a linear variation in thickness along the x-direction and the y- direction. The same study was conducted to determine the vibration behavior of such shell mode of graphite epoxy used for some aerospace structural components

***Attaf*** and ***Hollaway*** [٤٣] **(١٩٩٠)** presented and studied the dynamic response of stiffened and unstiffened composite structures subjected to static in-plane loads. A finite element package was also used to predict the dynamic behavior. The critical load values of the complete structures have been estimated from the stability and vibrational analysis. The aims of the studies were to

investigate the resonant frequency characteristics for stiffened and unstiffened composite structures.

***Suzuki, et al.*** [٤٤] **(١٩٩٤)** presented an exact solution procedure for solving free vibration problems for laminated composite noncircular shells. Based on the classical lamination theory, strain energy and kinetic energy functions were first derived for shells having arbitrary layer stacking sequences. These functions were useful for a general analysis based upon energy principles. Frequencies were presented for a set of elliptical cylindrical shells, and the effects of various parameters upon them were also discussed.

***Dipankark, et al.*** [٤٥] **(١٩٩٨)** applied the finite element method to solve free and forced vibration problems of isotropic and laminated composite shells with and without cutouts employing eight-node isoparametric finite element formulation. Specific numerical problems of earlier investigators were solved to compare their results. Moreover, free vibration problems of cylindrical, spherical, saddle (hyperbolic paraboloid bounded by parabolas), hypar (hyperbolic paraboloid bounded by straight lines), and conical shells with cutouts and forced vibration of composite hypar and conical shells without cutouts were examined to arrive at some conclusions useful to the designers.

***Yen and Cassin*** [٤٦] **(١٩٩٩)** developed a composite failure criterion for dynamic analysis of composite structures. The proposed progressive failure criterion has been integrated into an explicit dynamic analysis code for failure prediction of thin composite tubes subjected to drop weight impact tests. The results provided good correlation with experimental data for impact force histories and some critical damage modes.

***Nayfeh and Rivieccio*** [٤٧] **(٢٠٠٠)** presented the analysis of vibration of shallow, simply supported, non symmetric unbalanced composite shell. The discretized Lagrangian method of multiple scales solution technique was applied. The system of Lagrangian was developed and integrated over the spatial domain and substituted into Lagrange's equation. The resulted equation of

motion was a second frequency temporally nonlinear ordinary differential equation in the form of Doffing oscillator.

***Liew, et al.*** [٤٨] **(٢٠٠٢)** presented the free vibration analysis of axially loaded cross-ply laminated cylindrical shells with the consideration of centerfugal force as the initial hoop tension due to rotation. The frequency characteristic analysis for shell of simply supported boundary conditions was examined and the frequency characteristics of various laminated schemes were also investigated.

The results from the analysis were compared with the available solutions to validate its accuracy.

## ٢.٤ Closing Remarks

Many remarks are extracted from reviewing the literature that is concerned with the principles of the current work, these are:

- ***Stavsky*** and ***Loewy*** [٣٣] **(١٩٧٤)** concluded that the heterogeneity through the thickness was found to considerably affect the results for the natural frequencies so that, for certain shells produced of a fixed amount of materials, differing only in their arrangement, a suitable composition raises the lowest frequency by a factor of (١.٥٠). Therefore, the stacking sequence must be considered in studying of the composite materials especially in the design processes.
- ***Govil, et al*** [١١] **(١٩٧٩)** applied an iterative method for optimal design of large scale wing-type structure that incorporates the concept of substructuring analysis to demonstrate its generality, effectiveness and efficiency. Therefore, this concept will be adopted in present work.
- It is concluded from the study of ***Greenberg*** and ***Stavsky*** [٣٧] **(١٩٨١)** that the fiber orientation was found to be quite considerable on the response of laminated composite shells. Therefore, the effect of fiber orientation will be studied deeply.

- ***Raj, et al.*** [٥] (١٩٨٢) presented the impact properties of the various glass fiber reinforced composites. They concluded that the composite materials sustain higher impact loads and excellent impact strength and smaller time response and presents higher stiffness and more stability.
- ***Shapana*** [٣٩] **(١٩٨٦)** concluded from his study that using of composite materials represents an effective passive control strategy due to the superiorities of stiffness to weight for these materials, thus it can be possible to investigate an optimized ratio of stiffness\weight according to this result.
- It is concluded from the study of ***Mustafa*** and ***Ali*** [٤٠] **(١٩٨٧)** that the maximum natural frequency of any mode is corresponding to the maximum structural stiffness. Then a further conclusion is extracted, saying that the optimum configurations of the laminated fiber-reinforced composite shell structure can be predicted if the maximum natural frequencies are derived as a function of those configurations. Therefore; an optimization technique will be suggested in the present work based upon these conclusions.
- ***Yunus*** and ***Khonke*** [٢٠] (١٩٨٩) presented an efficient numerical integration scheme for evaluating the matrices for doubly curved, multilayered composite, quadrilateral shell. Finite element formulation was based on three dimensional continuum mechanics theory and used to analyze a thin and moderately thick composite shell. They concluded that the formatted element can be applied for analysis of thin and moderately thick composite shells. Therefore, this element and its formulation will be adopted in present work.
- As shown from the study of ***Lee*** and ***Liu*** [٢٤] **(١٩٩٢)** , the layer reduction technique increases the computational efficiency in composite material by reducing (n-layer) laminate to a four-layer laminate, but retaining the easiness and accuracy in calculating the transverse stresses from constitutive equations directly.

***Langley*** [٣١] (٢٠٠٢) developed a tow-placed device to economically manufacture composite structures, which have spatially varying fiber orientation and tapered layer thickness. The layer thickness that was obtained is ٠.٠٠٥٥ inch. Therefore, a tapered thickness distribution with a smaller thickness can be achieved and accomplished in this work depending on the mentioned tow-placed device ability.

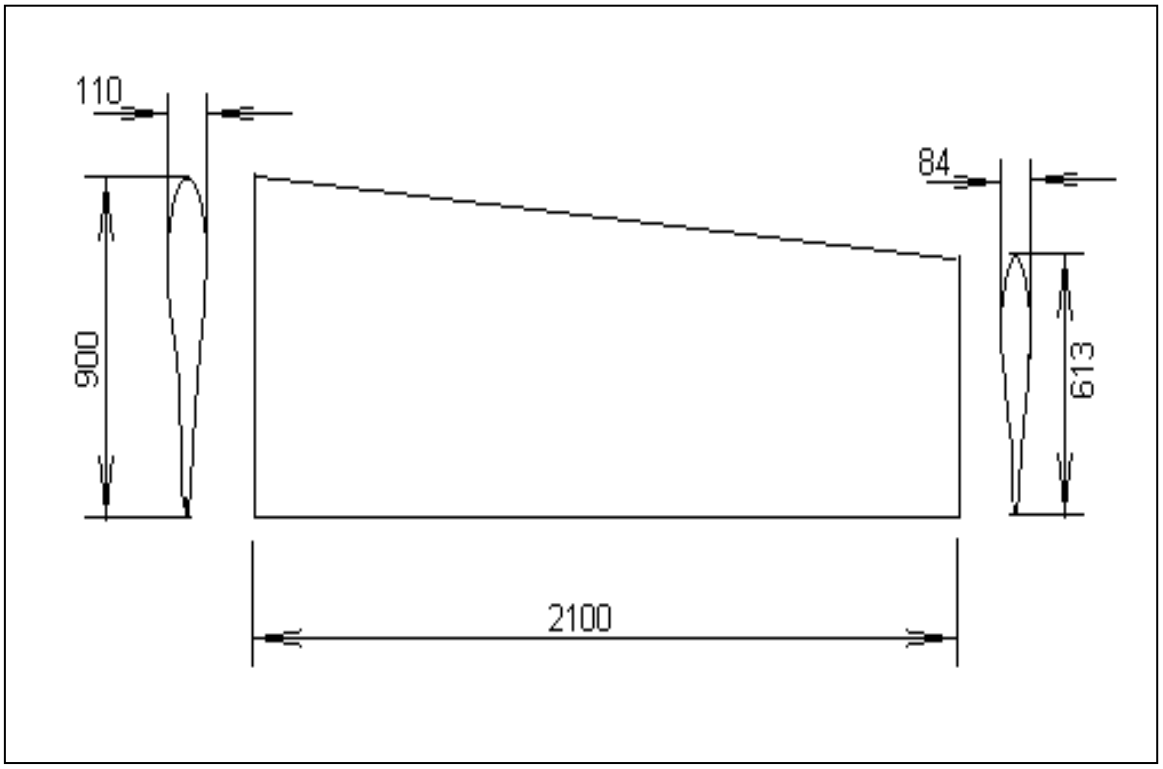


**Fig.(٣.١)**: The aerodynamic shape of wing of remotely guided aircraft

Note : all above dimensions are in mm

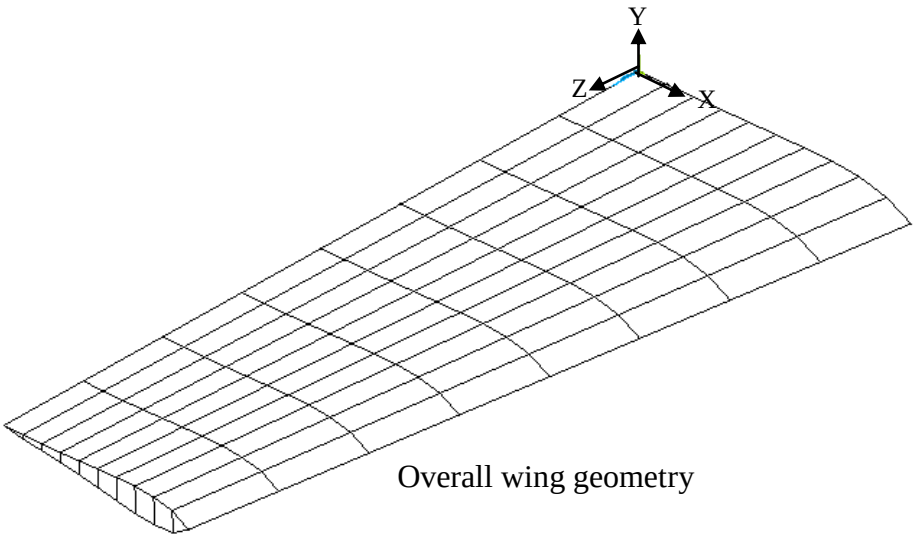


Overall wing geometry

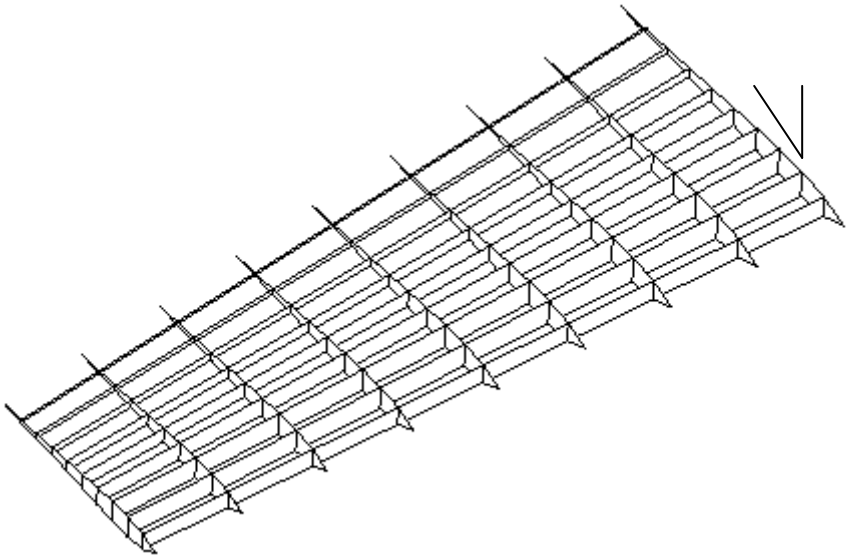

Stiffeners element
(spars and ribs)

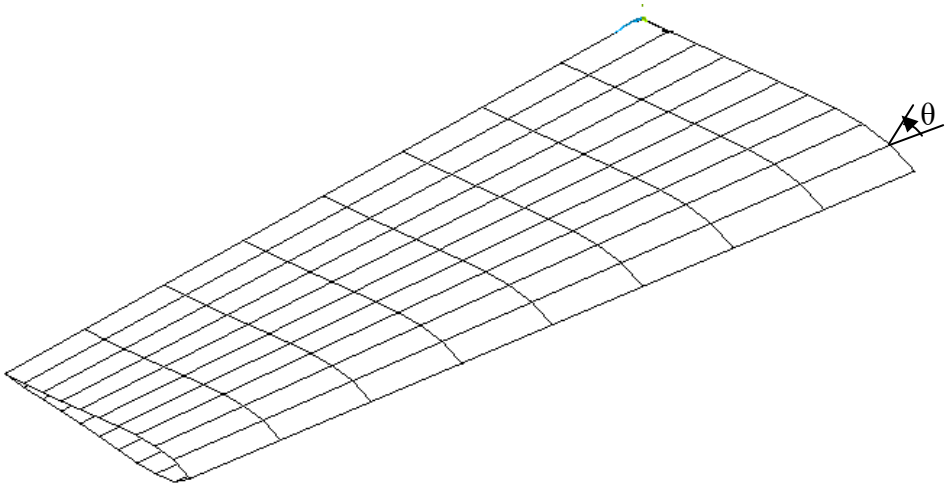


**Fig.(٣-٢)**: Wing finite elements model

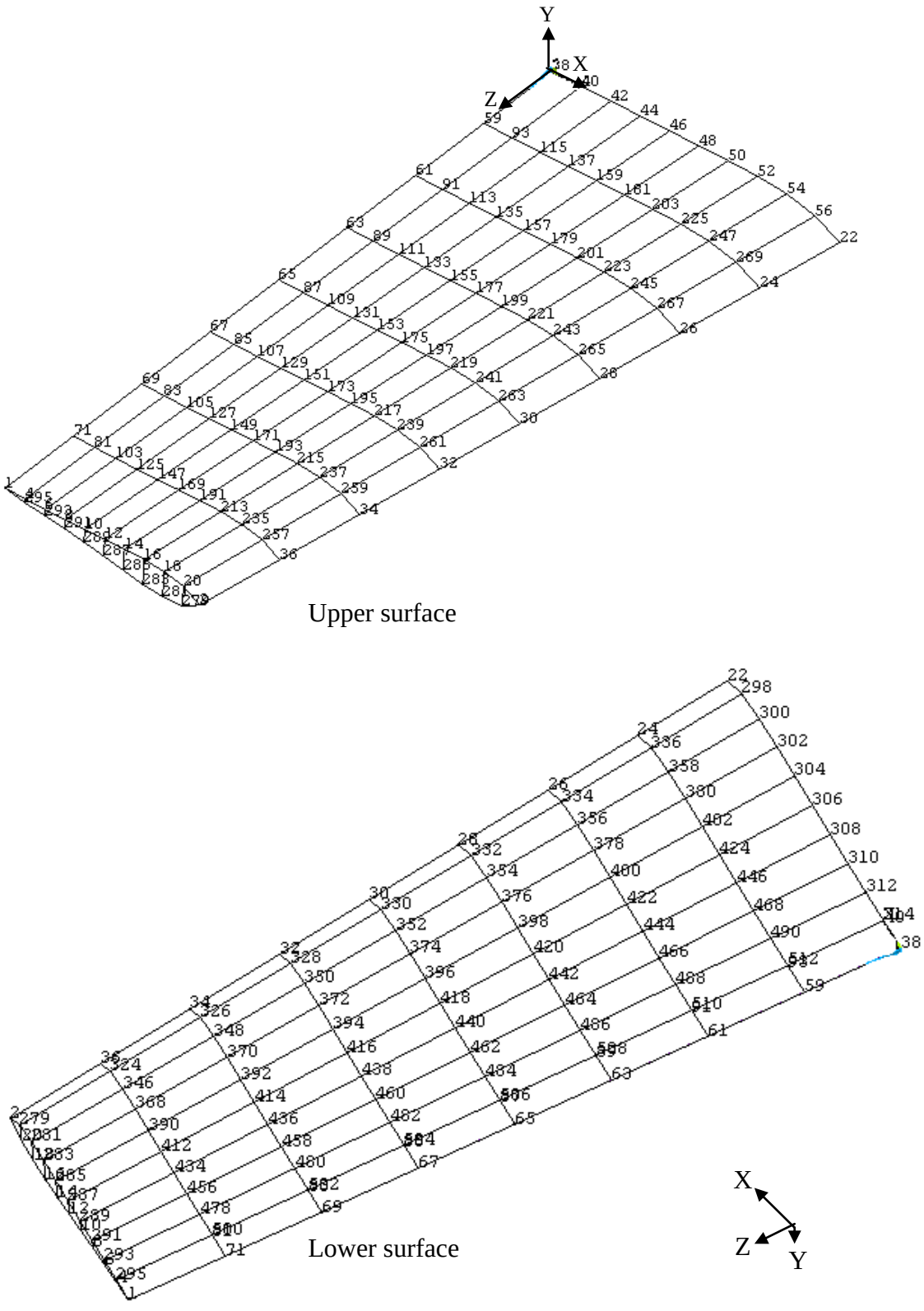


**Fig.(٣-٣)**: Locations and numbers
of the generated nodes of the wing finite element model.

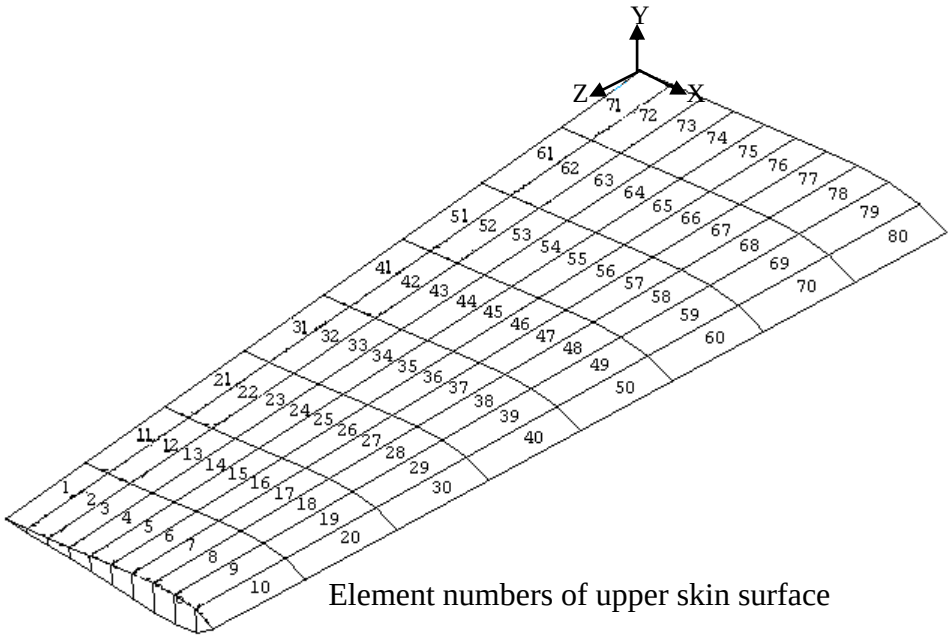


Element numbers of upper skin surface

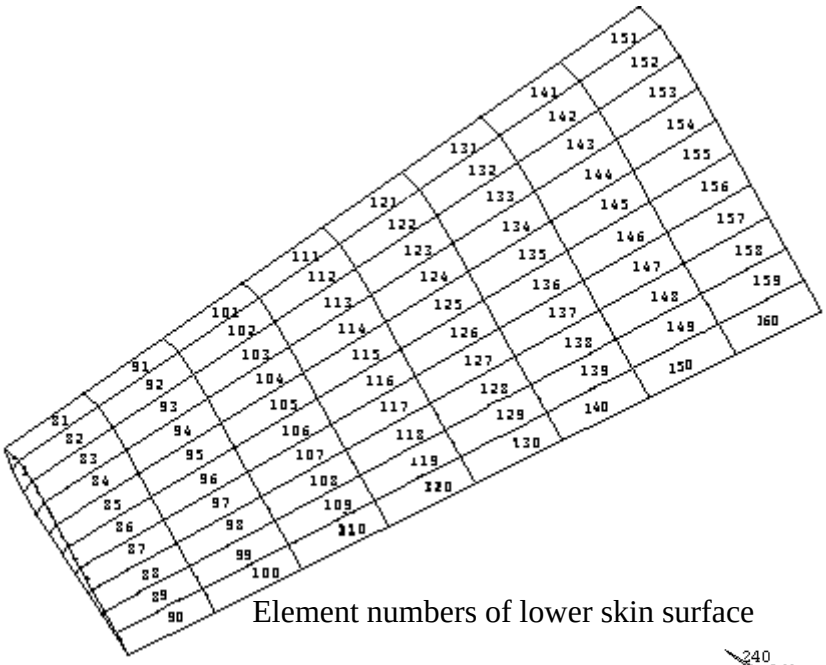

Element numbers of lower skin surface

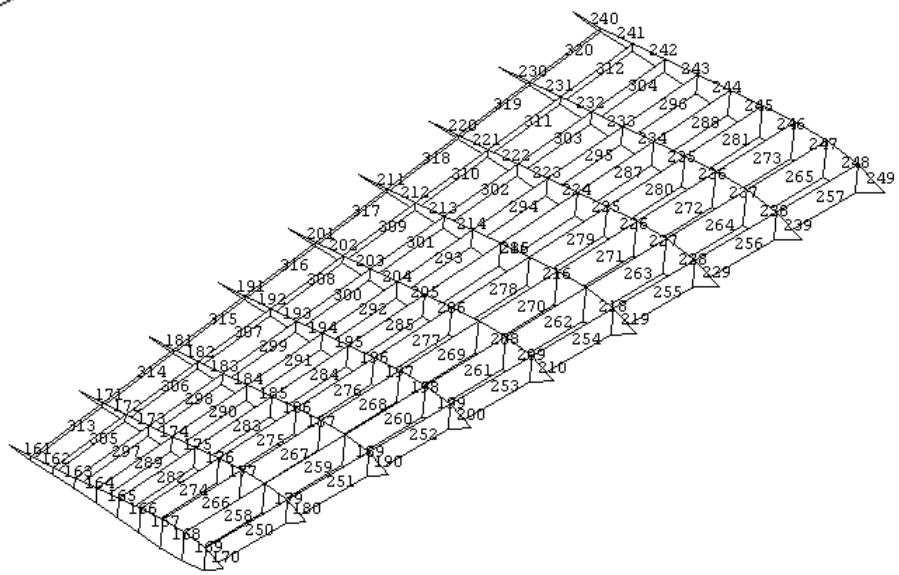

**Fig.(٣-٤)**: Locations and numbers of generated elements of wing.

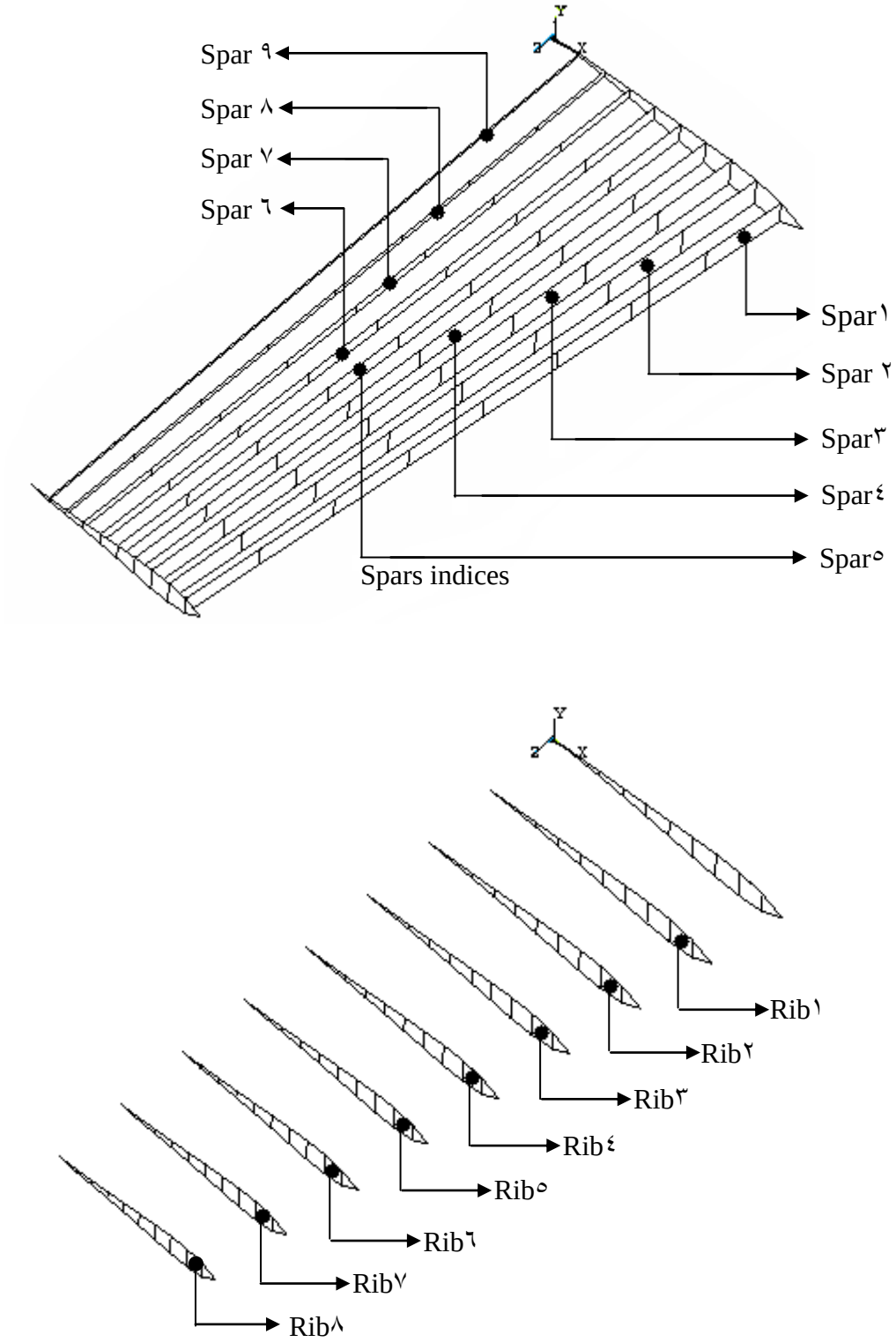


**Fig.(٣.٥.):** Presenting spars and ribs indices

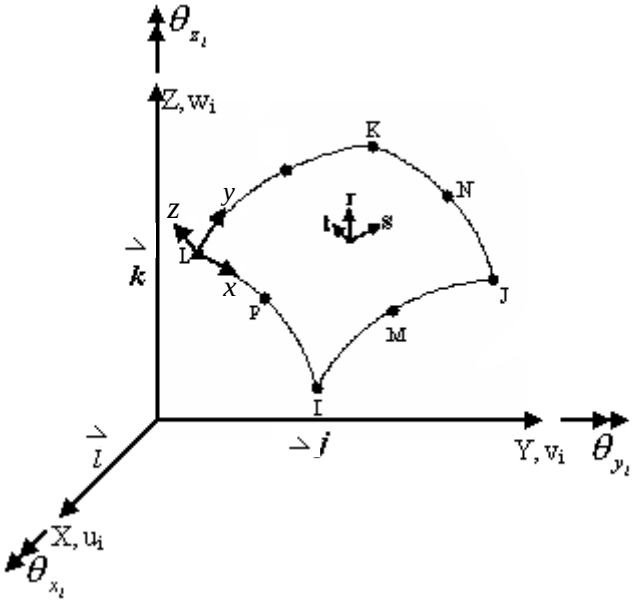


**Fig.(٣.٦):** Systems of Coordinates. (s,t,r) ,(*x,y,z*) , and (x,y,z) present Element, Nodal, and Global coordinates systems respectively.

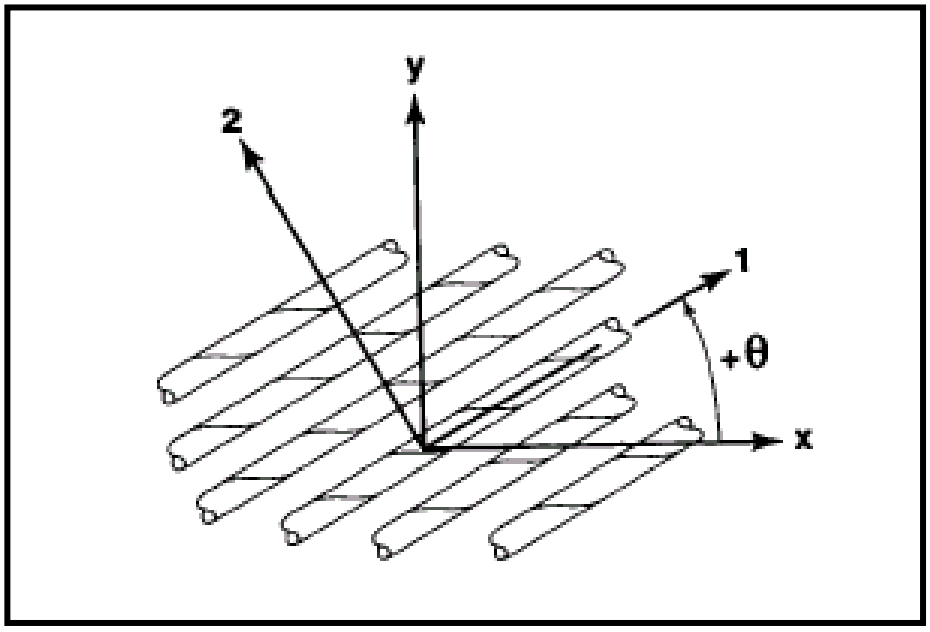


**Fig.(٣.٧)**: Positive rotation of principal material axes ١-٢ from x-y axes [١].

# *CHAPTER THREE*

## *THEORITICAL CONSIDERATION OF The SUGGESTED TECHNIQUE BY FEM*

## ٣.١ Introduction

includes the concerned theoretical concepts and application will be presented. The suggested technique is based upon the finite element method and iteration in order to predict the optimum design of laminated composite shells that used in the construction of aircraft structure subjected to certain load environments. The optimum design would basically includes:(١) the estimation of the optimum orientation angles of laminas,(٢) optimum thickness of composite laminas, in addition to the optimum stacking sequence of laminas through the shell thickness. All the above design parameters are estimated such that the induced stresses and strains maintained within the allowable values (safety factor) and the weight to be minimum. The suggested technique is examined to obtain the optimum design of a wing of a remotely guided aircraft structure shown in Figure (٣.١). The wing is constructed and fabricated by using laminated E-glass/epoxy composite laminas under the action of maximum aerodynamic loads that the wing may be subjected during flight duration.

The developments of suitable methods, more accurately, for analyzing various engineering structures are needed in order to investigate their behavior under different loading conditions. At present, the finite element method is the most powerful numerical technique, which offers approximate solution to realistic types of structures such as plates and shells. However, the term "finite elements" was first used by **Clough** in ١٩٦٠ (mentioned by ***Reddy,* ١٩٨٤**) [١٤]. In this method of analysis, a complex region defining a continuum is discretized into simple geometric shapes called "finite elements". The finite element analysis will be used in this work to obtain the displacements, stresses, natural frequencies, and the dynamic response as they are considered the main design criteria parameters.

In the present study, the ٨–noded isoparametric quadrilateral and ٦-noded triangular elements are used for discretization of layered shells. The derivations of the strain–displacement matrix [B], the elasticity matrix [E] and, as a result, the stiffness matrix of layered shells are presented. Also, the formulation of element mass matrix *[M]* and damping matrix *[C]* of layered shells are introduced. Finally, the numerical solutions are also presented in order to solve the basic structural modal, static, and the dynamic equilibrium equations.

## ٣.٢ Finite Element Modeling

A mesh is generated from the nodes of a "grid". The term grid is used in this work to define the set of node points, which put up the respective mesh.

Figure (٣.٢) shows the proposed finite element mesh model (wing), using isoparametric shell elements of triangular and quadrilateral shapes. *ANSYS* finite element program is used as a mathematical tool in the analysis of this model, according to the following steps:

**I.** The geometric domain of the wing aerodynamic shape can be considered as skin surface joining the root and tip airfoils, in addition to interior surfaces

representing the geometric domain of spars and ribs stiffeners. The boundary curves of each of root and tip airfoil, spar, and rib surfaces are defined through eight located points. The skin surface is created as a ruled surface between the root and tip airfoil curves, while any of the spars and ribs surfaces are created as edge surfaces within the boundaries of their corresponding curves.

**II.** The skin surface is discretized into eighty shell elements of quadrilateral shape, such that the mesh density is discretized into ten segments along airfoil sections and into eight segments along span direction as shown in Figure (٣.٢). Each of the spars surfaces are dicretized into eight shell elements of quadrilateral shape, while each of the rib surfaces is discretized into eight shell elements of quadrilateral shape and another two shell elements of triangular shape. Figure (٣.٣) shows the locations and numbers of the generated nodes while Figure (٣.٤) shows the locations and numbers of the generated elements.

At last, the three main parts of the wing model, skins, spars, and ribs are named under different indices for reorganization purposes. The longitudinal stiffeners (spars) are defined in different indices, they are: spar١, spar٢, spar٣ spar٤, spar٥, spar٦, spar٧, spar٨, and spar٩. The ribs are also named under rib١, rib٢, rib٣, rib٤, rib٥, rib٦, rib٧, and rib٨ as shown in Figure (٣.٥). **U**s and **L**s are the indices of the **u**pper and **l**ower **s**kins, respectively as shown in Figure (٣.٢).

## ٣.٣ Coordinates Systems

In general, there are three types of coordinates systems used to define any geometry such as the above wing model, these are: (١) Global coordinates system (٢) Nodal coordinates system and (٣) Element coordinates system.

The global coordinates system that is used in the above model is fixed Cartesian coordinates system as shown in Figure (٣.٦) and used in the wing model. All surfaces, nodes, and the elements of the model are drawn with respect to the global coordinates system. In addition, the directions of the

applied loads and the constraint degrees of freedom (boundary conditions) are defined along this coordinate system.

To describe the direction of the element degrees of freedom, a nodal coordinates system on each node must be used. The nodal coordinates system is located at each node as shown in Figure (٣.٦) such that the origin is located at the corresponding node position. Nodal $x$-axis is tangent to the curve joining this node and the subsequent nodes. Nodal $y$-axis is tangent to the element surface, its direction is perpendicular to that of nodal $x$-axis. The nodal $z$-axis is perpendicular to the $x-y$ plane, its direction is specified according to the orthogonal right-hand rule.

The element (local) coordinates system is located at each element as shown in Figure (٣.٦). This coordinates system is created on each element such that its origin is located at the element area center. The element ***s***-axis is tangent to the element surface at coordinate's origin along the direction of the curve joining first, fifth and second nodes for the quadrilateral element. The element ***t***-axis is tangent to the element surface at coordinate's origin; its direction is perpendicular to that of element ***s***-axis. The element ***r***-axis is perpendicular to the ***s-t*** plane; its direction is specified according to the orthogonal right-hand rule. Element coordinate system is used to describe the direction of the applied loads and directions of the stresses and strains that are induced in the elements.

## ٣.٤ Stress-Strain Relationship

The orthotropic stiffness properties are required to define the strain-stress relationship. The basic assumption of the composite material that can be treated in this work are, ***(Calcote, ١٩٦٩)*** [٥٤]:

١. The lamina is assumed to be:

- Macroscopically homogeneous.
- Linearly elastic.
- Macroscopically orthotropic.

- Initially stress-free.

٢. The fibers are assumed to be:

- Homogeneous.
- Linearly elastic.
- Isotropic.
- Regularly spaced
- Perfectly aligned

٣. The matrix material is assumed to be:

- Homogeneous.
- Linearly elastic.
- Isotropic.

Because of the linearly elastic behavior (assumption), the generalized Hooke's law is used for relating the stresses to strains. A material coordinate system is **x-y-z,** as shown in Figure (٣.٧) which introduced for the unidirectional reinforced lamina.

Hook's law gives the general anisotropic constitutive relation with respect to a material coordinate system ١–٢–٣ as follows ***(Jones, ١٩٧٥)*** [٣]:

$$\begin{Bmatrix} \sigma_1 \\ \sigma_2 \\ \sigma_3 \\ \tau_{23} \\ \tau_{13} \\ \tau_{12} \end{Bmatrix} = \begin{bmatrix} c_{11}\, c_{12}\, c_{13}\, c_{14}\, c_{15}\, c_{16} \\ c_{21}\, c_{22}\, c_{23}\, c_{24}\, c_{25}\, c_{26} \\ c_{31}\, c_{32}\, c_{33}\, c_{34}\, c_{35}\, c_{36} \\ c_{41}\, c_{42}\, c_{43}\, c_{44}\, c_{45}\, c_{46} \\ c_{51}\, c_{52}\, c_{53}\, c_{54}\, c_{55}\, c_{56} \\ c_{61}\, c_{62}\, c_{63}\, c_{64}\, c_{65}\, c_{66} \end{bmatrix} \begin{Bmatrix} \varepsilon_1 \\ \varepsilon_2 \\ \varepsilon_3 \\ \gamma_{23} \\ \gamma_{13} \\ \gamma_{12} \end{Bmatrix} \quad \ldots$$

***(٣.١)***

i.e., twenty-one independent material constants are used to describe the stress-strain relationship. For the composite lamina illustrated in Figure (٣.٧), there are two orthogonal planes of material property symmetry and the material is termed ***orthotropic***.

The stress–strain relations in coordinates aligned with principal material directions are given by, ***(Yunus and Khonke, ١٩٨٩)*** [٢٠]:

$$\begin{Bmatrix}\sigma_1\\ \sigma_2\\ \sigma_3\\ \tau_{23}\\ \tau_{13}\\ \tau_{12}\end{Bmatrix}=\begin{bmatrix}c_{11} & c_{12} & 0 & 0 & 0 & 0\\ c_{21} & c_{22} & 0 & 0 & 0 & 0\\ 0 & 0 & c_{33} & 0 & 0 & 0\\ 0 & 0 & 0 & c_{44} & 0 & 0\\ 0 & 0 & 0 & 0 & c_{55} & 0\\ 0 & 0 & 0 & 0 & 0 & c_{66}\end{bmatrix}\begin{Bmatrix}\varepsilon_1\\ \varepsilon_2\\ \varepsilon_3\\ \gamma_{23}\\ \gamma_{13}\\ \gamma_{12}\end{Bmatrix} \quad \dots$$

***(٣. ٣)*** or

$$\{\sigma\}=[\mathrm{E}]\{\varepsilon\} \quad \dots (٣. ٣)$$

where

$c_{١١} = \boldsymbol{A}\, E_{١,j}$ $\quad c_{٣٣} = E_{٣,j}\, \mathrm{B}$

$c_{١٢} = \boldsymbol{A}\nu_{12}\, E_{١,j}$ $\quad c_{٦٦} = G_{١٢,j}$ $\quad \dots (٣. ٤)$

$c_{٢٢} = \boldsymbol{A}\, E_{٢,j}$ $\quad c_{٤٤} = f\, G_{٢٣}$ $\quad c_{٥٥} = f\, G_{١٣}$

$\boldsymbol{A} = E_{٢,j} / (E_{٢,j} - \nu_{12,j} E_{١,j})$ , $\mathrm{B} = ١٠^{-٦}$

$١/f = ١.٢$, a derivation of the factor $f$ is illustrated in **Appendix-A**

To obtain the stress–strain relations for the lamina of arbitrary orientation, the transformation equations are used for expressing stresses in ***x-y-z*** coordinate system in terms of stresses in ١-٢-٣ coordinate system ***(Calcote, ١٩٦٩)*** [٥٤]:

$$\begin{Bmatrix}\sigma_x\\ \sigma_y\\ \sigma_z\\ \tau_{yz}\\ \tau_{xz}\\ \tau_{xy}\end{Bmatrix}=\begin{bmatrix} & & \\ & \mathrm{T_m} & \\ & & \end{bmatrix}^{-1}\begin{bmatrix} & & \\ & \mathrm{E} & \\ & & \end{bmatrix}\begin{bmatrix} & & \\ & \mathrm{T_m} & \\ & & \end{bmatrix}\begin{Bmatrix}\varepsilon_x\\ \varepsilon_y\\ \varepsilon_z\\ \gamma_{yz}\\ \gamma_{xz}\\ \gamma_{xy}\end{Bmatrix} \quad \dots$$

***(٣. ٥)***

where

$$T_m = \begin{bmatrix} c^2 & s^2 & 0 & sc & 0 & 0 \\ s^2 & c^2 & 0 & -sc & 0 & 0 \\ 0 & 0 & 1 & 0 & 0 & 0 \\ -2sc & 2sc & 0 & c^2-s^2 & 0 & 0 \\ 0 & 0 & 0 & 0 & c & -s \\ 0 & 0 & 0 & 0 & s & c \end{bmatrix} \quad \dots$$

***(٣.٦)*** in which, ***c = Cos θ***, ***s = Sin θ***, and $\theta$ is the fiber orientation angle in degrees.

Using the above transformations, the stress–strain relations for arbitrary lamina orientation can be written as:

$$\begin{Bmatrix} \sigma_x \\ \sigma_y \\ \sigma_z \\ \tau_{yz} \\ \tau_{xz} \\ \tau_{xy} \end{Bmatrix} = \begin{bmatrix} Q_{11} & Q_{12} & 0 & Q_{14} & 0 & 0 \\ Q_{21} & Q_{22} & 0 & Q_{24} & 0 & 0 \\ 0 & 0 & Q_{33} & 0 & 0 & 0 \\ 0 & 0 & 0 & 0 & Q_{55} & Q_{56} \\ 0 & 0 & 0 & 0 & Q_{65} & Q_{66} \\ Q_{41} & Q_{42} & 0 & Q_{44} & 0 & 0 \end{bmatrix} \begin{Bmatrix} \varepsilon_x \\ \varepsilon_y \\ \varepsilon_z \\ \gamma_{yz} \\ \gamma_{xz} \\ \gamma_{xy} \end{Bmatrix} \quad \dots$$

***(٣.٧)***

A generally orthotropic composite lamina is an orthotropic lamina in which the principal material axes are not aligned with the structural axes and the constitutive matrix (**Q)** is as defined above in Equation (٣.٧). All coefficients of the constitutive matrix are derived and listed in **Appendix-A.**

Finally, Poisson's ratio for orthotropic material is generally defined as ***(Calcote, ١٩٦٩)*** [٥٤]:

$$\upsilon_{ij} = -\frac{\varepsilon_j}{\varepsilon_i} \quad \dots (٣.٨)$$

where $\varepsilon_i$ is the strain produced by $\sigma_i$ and $\varepsilon_j$ is the corresponding lateral strain.

There are three reciprocal relations that must be satisfied for the general orthotropic material, these are ***(Calcote, ١٩٦٩)*** [٥٤]:

$$\frac{\upsilon_{ij}}{E_i} = \frac{\upsilon_{ji}}{E_j} \qquad i, j = ١, ٢, ٣ \qquad \ldots (٣.٩)$$

Then:

$$\frac{\upsilon_{12}}{E_1} = \frac{\upsilon_{21}}{E_2} \qquad \ldots$$

**(٣.١٠)**

$$\frac{\upsilon_{13}}{E_1} = \frac{\upsilon_{31}}{E_3} \qquad \ldots$$

**(٣.١١)**

$$\frac{\upsilon_{23}}{E_2} = \frac{\upsilon_{32}}{E_3} \qquad \ldots$$

**(٣.١٢)**

Then only nine independent elastic properties are needed for a full definition of the stress-strain relationship of the general orthotropic material. These nine independent stiffness properties are: $\upsilon_{١٢}$, $\upsilon_{٢٣}$, $\upsilon_{١٣}$, $E_١$, $E_٢$, $E_٣$, $G_{١٢}$, $G_{٢٣}$, and $G_{٣١}$ then the material which requires this number of stiffness properties for full definition of stress-strain relationship is called ***three-dimensional orthotropic material*.**

## ٣.٥ Element Parameters

A quadratic element of quadrilateral shape which consists of eight nodes, all of which are located on the element boundary, have been used to define the wing finite element model, while that of triangular shape consists of six nodes, all of which are located at the ends of the transverse stringers (ribs). These types of elements are used for plates and shells applications and for membrane and flexural load conditions ***(Yunus and Khonke, ١٩٨٩)*** [٢٠]. In this section, the parameters that are concerned with the selected elements are discussed. These parameters basically include the element properties and the element degrees of

freedom. The element properties have included the material properties of the composite in addition to the thickness of each element. The fiber orientation is defined uniformly through the element real constants. The shell is composed of N layers in its thickness direction (r). The formulation of such shell is based on three-dimensional elasticity theory. It is assumed that the normal to the middle-plane remain straight after deformation, but not necessarily normal to the middle-plane.

The displacement at any point within the element is written in terms of nodal translations and rotations (degenerated element) as:

$$\begin{Bmatrix} u \\ v \\ w \end{Bmatrix} = \sum_{i=1}^{n} N_i \begin{Bmatrix} u_i \\ v_i \\ w_i \end{Bmatrix} + \sum_{i=1}^{N} N_i \frac{rt_i}{2} \begin{bmatrix} a_i^u & b_i^u & c_i^u \\ a_i^v & b_i^v & c_i^v \\ a_i^w & b_i^w & c_i^w \end{bmatrix} \begin{Bmatrix} \theta_{xi} \\ \theta_{yi} \\ \theta_{zi} \end{Bmatrix} \quad \ldots$$

***(٣.١٣)***

Where, n is the number of element nodes

$N_i$= shape functions. They are illustrated in **Appendix-A**.

$u_i, v_i, w_i$ =global nodal displacements.

$\theta_{xi}, \theta_{yi}, \theta_{zi}$ =global nodal rotations.

$t_i$ = nodal thickness.

$r$ = natural coordinate along thickness direction but normal to the shell surface.

$a_i^u$, $a_i^v$, $a_i^w$ = direction cosines of *u*, *v*, and *w* with respect to the nodal coordinate system at node *i*.

The first row of transformation matrix represents the direction cosines of each of nodal coordinate axis with respect to the global x-axis. The second row of transformation matrix represents the direction cosines of each of nodal coordinate axis with respect to the global y-axis. The third row of transformation matrix represents the direction cosines of each of nodal coordinate axis with respect to the global z-axis.

It is obvious that, each node has six degrees of freedom, then the second order shell element is of (٤٨) degrees of freedom, while the second order triangular element is of (٣٦) degrees of freedom.

## ٣.٦ Derivation of Strain-Displacement Matrix

In this section, the strain-displacement relations are developed to explicitly express their dependence on the through-thickness coordinate. The integration through thickness can then carried out separately. Thus, a separate numerical integration rule can be used for each layer through the thickness of the element.

The strains are first written in terms of the global derivatives of displacements as:

$$\{\varepsilon\} = [H]\{E\} \quad \ldots$$

***(٣.١٤)*** where,

$$\{\varepsilon\} = \lfloor \varepsilon_x \quad \varepsilon_y \quad \varepsilon_z \quad \varepsilon_{xy} \quad \varepsilon_{yz} \quad \varepsilon_{xz} \rfloor^T \quad \ldots$$

***(٣.١٥)***
$$[H] = \begin{bmatrix} 1 & 0 & 0 & 0 & 0 & 0 & 0 & 0 & 0 \\ 0 & 0 & 0 & 0 & 1 & 0 & 0 & 0 & 0 \\ 0 & 0 & 0 & 0 & 0 & 0 & 0 & 0 & 1 \\ 0 & 1 & 0 & 1 & 0 & 0 & 0 & 0 & 0 \\ 0 & 0 & 0 & 0 & 0 & 1 & 0 & 1 & 0 \\ 0 & 0 & 1 & 0 & 0 & 0 & 1 & 0 & 0 \end{bmatrix}$$

$$\{E\} = \lfloor \lfloor E^u \rfloor \quad \lfloor E^v \rfloor \quad \lfloor E^w \rfloor \rfloor^T \quad \ldots$$

***(٣.١٦)***
$$\lfloor E^u \rfloor = \left\lfloor \frac{\partial u}{\partial x} \quad \frac{\partial u}{\partial y} \quad \frac{\partial u}{\partial z} \right\rfloor$$

***(٣.١٧)*** ...
$$\lfloor E^v \rfloor = \left\lfloor \frac{\partial v}{\partial x} \quad \frac{\partial v}{\partial y} \quad \frac{\partial v}{\partial z} \right\rfloor$$

$$\left\lfloor E^{w} \right\rfloor = \left\lfloor \frac{\partial w}{\partial x} \quad \frac{\partial w}{\partial y} \quad \frac{\partial w}{\partial z} \right\rfloor \qquad \text{...} \quad (٣.١٨)$$

... (٣.١٩)

The global Cartesian derivatives are related to the local coordinate as:

$$\{E\} = [\Gamma]\{e\} \qquad \text{...}$$

(٣.٢٠) where,

$$[\Gamma] = diag\left[ \ [J]^{-1} \quad [J]^{-1} \quad [J]^{-1} \right] \qquad \text{...}$$

$$(٣.٢١) \quad \{e\} = \left\lfloor \ \left\lfloor e^{u} \right\rfloor \ \left\lfloor e^{v} \right\rfloor \ \left\lfloor e^{w} \right\rfloor \ \right\rfloor^{T} \qquad \text{...}$$

(٣.٢٢)

$$\left\lfloor e^{u} \right\rfloor = \left\lfloor \frac{\partial u}{\partial s} \quad \frac{\partial u}{\partial t} \quad \frac{\partial u}{\partial r} \right\rfloor \qquad \text{...}$$

(٣.٢٣)

and $\left\lfloor e^{v} \right\rfloor$ and $\left\lfloor e^{w} \right\rfloor$ are defined similarly to $\left\lfloor e^{u} \right\rfloor$.

$[J]$ is the Jacobian matrix

***r, s,*** and ***t*** are the local coordinates system.

The local coordinate displacement derivatives are expressed in terms of the nodal displacements as:

$$\{e\} = [\eta_t] \ \{u_t\} + [\eta_\theta] \ [\tau_\theta] \ \{u_\theta\} \qquad \text{...}$$

(٣.٢٤)

where

$$[\eta_t] = diag[ \ [\eta_1] \quad [\eta_1] \quad [\eta_1] \ ] \qquad \text{...}$$

(٣.٢٥)

$$[\eta_\theta] = diag[ \ [\eta_2] \quad [\eta_2] \quad [\eta_2] \ ] \qquad \text{...}$$

(٣.٢٦)

$$[\eta_1]=\begin{bmatrix} \frac{\partial N_1}{\partial s} & \frac{\partial N_2}{\partial s} & \cdots & \frac{\partial N_8}{\partial s} \\ \frac{\partial N_1}{\partial t} & \frac{\partial N_2}{\partial t} & \cdots & \frac{\partial N_8}{\partial t} \\ 0 & 0 & \cdots & 0 \end{bmatrix} \quad \ldots$$

**(٣.٢٧)**

$$[\eta_2]=\frac{1}{2}\begin{bmatrix} rt_1\frac{\partial N_1}{\partial s} & rt_2\frac{\partial N_2}{\partial s} & \cdots & rt_8\frac{\partial N_8}{\partial s} \\ rt_1\frac{\partial N_1}{\partial t} & rt_2\frac{\partial N_2}{\partial t} & \cdots & rt_8\frac{\partial N_8}{\partial t} \\ t_1N_1 & t_2N_2 & \cdots & t_8N_8 \end{bmatrix} \quad \ldots$$

**(٣.٢٨)**

$$\{u_t\}=\lfloor \lfloor u_t^u \rfloor \ \lfloor u_t^v \rfloor \ \lfloor u_t^w \rfloor \rfloor^T \quad \ldots$$

**(٣.٢٩)**

$$\lfloor u_t^u \rfloor=\lfloor u_1 \ \ u_2 \ \ \cdots \ \ u_8 \rfloor \quad \ldots$$

**(٣.٣٠)** $\lfloor u_t^v \rfloor$ and $\lfloor u_t^w \rfloor$ are defined similarly,

$$\{u_\theta\}=\lfloor \theta_{x1} \ \ \theta_{y1} \ \ \theta_{z1} \ \ \cdots \ \ \theta_{x8} \ \ \theta_{y8} \ \ \theta_{z8} \rfloor \quad \ldots$$

**(٣.٣١)**

$$[\eta_\theta]=\begin{bmatrix} [\tau_u] \\ [\tau_v] \\ [\tau_w] \end{bmatrix} \quad \ldots$$

**(٣.٣٢)**

$$[\tau_u]=\begin{bmatrix} a_1^u & b_1^u & c_1^u & 0 & 0 & 0 & \cdots & 0 & 0 & 0 \\ 0 & 0 & 0 & a_2^u & b_2^u & c_2^u & \cdots & 0 & 0 & 0 \\ \cdots & \cdots & \cdots & \cdots & \cdots & \cdots & \cdots & 0 & 0 & 0 \\ 0 & 0 & 0 & 0 & 0 & 0 & \cdots & a_8^u & b_8^u & c_8^u \end{bmatrix} \quad \ldots$$

**(٣.٣٣)**

$[\tau_v]$and $[\tau_w]$ are defined similarly to$[\tau_u]$. The matrix equation (٣.٢٤) is now partitioned and the top partition of $\{e^u\}$ can be written as:

$$\{e^u\}=[\eta_1]\ \{u_t^u\}+[\eta_2]\ [\tau_u]\ \{u_\theta\} \quad \ldots$$

**(٣.٣٤)**

The terms in matrix$[\eta_2]$contain the variable *r*. Equation (٣.٣٤) is expressed and written to explicitly express its dependency on r as, ***(Yunus and Khonke, ١٩٨٩)***[٢٠]:

$$\{e^u\}=[\eta_1]\ \{u_t^u\}+\left(r[\eta_{21}]+[\eta_{22}]\right)[\tau_u]\ \{u_\theta\} \quad \ldots \textbf{(٣.٣٥)}$$

where,

$$[\eta_{21}]=\frac{1}{2}\begin{bmatrix} t_1\dfrac{\partial N_1}{\partial s} & t_2\dfrac{\partial N_2}{\partial s} & \cdots & t_8\dfrac{\partial N_8}{\partial s} \\ t_1\dfrac{\partial N_1}{\partial t} & t_2\dfrac{\partial N_2}{\partial t} & \cdots & t_8\dfrac{\partial N_8}{\partial t} \\ 0 & 0 & \cdots & 0 \end{bmatrix} \quad \ldots$$

**(٣.٣٦)**

$$[\eta_{22}]=\frac{1}{2}\begin{bmatrix} 0 & 0 & \cdots & 0 \\ 0 & 0 & \cdots & 0 \\ t_1N_1 & t_2N_2 & \cdots & t_8N_8 \end{bmatrix}. \quad \ldots$$

**(٣.٣٧)**

Equation (٣.٣٥) can be rearranged as:

$$\{e^u\} = [\eta_1]\ \{u_t^u\} + \left(r\left[\eta_{21}^u\right] + \left[\eta_{22}^u\right]\right)\ \{u_\theta\} \quad \ldots (٣.٣٨)$$

where,

$$\left[\eta_{21}^u\right] = [\eta_{21}]\ [\tau_u] \quad \ldots (٣.٣٩)$$

and,

$$\left[\eta_{22}^u\right] = [\eta_{22}]\ [\tau_u]. \quad \ldots (٣.٤٠)$$

The strain-displacement relationship can now be written with its dependence explicitly expressed as:

$$\{\varepsilon\} = [B]\{u_i\} \quad \ldots (٣.٤١)$$

where,

$$[B] = [B_0] + r\ [B_1] + r^2[B_2] \quad \ldots (٣.٤٢)$$

$$[B_0] = [H]\begin{bmatrix} [b_0^u] \\ [b_0^v] \\ [b_0^w] \end{bmatrix} \quad \ldots (٣.٤٣)$$

$$[B_1] = [H]\begin{bmatrix}[b_1^u]\\ [b_1^v]\\ [b_1^w]\end{bmatrix} \quad \ldots$$

**(٣.٤٤)**

$$[B_2] = [H]\begin{bmatrix}[b_2^u]\\ [b_2^v]\\ [b_2^w]\end{bmatrix} \quad \ldots \textbf{(٣.٤٥)}$$

$$[b_0^u] = [J_a]^{-1}\begin{bmatrix}[\eta_1] & [0] & [0] & [\eta_{22}^u]\end{bmatrix} \quad \ldots$$

**(٣.٤٦)**

$$[b_1^u] = [J_v]^{-1}\begin{bmatrix}[\eta_1] & [0] & [0] & [\eta_{22}^u]\end{bmatrix} + [J_a]^{-1}\begin{bmatrix}[0] & [0] & [0] & [\eta_{21}^u]\end{bmatrix} \quad \ldots$$

**(٣.٤٧)**

and,

$$[b_2^u] = [J_v]^{-1}\begin{bmatrix}[0] & [0] & [0] & [\eta_{21}^u]\end{bmatrix} \quad \ldots$$

**(٣.٤٨)**

All elements of the strain–displacement matrix, $[B]$, are derived in terms of the shape function derivatives and the Jacobian matrix in **Appendix-B**.

## ٣.٧ Derivation of Element Stiffness-Matrix

In general, the basic concept of the finite elements method is to discretize the continuum into a definite numbers of small elements connected together at their common nodes. The strain-displacement matrix,$[B]$, as shown previously is given by:

$$\{\varepsilon\} = [B]\{u_i\}$$

The total solution domain is discretized into a number of elements **(NE)** [sub–domain] such that:

$$\pi(u) = \sum_{e=1}^{NE} \pi^e(u) \quad \ldots$$

**(٣.٤٩)**

where, $\pi$ and $\pi^e$ are the potential energies of the total solution domain and the sub–domain, respectively. The potential energy for an element, **e**, can be expressed in terms of the internal strain energy, SE, and external work done, **WF**, generally, such that:

$$\pi^e(u) = SE - WF \quad \ldots$$

**(٣.٥٠)**

in which (u) is the vector of nodal degrees of freedom of an element.

The internal strain energy of a linearly elastic body is given by:

$$SE = \frac{1}{2}\int_V \varepsilon^T \sigma \ dv \quad \ldots$$

**(٣.٥١)**

where the integration is over the volume of the element.

By substitution of Equations (٣.٣) and (٣.٤١) into Equation (٤.٥١), then:

$$SE = \frac{1}{2}\{u\}^{eT} \int_V [B]^T [E][B] \ dV \ \{u\} \quad \ldots$$

**(٣.٥٢)**

The external work done by uniformly distributed load is given by:

$$W_f = \int_V \{u\} \lfloor P \rfloor \ dV \quad \text{(If } p \text{ per unit volume is body force).} \quad \ldots$$

***(٣.٥٣)*** But, the displacement vector **{u}** can also be defined as:

$$\{u\} = [N]\{u_i\}^e \quad \ldots$$

**(٣.٥٤)**

Also, by substitution of Equation (٤.٥٤) in Equation (٤.٥٣) then:

$$W_f = \int_V \{u\}^{eT} [N]^T \lfloor \mathrm{P} \rfloor \mathrm{dV} \quad \ldots$$

$$\textbf{(٣.٥٥)} \quad \pi^e(\mathrm{u}) = \frac{1}{2}\{\mathrm{u}\}^{e\mathrm{T}} \int_V [\mathrm{B}]^T [\mathrm{E}][\mathrm{B}]\, dV\ \{u\}^e - \int_V \{\mathrm{u}\}^{e\mathrm{T}} [N]^{\mathrm{T}} \lfloor \mathrm{P} \rfloor\ dV$$

**... (٣.٥٦)**

To obtain the Equilibrium State of the element, the potential energy must be minimized with respect to the nodal displacements as follows:

$\{\frac{\partial \pi}{\partial u^e}\} = \{0\}$ with respect to one element.

**... (٣.٥٧)**

By substitution of Equation (٣.٥٦) in Equation (٣.٥٧) and carrying out the partial differentiation, then:

$$\{\frac{\partial \pi}{\partial u^e}\} = \int_V [\mathrm{B}]^T [\mathrm{E}][\mathrm{B}]\, dV\ \{u\}^e - \int_V [N]^{\mathrm{T}} \lfloor \mathrm{P} \rfloor\ dV = \{0\} \quad \textbf{... (٣.٥٨)}$$

or

$$[k]^e\{u\}^e - [F]^e = \{0\} \quad \ldots$$

**(٣.٥٩)**

where,

$$[k]^e = \int_V [\mathrm{B}]^T [\mathrm{E}][\mathrm{B}]\, dV = \int_{-1}^{1}\int_{-1}^{1}\int_{-1}^{1} [\mathrm{B}]^T [\mathrm{E}][\mathrm{B}] \det\ [J]\ dr\ ds\ dt \quad \ldots$$

**(٣.٦٠)**

in which,

$[K]^e$: is the element stiffness matrix,

$[F]^e$: is the element external applied force vector,

$|J|$: is the determinant of the Jacobian matrix.

For layered element, equation **(٣.٦٠)** can be written as:

$$[K]^e = \int_{-1}^{1}\int_{-1}^{1}\sum_{j=1}^{N_1}\int_{r_j^{bt}}^{r_j^{tp}} [\mathrm{B}]^T [\mathrm{E}]_j [\mathrm{B}]\ dr \det\ [J]\ ds\ dt \qquad \ldots (٣.٦١)$$

where,

$N_١$ = number of layers.

$r_j^{tp}$ and $r_j^{bt}$ =coordinates of the top and bottom of the layer j, respectively.

The determinant of Jacobian matrix depends on the thickness variable, *r*, for curved shell. This dependence can be explicitly written in the form:

$$\Delta = \Delta_a\left(1 + r\frac{\Delta_v}{\Delta_a}\right) \qquad \ldots (٣.٦٢)$$

where,

$$\Delta^2 = \det[J] \qquad \ldots (٣.٦٣)$$

$$\Delta_a = \frac{1}{2}\left(\Delta_t + \Delta_b\right) \qquad \ldots (٣.٦٤)$$

$$\Delta_v = \frac{1}{2}\left(\Delta_t - \Delta_b\right) \qquad \ldots (٣.٦٥)$$

$$\Delta_t = \Delta\big|_{r=1.0} \quad \ldots$$

$$\Delta_b = \Delta\big|_{r=-1.0} \quad \ldots \quad (٣.٦٦)$$

$$(٣.٦٧)$$

Combining the definition of *[B]* and *det [J]* given in Equations (٣.٤١) and (٣.٦٢), respectively, into Equation (٣.٦١) leads to the element stiffness matrix as:

$$[K_1] = \int_{-1}^{1}\int_{-1}^{1} ( [B_0]^T [E_0] [B_0] + [B_0]^T [E_1] [B_1] + [B_1]^T [E_1] [B_0] +$$

$$[B_0]^T [E_2] [B_2] + [B_2]^T [E_2] [B_0] + [B_2]^T [E_3] [B_1] + [B_1]^T [E_3] [B_2] +$$

$$[B_2]^T [E_4] [B_2] ) ds\ dt \quad . \quad \ldots (٣.٦٨)$$

where,

$$[E_0] = \sum_{j=1}^{N_1} \int_{r_j^{bt}}^{r_j^{tp}} \left(1 + r\frac{\Delta_v}{\Delta_a}\right)^2 [T_m]_j^T [E]_j [T_m]_j \, dr \quad \ldots$$

$$(٣.٦٩)$$

$$[E_1] = \sum_{j=1}^{N_1} \int_{r_j^{bt}}^{r_j^{tp}} r \left(1 + r\frac{\Delta_v}{\Delta_a}\right)^2 [T_m]_j^T [E]_j [T_m]_j \, dr \quad \ldots (٣.٧٠)$$

$$[E_2] = \sum_{j=1}^{N_1} \int_{r_j^{bt}}^{r_j^{tp}} r^2 \left(1 + r\frac{\Delta_v}{\Delta_a}\right)^2 [T_m]_j^T [E]_j [T_m]_j \, dr \quad \ldots$$

$$(٣.٧١)$$

$$[E_3] = \sum_{j=1}^{N_1} \int_{r_j^{bt}}^{r_j^{tp}} r^3 \left(1 + r\frac{\Delta_v}{\Delta_a}\right)^2 [T_m]_j^T [E]_j [T_m]_j \, dr \quad \ldots (٣.٧٢)$$

$$[E_4] = \sum_{j=1}^{N_1} \int_{r_j^{bt}}^{r_j^{tp}} r^4 \left(1 + r\frac{\Delta_v}{\Delta_a}\right)^2 [T_m]_j^T [E]_j [T_m]_j \, dr \quad \ldots (٣.٧٣)$$

It is noted that the present formulation requires an additional set of integrations for the material effect through thickness to obtain the matrices $[E_0]$, $[E_1]$, $[E_2]$, $[E_3]$, and $[E_4]$, respectively. These integrations, however, are relatively simple as they do not involve the shape functions. In addition, the present formulation allows the direct input of matrices that reflect the integrated effects of the material properties through the thickness ***(Yunus and Khonke, ١٩٨٩)***[٢٠].

## ٣.٨ Derivation of Element Mass- Matrix

When the shape functions used for the derivation of the mass matrix are identical to those used in formulating the element stiffness matrix; matrix **[M]** is called the consistent mass matrix. This matrix was first derived by **Archer** in ١٩٦٣ ***(Hyder, ٢٠٠٠)***[٦٤].

To derive the consistent mass matrix, one can consider the kinetic energy of the total solution domain discretized into number of elements **(NE**) such that:

$$TI(\dot{u}) = \sum_{e=1}^{NE} TI^{e}(\dot{u}) \quad \ldots$$

***(٣.٧٤)***

where **TI** and **TI$^{e}$** are the kinetic energies of the total solution domain and the sub–domain respectively. The kinetic energy of the element can be expressed as:

$$TI^{e} = \frac{1}{2}\int_{V} \{\dot{u}\}^{T}[m]\{\dot{u}\}\ dV \quad \ldots$$

***(٣.٧٥)***

The velocity vector within an element is related such that:

$$\{\dot{u}\} = \sum_{i=1}^{n} N_i\{\dot{u}_i\}, \quad \text{n (number of nodes)} \quad \ldots (٣.٧٦)$$

By substituting Equation (٣.٧٦) into Equation (٣.٧٥), then:

$$TI^{e} = \frac{1}{2}\sum_{i=1}^{n}\{\dot{u}_i\}^T\left(\int_V N_i{}^T[m]\,N_i\,dV\right)\{\dot{u}_i\} \quad \ldots$$

***(٣.٧٧)*** or in a matrix form:

$$TI^{e} = \frac{1}{2}\{\dot{u}\}^T\int_V [N]^T[m][N]dV\{\dot{u}\} = \frac{1}{2}\{\dot{u}\}^T[M]^e\{\dot{u}\} \quad \ldots (٣.٧٨)$$

Thus, the mass matrix of the presented curved shell element is written as: ***(Yunus and Khonke, ١٩٨٩)***[٣٠]:

$$[M_1] = diag\ \ [[M_0]\ \ [M_0]\ \ \ [M_0]\ \ [0]]$$

where

$$[M_0] = \int_V \sum_{j=1}^{N_1}\rho_j\{N\}\{N\}^T dV \quad \ldots$$

***(٣.٧٩)***

where, $\rho_j$ is density of layer j. $\{N\}$is a vector of the shape functions for inplane motions involving only the nodal translations which are functions of ***s*** and ***t*** only. $[0]$ is a null matrix of size ٢٤*٢٤. Equation (٣.٧٩) can be written in

an expanded form as:

$$[M_0] = \int_{-1}^{1}\int_{-1}^{1}\sum_{j=1}^{N_1}\rho\ \int_{r_j^{bt}}^{r_j^{tp}}\det[J]dr\ \ \{N\}\ \{N\}^T ds\ dt \quad \ldots$$

***(٣.٨٠)*** Using equation (٣.٦٢) in equation (٣.٨٠) above, then

$$[M_0] = \int_{-1}^{1}\int_{-1}^{1}\Delta_a^2\sum_{j=1}^{N_1}\rho_j\ \int_{r_j^{bt}}^{r_j^{tp}}\left(1+r\frac{\Delta_v}{\Delta_a}\right)^2\det[J]dr\ \ \{N\}\ \{N\}^T ds\ dt \quad \ldots (٣.٨١)$$

Defining a weighted average density, $\rho_a$, as:

$$\rho_a = \frac{1}{2}\sum_{j=1}^{N_1}\int_{r_j^{bt}}^{r_j^{tp}}\rho_j\left(1+r\frac{\Delta_v}{\Delta_a}\right)\,dr \quad \ldots (٣.٨٢)$$

then

$$[M_0] = \rho_a\int_{-1}^{1}\int_{-1}^{1}\ \Delta_a^2\{N\}\ \{N\}^T ds\ dt \quad \ldots (٣.٨٣)$$

Only a ٢*٢ spatial Gauss integration scheme is required. All values of the mass matrix are derived in **Appendix-B**.

## ٣.٩ Free Vibration Analysis

The free vibration analysis is the first step in the dynamic analysis, the natural frequency, **ω**, of the structure is important to give an idea about the oscillation of the system with time, stiffness to weight ratios for different modes of oscillations, and to determine the natural period **(T)** of vibration which represents the time for which the vibration repeats itself, as:

$$T = ٢\pi/\omega \quad \ldots (٣.٨٤)$$

Therefore; the free vibration (modal analysis) is used to determine the basic vaibrational characteristic of structures, which are the natural frequencies and mode shapes (normal modes). Natural frequencies and mode shapes are important parameters in the design of a structure under dynamic loading conditions. They are also needed if it is required doing dynamic analysis such as frequency, transient and spectrum analysis. To determine the natural frequencies of a structure, the governing differential equation of motion for the free vibration problem (no external applied loads) and undamped case is assumed in general, ***(Weaver*** and ***Johnston, ١٩٨٧)*** [٥٨]:

$$[M_0]\{\ddot{X}\} + [K_1]\{X\} = \{0\} \quad \ldots (٣.٨٥)$$

Assuming harmonic motion that is:

$$\{X_i\} = \{\phi_i\} \sin \omega_i t \quad ; \quad i = 1,2,...k \quad \ldots$$

**(٣.٨٦)** where:

k : the number of D.O.F. of the system

$\{\phi_i\}$ : the mode shape vector for the **i**$^{th}$ mode of vibration, and

$\omega_i$ : the angular frequency of mode **i**.

Differentiating Equation (٣.٨٦) twice with respect to time yields:

$$\{\ddot{X}_i\} = -\omega_i^2\{\phi_i\}\sin\omega_i t \quad \ldots$$

***(٣.٨٧)*** Then, substituting Equations (٣.٨٦) and (٣.٨٧) into Equation (٣.٨٥) yields, after canceling the term (**sin $\omega_i$t** ):

$$([K_1] - \omega_i^2[M_0])\{\phi_i\} = \{0\} \quad \ldots \textbf{(٣.٨٨)}$$

Equation (٣.٨٨) has the form of the algebraic eigenvalue problem (**K$\phi$=$\lambda$M$\phi$**). From the theory of homogeneous equations, nontrivial solutions exist only if the determinant of the coefficient matrix is equal to zero. Thus:

$$\left|[K_1] - \omega_i^2[M_0]\right| = \{0\} \quad \ldots$$

***(٣.٨٩)*** Expansion of the determinant yields a polynomial of order NR called characteristic equation. The NR roots of this polynomial **($\omega_i^2$)** are the characteristic values or the eigenvalues. The cyclic natural frequency ($f_i$) is then obtained from:

$$f_i = \omega_i / 2\pi \quad \ldots\textbf{(٣.٩٠)}$$

Substitution of these roots (one at each time) into the homogeneous equation, (٣.٨٩), produces the characteristic vectors or the eigenvectors **{$\phi_i$}** within arbitrary constants. A number of solution algorithms have been developed for the solution of the eigenvalue problem. However, the inverse iteration method will be presented and used in this work.

## ٣.٩.١ Inverse Iteration Method

This technique is very effective in calculating the smallest eigenvalue and the corresponding eigenvector, which are the most important eigenpair in structural dynamics.

The basic steps for solving the eigenvalue problem of the form (**D $\phi$= $\lambda$ I$\phi$**) using the inverse iteration method are ***(Hussain et al., ٢٠٠٢)*** [٦٥]:

١. Computing the dynamic matrix **[D]** as follows :

$$[D] = [M_0]^{-1}[K_1] \quad \ldots \textbf{(٣.٩١)}$$

٢. Assuming initial trial vector **{ϕ١}** almost with all terms equal ١.٠.

٣. Substituting the vector, **{ϕ١}**, in the following equation:

$$( [D] - (1/\lambda) [I] ) \{ \phi^{(1)} \} = 0$$

**...(٣.٩٢)**

٤. Approximate value of **(١/λ)** is obtained by dividing the first element of the column matrix **[D]** $\{\phi^{(1)}\}$ by $\phi_1^{(1)}$, that is:

$$\lambda^1 = \frac{(first\ row\ of\ D) \times \left\{ \phi^{1\,(1)} \right\}}{\phi^{(1)}_1} \quad \ldots$$

**(٣.٩٣)**

where $\phi^{(1)}_1$ is the first element of the matrix $\{\phi^{(1)}\}$.

**٥.** The second approximate value of the characteristic vector $\{\phi^{(2)}\}$ is obtained by:

$$\left\{ \phi_{appr.} \right\} = \frac{[D]\left\{ \phi^{(1)} \right\}}{(1/\lambda)} \quad \ldots (٣.٩٤)$$

These steps can be continued until the errors become sufficiently small where the used error criterion is the absolute difference, such that:

$$\varepsilon_r = \sum |\phi_i - \phi_{i-1}| \quad \ldots$$

***(٣.٩٥)*** For the composite wing structure, modal analysis is done to predict the relationships between the natural frequencies and corresponding mode shapes with the orientation angles of composite laminas. For this purpose, the element properties are created such that the orientation angles of a single unidirectional fibers lamina are assigned to ten iterated angles (٠, ١٠, ٢٠... ٩٠).

## ٣.٩.٢ Optimum Orientation Angle

The superiority of any structure mainly depends on the strength and properties of the materials that are used in the structure. It is well known that as each composite is a blend of materials with unique direction-dependent materials properties, the strength of composite lamina basically depends on the orientation of the fiber-reinforcement in each layer and the lay-up sequence of a laminate which play an essential role in obtaining its most attractive features of high stiffness/ strength-to-weight ratio. Therefore, in this section, the aim is to find the orientation angles which correspond to the stacking maximum ($m^{th}$) natural frequency. Because of the testing of modal analysis at different value of orientation (٠, ١٠, ٢٠ …٩٠), the calculus of variation principles can be possible to apply to find the corresponding frequency at a certain orientation. RAYLEIGH-RITZ method can be applied herein to estimate the optimum orientation as shown in **Appendix-C**.

## ٣.١٠ Static Analysis

A static analysis calculates the effects of steady loading conditions on a structure, while ignoring inertia and damping effects, such as those caused by time-varying loads. The static analysis is governed by the following equilibrium equation:

$$[K]\cdot\{u\}=\{F\} \quad \ldots$$

**(٣.٩٦)**

where, [K] : the assembled stiffness matrix.

The above equilibrium equation is solved by Newton-Raphson method to obtain the unknowns {u} vector. The results of the static analysis would be including the following items:

١. The element stresses along element coordinates axis.

٢. The linear and angular displacements of the nodes $(u, v, w, \theta_{xi}, \theta_{yi}, \theta_{zi})$ along global coordinate axis.

٣. The element criteria stress index $\Psi$, according to ***Tsi-Wu*** (quadratic) yield criteria ***(Abdul-Raheem, ٢٠٠٠)*** [٧], which is used for orthotropic materials and cited in **Appendix-C**.

The wing structure is subjected to static nodal forces that are shown in **Appendix-A**. Preliminary design of this structure against those loads is assumed, in which a three of the E-glass/epoxy laminas is of same assumed thickness of (٣ mm), and oriented by the optimum angles that correspond to the first five mode shapes for each of spars, ribs, and skins. Composite and stiffener laminas are arranged through the thickness in a scheme such that, honeycomb stiffener lamina is surrounded from each side with three of composite laminas.

## ٣.١٠.١ Optimum Layer Thickness and Its Arrangements

Since the use of composite materials became widespread in aerospace, defense and automotive applications three or four decades ago, laminated structural elements (such as plates and shells) made of layers of fiber-reinforced composite materials (high stiffness and strength-to-weight ratios) have been most often adopted in these applications. Thicknesses of the layers of a laminate are available as structural variables in the case of fiber composite structures.

Therefore, an important issue is that, how a laminated composite structural element can be designed by choosing the best layers thicknesses, so that the most efficient performance can be achieved together with the fulfillment of the required design specification. A great deal of this section is to obtain the

optimum thickness and arrangement for each layer of composites. The allowable limit of criteria stress index depends upon the required safety factor, which is further depending upon the function of the structure. The safety factor is defined as ***(Abdul-Raheem, ٢٠٠٠)*** [٧]:

$$S.F = 1/\Psi \quad \ldots (٣.٩٧)$$

where, ***S.F*** is the safety factor and $\Psi$ is the failure index.

Due to the applied load on the structure, it is subjected to general stress state in which the shell elements be under both membrane and flexure stress condition. Membrane stresses are uniformly distributed through shell thickness, while flexure stresses are distributed through shell section in a manner such that, they are maximum at the outer or inner surfaces of the shell elements ***(Hate, ٢٠٠٣)*** [٥٥]. Then it is preferable to arrange the laminas through shell section according to the behavior of the structure if constructed of a single unit of them (each considered separately) under the action of applied load such that the laminas of lower induced stresses are located near outer or inner surfaces of shell section, then a priority in the thickness fraction (with respect to composite total thickness) is given to that laminas. Total thickness of composite is the summation of that of laminas, and then optimum value of each one of them is specified according to the following steps:

I- In order to recognize the behaviors of the structure if constructed from only a single of the three laminas, static analysis is performed to the structure (for each lamina) under the action of the applied load.

II- From results of static analysis, ***Tsi-Wu*** failure criteria indices are extracted for each lamina, then laminas are arranged through shell section such that the laminas of minimum indices are located near outer or inner shell surface, and that of maximum indices are located near honeycomb stiffeners (spars and ribs) lamina which is placed at intermediate plane of the shell so that the optimized

fraction of a layer thickness is obtained from the division of its failure index to the summation of layers failure indices as follows:

$\beta_i=(1/\Psi_i) / (1/ \Psi_1+1/ \Psi_2+1/ \Psi_3)$ ...(٣.٩٨)

Then the optimum layer thickness would be estimated as a fraction of the total composite thickness as:

$T_i=T_t*\beta_i$ ...(٣.٩٩)

where $T_t$ is the total composite thickness.

## ٣.١٠.٢ Tapered Distribution in Global Thickness of the Structure

In the previous section, the optimum thickness arrangement across the layers of composite lamina (the optimum arrangement of the layers thicknesses along the total thickness of composite lamina) is obtained. In addition, the total thickness ($T_t$) for each one of the layered elements (regions) along the span and chord have the same opimized value. With the manufacturing process, it is possible to produce variable thicknesses for layered elements by a regional application. In order to fully utilize these manufacturing possibilities in the design model and to guarantee maximum flexibility, the general design model must also allow regionally variable layer thicknesses.

In the finite element method, the FE-mesh already divides the structure into substructures in the form of finite elements. Within each composite finite element the fiber orientations and thicknesses are defined independently. Thus, the finite element properties (thicknesses and fiber orientations) can be used for the design model formulation as principal independent structural variables.

In this section, the total thickness for each element along the wing struture from the root to the tip will make a different value depending upon the ***Tsi-Wu*** failure indices of these elements. That it is, the element of large value of failure index will take large thickness and the element of minimum failure index will

take the minimum thickness but does not exced the allowable value of ٠.١٢٥mm for each layer ***(Liu and Haftka, ٢٠٠١)*** [٥٢]

In general, if the maximum obtained failure index is denoted by($\Psi_{max}$), then for each element of a failure index of ($\Psi_{el}$) would have a thickness of :

$$T_{ti} = (\Psi_{ei} / \Psi_{max}) * T_t \qquad \ldots (٣.١٠٠)$$

where $T_{ti}$ represents the total thickness of element number i. Based on this criterion, a tapered thickness distribution along the wing domain is obtained. This distribution gives a superiority in weight reduction; thus increasing in the stiffness matrix by decreasing in the values of mass matrix. It is importanat to be noted that the present step is the final step of the suggested technique that was mentioned previously. A flow-chart presenting the sequence of optimization procedure of all the above steps is sited in **Appendix-C**.

## ٣.١١ Dynamic Analysis

Majority of today's structures are subjected to the load which varies with time. In fact, with possible exception of dead load, imposed loads cannot really be considered as static. However, in many cases the variation of the force is slow, which allows the structures to be treated as static. For aerospace and aeroplane flying through storm as an example, the dynamic effect associated with the load must be accurate for the proper evaluation of safety, performance, and reliability of these systems ***(Warburton, ١٩٧٦)*** [٥٣].

### ٣.١١.١ Dynamic Equilibrium Equation

The dynamic equation for a system can be formulated by directly expressing the equilibrium of all forces acting on the mass. In general, four types of forces will be involved; the externally applied load and three forces namely, inertia,

damping, and the elastic forces. Thus, the dynamic equation may be expressed in a matrix form as follows ***(ANSYS$^R$, ١٩٩٨)*** [٥٦]**:**

$$[M]\{\ddot{u}\}+[C]\{\dot{u}\}+[K]\{u\}=\{F(t)\} \quad \ldots (٣.١٠١)$$

where :

$[M]$: structural mass matrix.

$[C]$: structural damping matrix.

$[K]$: structural stiffness matrix.

$\{\ddot{u}\}$: nodal acceleration vector.

$\{\dot{u}\}$: nodal velocity vector.

$\{u\}$ = nodal displacement vector.

$\{F(t)\}$ = applied load factor as a function of time.

The above equilibrium equation is solved by Newmark Family method to obtain the unknowns $\{u_{n+١}\}$ vector. The results of the dynamic analysis include the following items:

١. The linear and angular displacements of the nodes ( $u, v, w, \theta_x, \theta_y, \theta_z$) along global coordinate axis as a function of time.

٢. The element stresses along element coordinates axis as a function of time.

٣. Dynamic load factor (***Magnification Factor***) for all nodes presented in the structure.

The ***Dynamic Load factor*** (***DLF***) is defined as the ratio of dynamic displacement at any instant of time to the static displacement. It is non-dimensional and independent on the magnitude of the load. The maximum dynamic load factor is known as the ***Magnification Factor***. In many structural problems, the magnification factor is of importance ***(Warburton, ١٩٧٦)*** [٥٣].

### ٣.١١.٢ Formulation of Damping Properties

In the analysis of dynamic problems, it is assumed that the amplitude of free vibration remains constant with time, but experience shows that the amplitude diminishes with time and that the vibrations are gradually damped out.

To bring the vibration analysis into better agreement with reality, the equation of motion for a discretized body or structure, often, must include a term to account for energy dissipation, i.e. damping forces. These forces may arise from several causes, such as friction, air or fluid resistance, internal friction due to imperfect elasticity of materials, and so on. Among all of these sources of energy dissipation, the case where the damping force is proportional to velocity is called viscous damping, and this is the simplest to deal with mathematically. For this reason, resisting forces of a complicated nature are replaced for purpose of analysis by equivalent viscous damping ***(Timoshenko et al., ١٩٧٤)*** [٥٧].

### ٣.١١.٣ Effect of Damping

In most cases the effect of damping on the response of a vibratory system is minor and thus, it can be ignored. However, for vibratory system with a periodic excitation and a frequency at or near the natural frequency, i.e. the resonance phenomenon, damping will be of primary importance and must be taken into account ***(Timoshenko et al., ١٩٧٤)*** [٥٧].

Figure (٣.٨) shows the relationship between the magnification factor ($\beta$) which represents the ratio of dynamic response to static response (function of dynamic response of the system), and the ratio ($\Omega/\omega$) which represents the ratio of the angular frequency ($\Omega$) of a simple harmonic force function ($P\sin\Omega t$ or $P\cos\Omega t$) to the natural frequency of the system, $\omega$, plotted for various levels of damping ratios ($\gamma$). As for undamped case, the value of ($\beta$) is approximately unity for small values of ($\Omega/\omega$), and approaches zero for large values of ($\Omega/\omega$).

However, as the value of **Ω** approaches **ω** (i.e. (**Ω/ω**) approaches unity), the magnification factor grows rapidly.

Furthermore, the value of **β** at or near resonance is very sensitive to the amount of damping. Thus, while the damping has only a minor effect when the system is remote from resonance, it has a dramatic effect at or near resonance. In structural dynamics the influence of damping is critical for this case and represents its most important application ***(Weaver*** and ***Johnston, ١٩٨٧)*** [٥٨]**.**

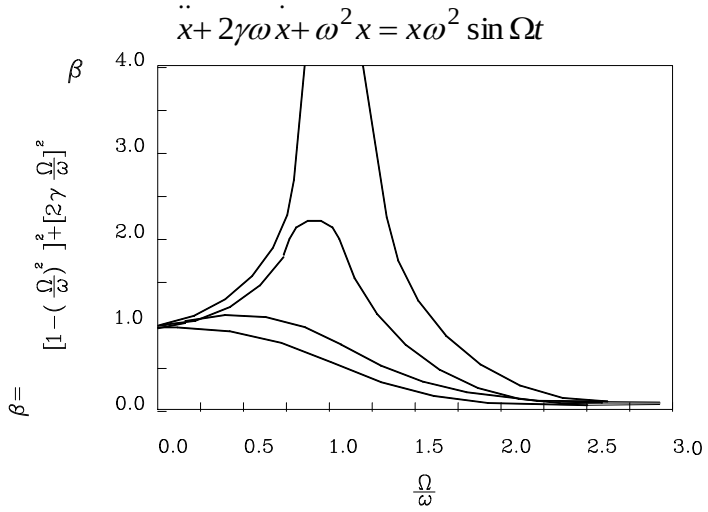


**Figure (٣.٨):** Effect of damping on the magnification factor [٥٨].

## ٣.١١.٤ Damping Matrix

With the present understanding of damping in structures, it is not possible to formulate an explicit damping matrix for distributed damping throughout a structure, in a manner similar to that followed for the stiffness **[K]** and mass **[M]** matrices ***(Pytet, ١٩٩٠)*** [٦٠]. In practice, damping is usually expressed in terms of damping ratios for each of the natural frequency modes. These ratios are established from experiments on similar structures.

The most common form of representation of the damping matrix **[C]** is the so-called Rayleigh-type damping ***(Timoshenko et al., ١٩٧٤)*** [٥٧] as a linear combination of mass and stiffness matrices which is given as:

$$[C] = a_o [M] + a_1 [K] \quad \ldots (٣.١٠٢)$$

in which **($a_o$)** and **($a_1$)** are arbitrary proportionality factors which make the damping matrix satisfy the orthogonality condition with respect to the modal matrix **[ϕ]** in the same way of the orthogonality conditions for the mass and stiffness matrices that is ***(Bathe, ١٩٩٦)*** [٥٩]:

$$[\phi]^T [M] [\phi] = [I] \quad \ldots (٣.١٠٣)$$

$$[\phi]^T [K] [\phi] = [\Lambda] \quad \ldots (٣.١٠٤)$$

$$[\phi]^T [C] [\phi] = ٢ [\gamma] [\Lambda]^{1/2} \quad \ldots (٣.١٠٥)$$

where:

[ϕ] = Modal matrix whose columns represent the natural modal shapes and the superscript (**T**) denotes transpose,

[I] = Identity matrix.

[Λ] = Spectral matrix, which is diagonal with elements representing the squares of the natural frequencies ($\omega_i^2$) and

[γ] = Modal damping matrix which is also diagonal with elements representing the damping ratios for the system modes ($\gamma_i$).

Premultiplying Equation (٣.١٠٢) by **[ϕ]**$^T$ and post-multiplying it by **[ϕ]** yields:

$$[\phi]^T [C] [\phi] = a_o [\phi]^T [M] [\phi] + a_1 [\phi]^T [K] [\phi] \quad \ldots (٣.١٠٦)$$

Substituting Equations (٣.١٠٣) to (٣.١٠٥) into Equation (٣.١٠٦) gives:

$$٢ [\gamma] [\Lambda]^{1/2} = a_o [I] + a_1 [\Lambda] \quad \ldots (٣.١٠٧)$$

**...(٣.١٠٧)** The two factors, $a_o$ and $a_1$, can be determined by specifying damping

ratios for two modes, for example ١ and ٢, and substituting into Equation (٣.١٠٧) as ***(Pytet, ١٩٩٠)*** [٦٠]:

$$2\gamma_1\omega_1 = a_o + \omega_1^2 a_1 \quad \ldots$$

***(٣.١٠٨)*** $$2\gamma_2\omega_2 = a_o + \omega_2^2 a_1 \quad \ldots$$

***(٣.١٠٩)*** where $\omega_1$ and $\omega_2$ are the natural frequencies for modes ١ and ٢ respectively.

Solving the above two Equations, then

$$a_o = \frac{2\omega_1\omega_2(\omega_2\gamma_1 - \omega_1\gamma_2)}{(\omega_2^2 - \omega_1^2)} \quad \ldots$$

***(٣.١١٠)*** $$a_1 = \frac{2(\omega_2\gamma_2 - \omega_1\gamma_1)}{(\omega_2^2 - \omega_1^2)}$$

***... (٣.١١١)*** Then, the values of $a_o$ and $a_1$ are substituted into Equation (٣.١٠٢) to get the required damping matrix. The natural frequencies ($\omega_i$) which are used in the above equations can be obtained from the solution of the eigenvalue problem for the undamped case ***(Timoshenko et al, ١٩٧٤)*** [٥٧]. As will be shown later, the corresponding damping ratios ($\gamma_i$) can be obtained by finding the damping ratio $\gamma_1$ , related to the first mode of vibration, using field testing of a structure or from previous experience or even by assuming it within an acceptable range according to the type of the structure. With the value $\gamma_1$ on hand, other values of $\gamma_i$ can be extrapolated using the approximate formula ***(Weaver*** and ***Johnston, ١٩٨٧)*** [٥٨]:

$$\gamma_i \approx \gamma_1 \left(\frac{\omega_i}{\omega_1}\right)^{el} \quad ; (٠.٥ \le el \le ٠.٧) \quad \ldots$$

***(٣.١١٢)*** Rewriting Equation (٣.١٠٧) for an arbitrary mode ( i ) gives:

$$2\gamma_i\omega_i = a_o + a_1\omega_1^2 \quad \ldots$$

***(٣.١١٣)*** from which the damping ratio ($\gamma_i$ ) can be defined as:

$$\gamma_i = \frac{a_o + a_1 \omega_i^2}{2\omega_i} \qquad \ldots$$

***(٣.١١٤)*** The relationship of Equation (٣.١١٤) between the natural frequency ($\omega_i$) and the damping ratio ($\gamma_i$) is illustrated in Figure (٣.٩) ***(Pytet, ١٩٩٠)*** [٦٠].

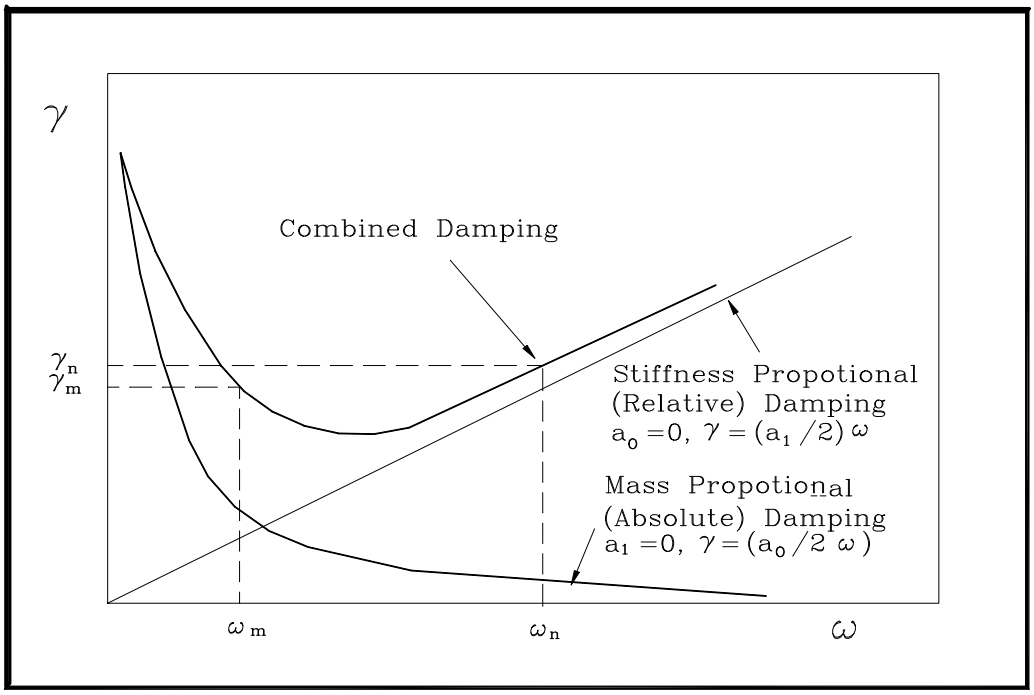


**Figure (٣.٩)**: Relationship between damping ratio and frequency for Rayleigh damping [٦٠]

## ٣.١٢ Numerical Method for the Dynamic Analysis

The dynamic equilibrium equation, equation (٣.١٠١), represents a system of linear differential equations of second order and, in principle; the solution of the equations can be obtained by standard procedures for the solution of differential equations with constant coefficients. However, the procedures proposed for the solution of general system of differential equations become very expensive if the order of the matrices is large. In practical finite element analysis, there are few

effective methods. These are mainly, direct time–integration and mode superposition. In the present work, the direct integration method is used.

In direct integration method, the dynamic equilibrium equations are integrated using a numerical step–by–step procedure. The term "direct" meaning that prior to the numerical integration and no transformation of the equation into different form is carried out.

In essence, direct numerical integration is based on two ideas. First, equation (٣.١٠١) is satisfied at discrete time intervals ($\Delta$**t**) apart. The second idea is that a variation of displacements, velocities, and accelerations within each time interval ($\Delta$**t**) is assumed. The available direct procedures can be further sub– divided into implicit and explicit methods.

The implicit algorithms are more effective for structural dynamic problems, in which the response is controlled by a relatively small number of low frequency modes, while explicit algorithms are very efficient for wave propagation problems, in which the contribution of intermediate and high frequency structural modes to the response is important (***Subbaraj*** and ***Dokainish***, ١٩٨٩) [٦١].

In the present study, only implicit methods will be considered because of their properties discussed above.

## ٣.١٢.١ The Newmark Familv of Methods

Newmark method is based on using the equilibrium conditions given by equation (٣.١٠١) at time **t+$\Delta$t** in order to calculate the displacements at this time. This method is based on the following assumptions:

$$\dot{X}_{t+\Delta t} = \dot{X}_t + \Delta t[(1-\alpha)\ddot{X}_t + \gamma\ddot{X}_{t+\Delta t}] \qquad \textbf{... (٣.١١٥a)}$$

and,

$$X_{t+\Delta t} = X_t + \Delta t\dot{X}_t + (\Delta t)^2[(\frac{1}{2} - \beta)\ddot{X}_t + \beta\ddot{X}_{t+\Delta t}] \quad \text{... (٣.١١٥b)}$$

where the parameters $\beta$ and $\alpha$ determine the stability and accuracy of the algorithm. Assuming different values for $\alpha$ and $\beta$, give different formulas within the Newmark family of methods. This method is unconditionally stable if $\alpha \geq 1/2$ and $\beta \geq (2\gamma+1)^2/16$.

Unless $\alpha$ taken to be **٠.٥,** the method introduces artificial damping which can be negative when $\gamma <$ **٠.٥ (*Pytet,* ١٩٩٠)** [٦٠] . Therefore, as remarked by Newmark, all schemes for which $\alpha \geq 1/2$ and $\beta \geq 1/4$ are unconditionally stable and indeed show no artificial damping, (***Zienkiewicz,*** ١٩٧٧) [٦٢].

In the present study, values of $\alpha$ and $\beta$ are **٠.٥** and **٠.٢٥,** respectively. Newmark method with these values of $\alpha$ and $\beta$ is called **constant –average-acceleration method**. This method is generally used in structural dynamics because it has been shown to have high degree of numerical stability, ( ***Al-Sarraf et al.,*** ٢٠٠٣) [٦٣]. The complete algorithm of the present method is given in (***Subbaraj*** and ***Dokainish***, ١٩٨٩) [٦١].

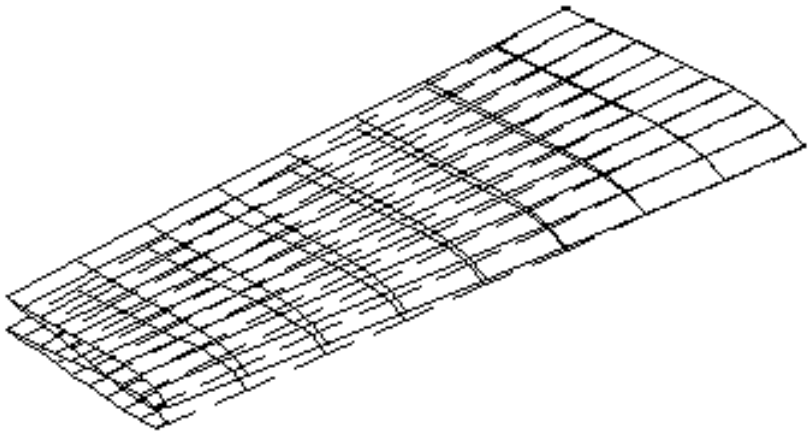

**Fig.(٤.١):** The first mode shape of the Skins**f** in term of deformed and undeformed shapes.

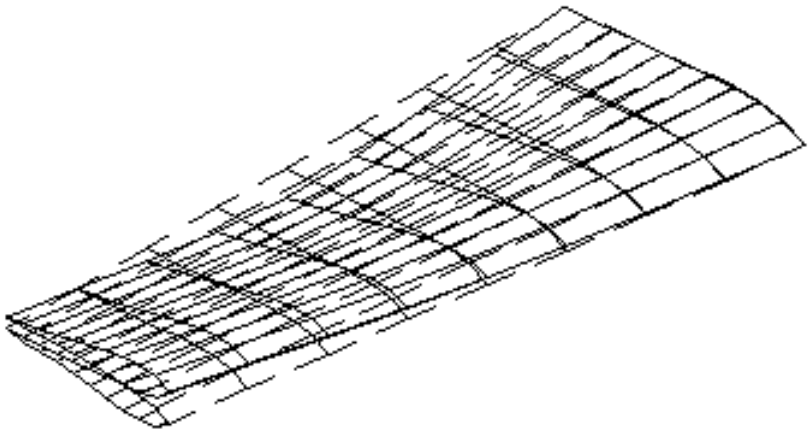

**Fig.(٤.٢):**The second mode shape of the Skins**f** in term of deformed and undeformed shapes.

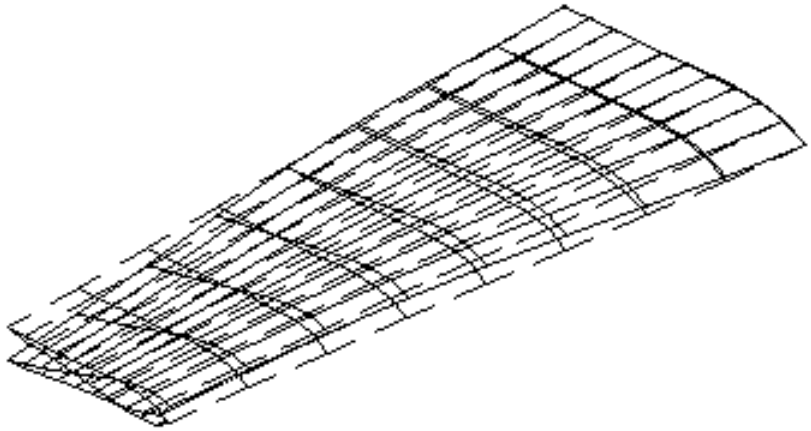

**Fig.(٤.٣):** The third mode shape of the Skins**f** in term of deformed and undeformed shapes.

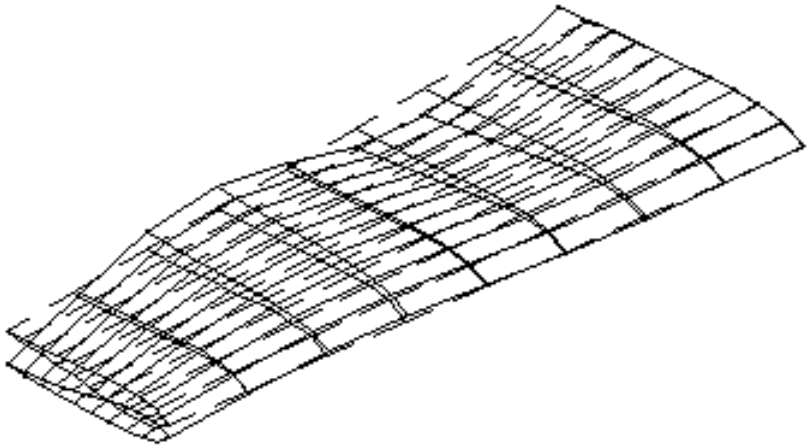

**Fig.(٤.٤):** The fourth mode shape of the Skins**f** in term of deformed and undeformed shapes.

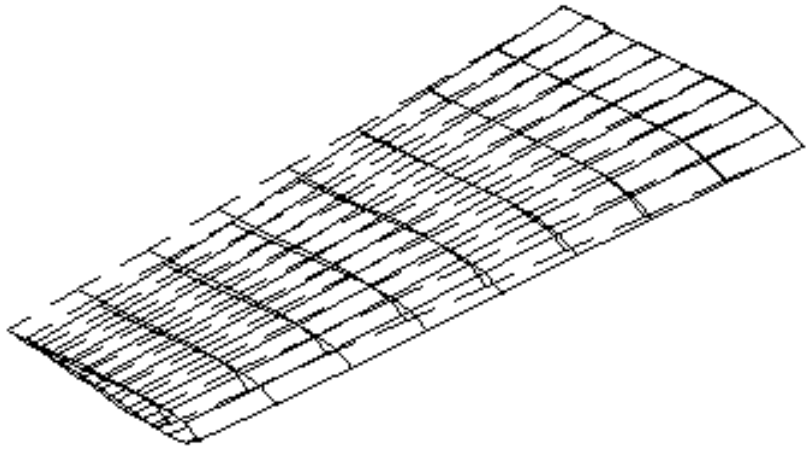

**Fig.(٤.٥):** The fifth mode shape of the Skins**f** in term of deformed and undeformed shapes.

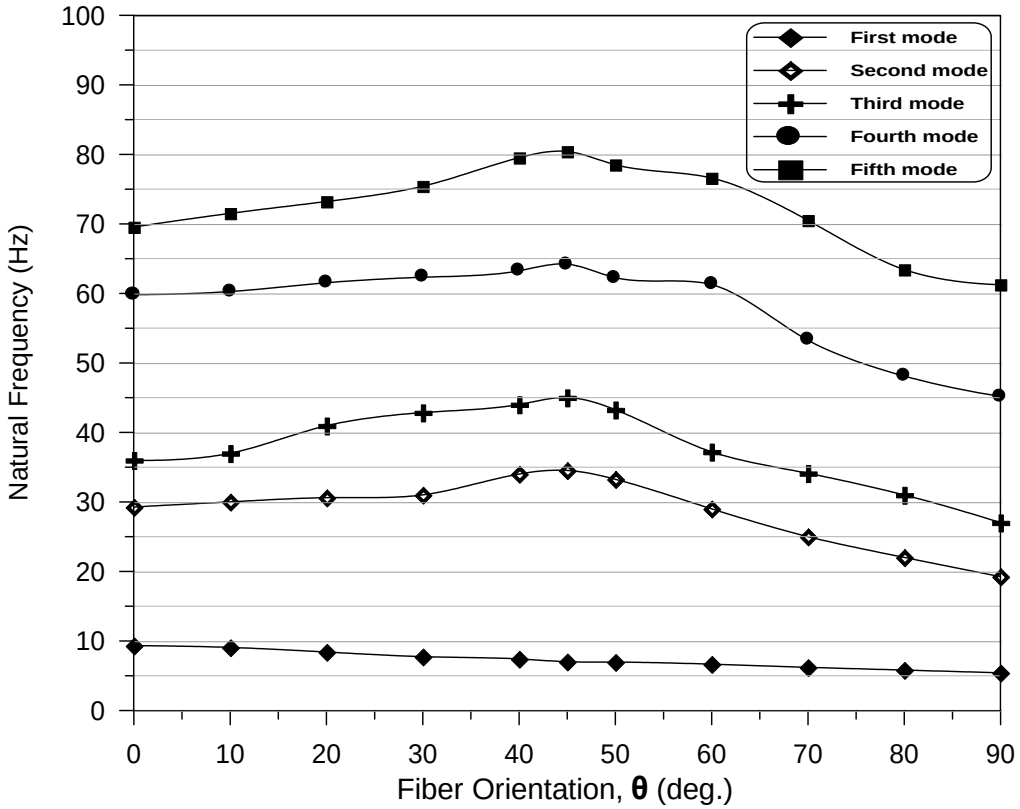


**Fig.(٤.٦):** Variation of natural frequency with orientation angles of Skins**f**.

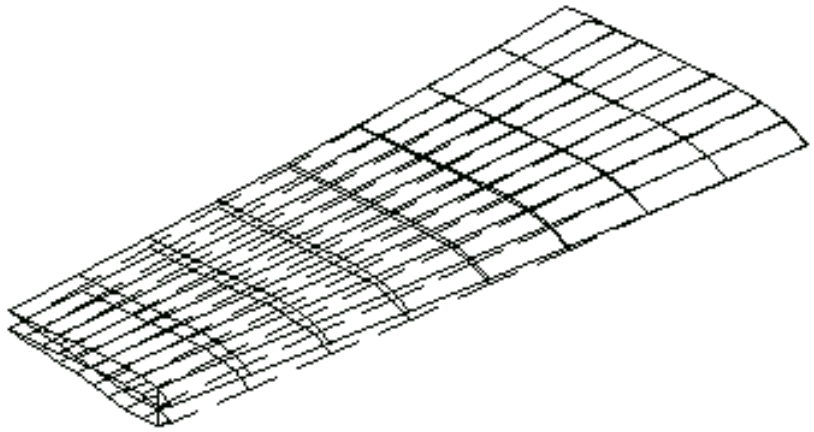

**Fig.(٤.٧):** The first mode shape of the Spar١**f** in Term of deformed and undeformed shapes.

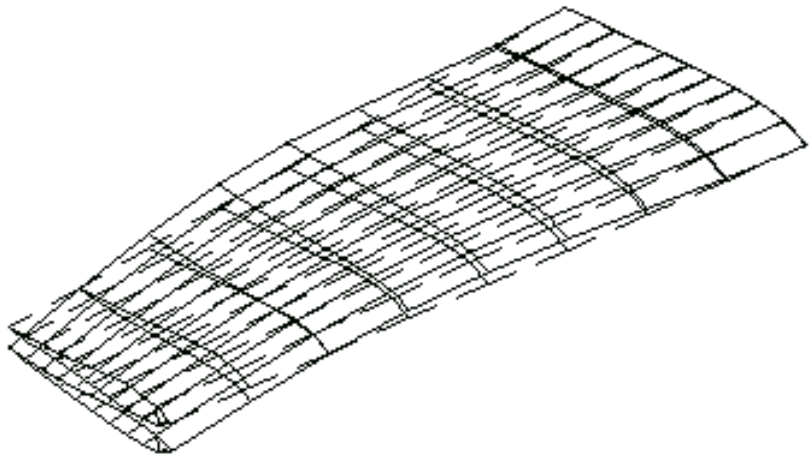

**Fig.(٤.٨):** The second mode shape of the Spar١**f** in Term of deformed and undeformed shapes.

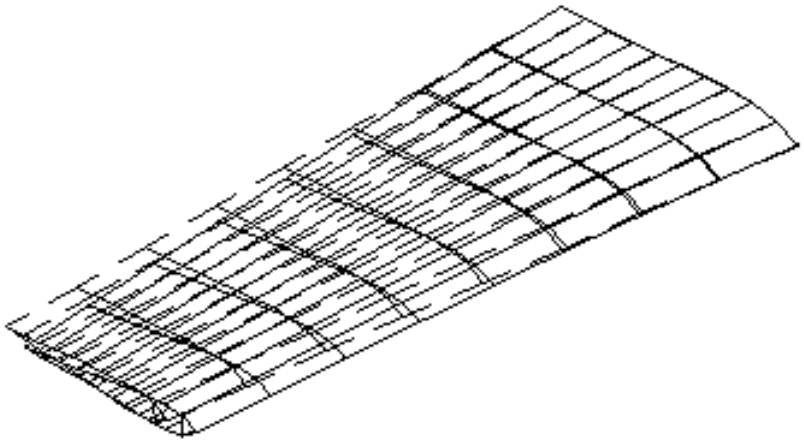

**Fig.(٤.٩):** The third mode shape of the Spar١**f** in term of deformed and undeformed shapes.

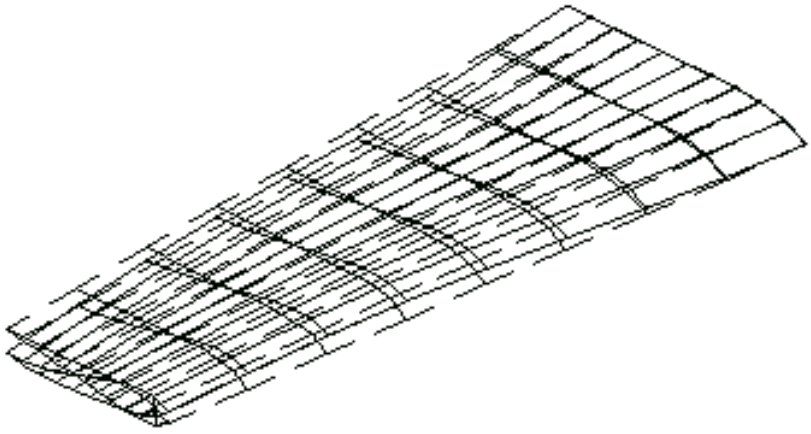

**Fig.(٤.١٠):** The fourth mode shape of the Spar١**f** in term of deformed and undeformed shapes.

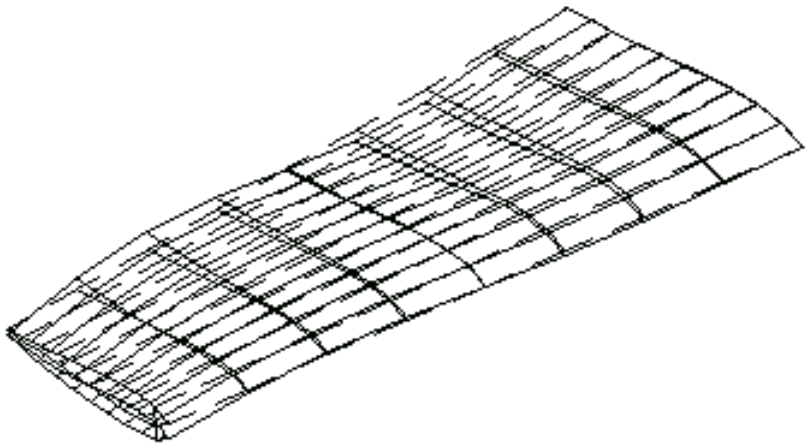

**Fig.(٤.١١):** The fifth mode shape of the Spar١**f** in term of deformed and undeformed shapes.

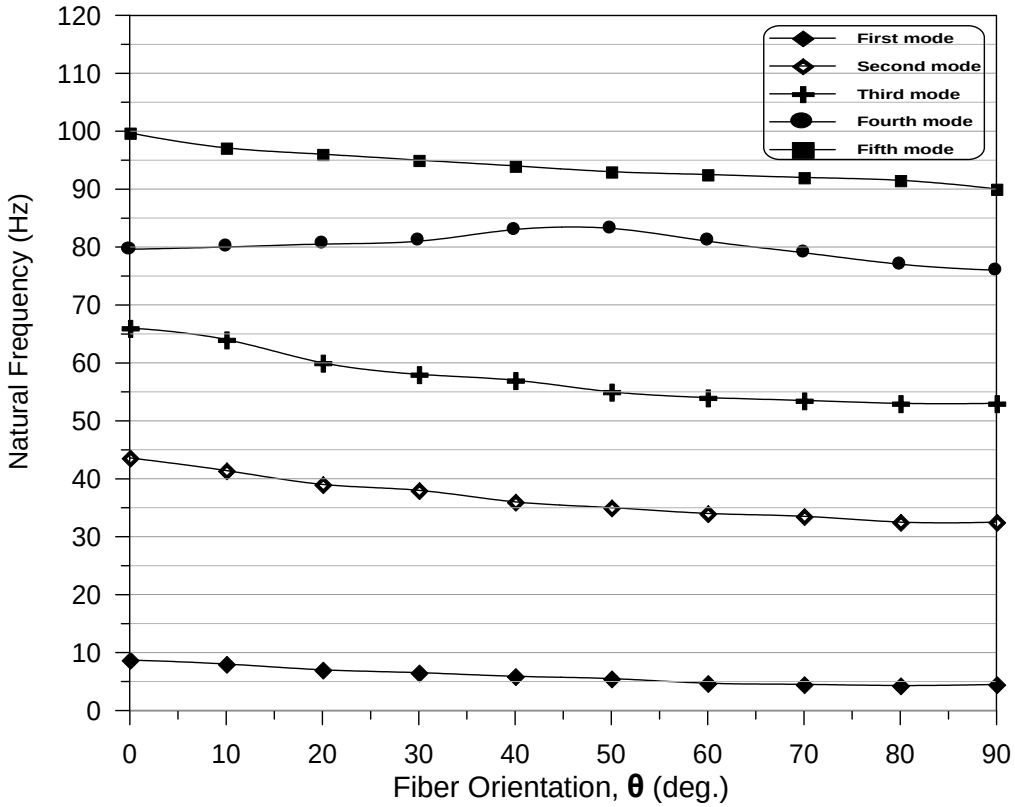


**Fig.(٤.١٢):** Variation of natural frequency with orientation angles of Spar١**f**.

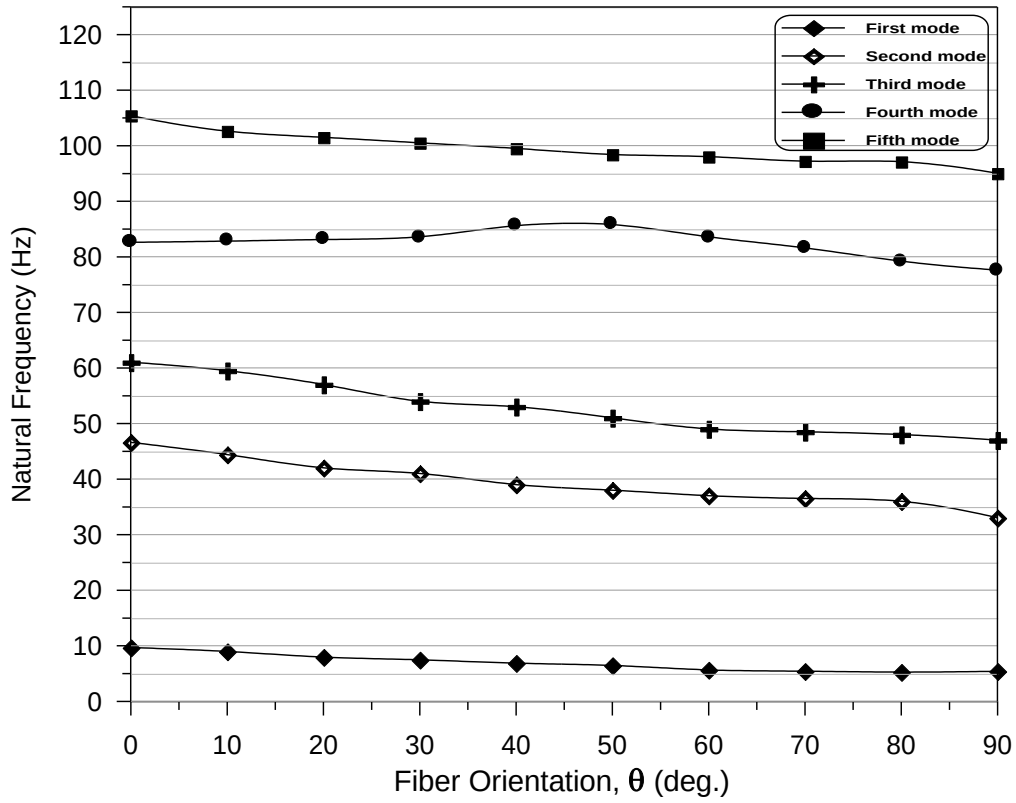


**Fig.(٤.١٣):** Variation of natural frequency with orientation angles of Spar٢**f**.

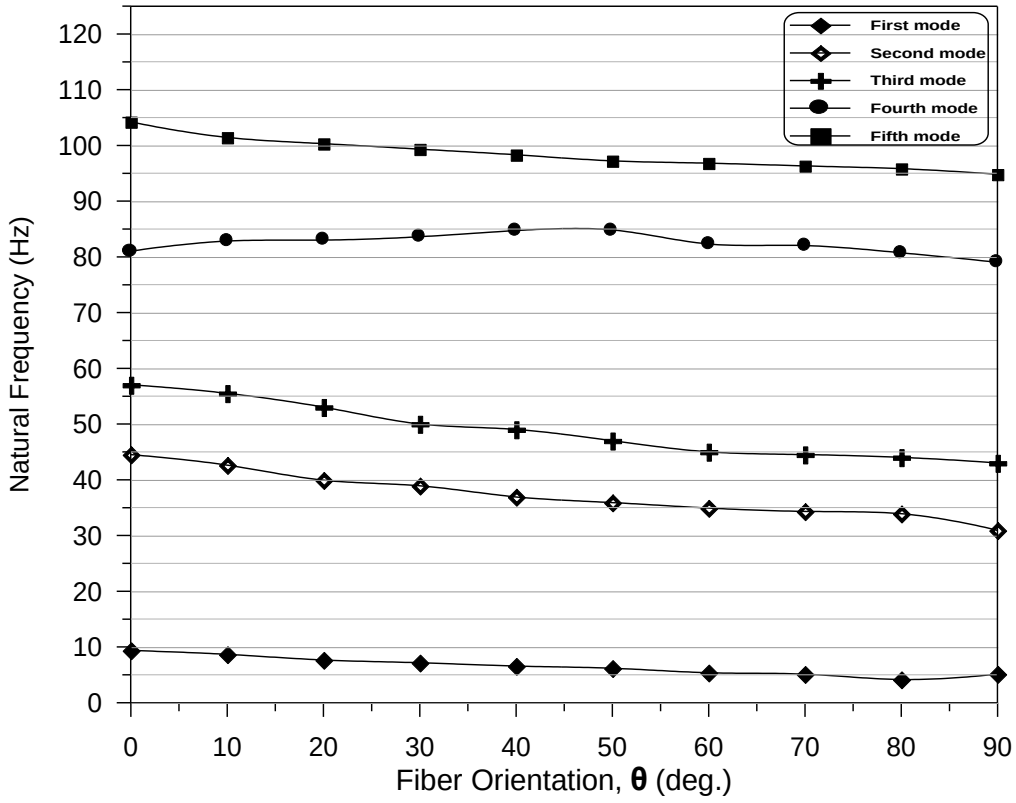


**Fig.(٤.١٤):** Variation of natural frequency with orientation angles of Spar٣**f**.

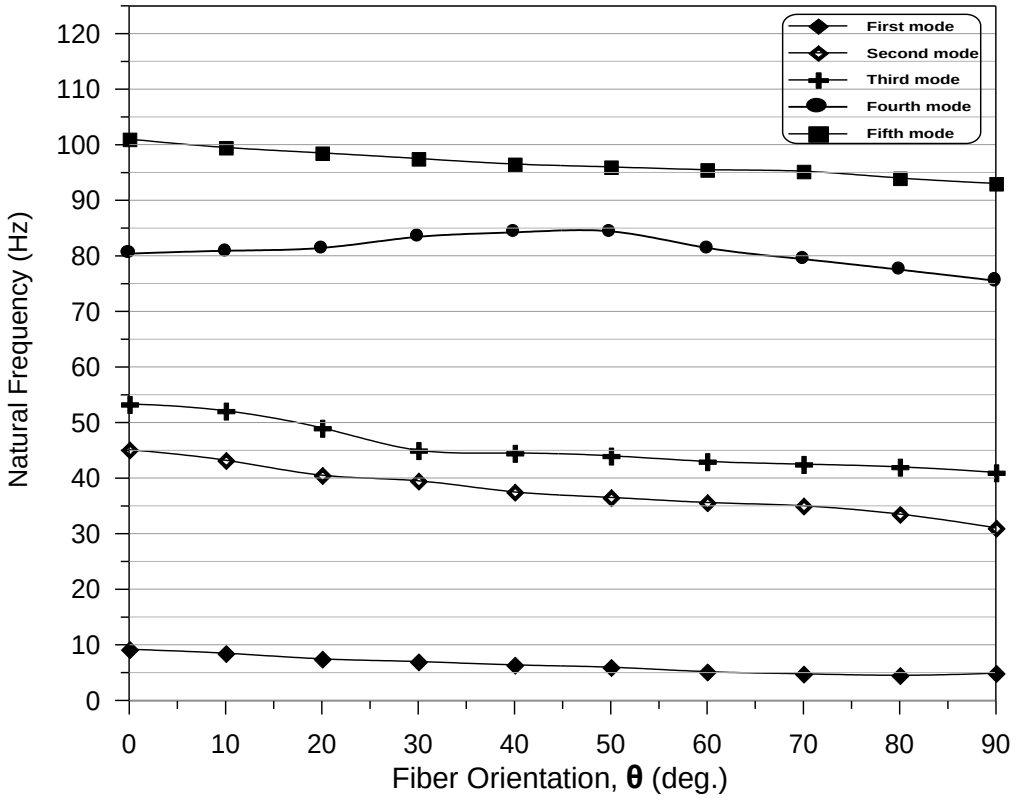


**Fig.(٤.١٥):** Variation of natural frequency with orientation angles of Spar٤**f**.

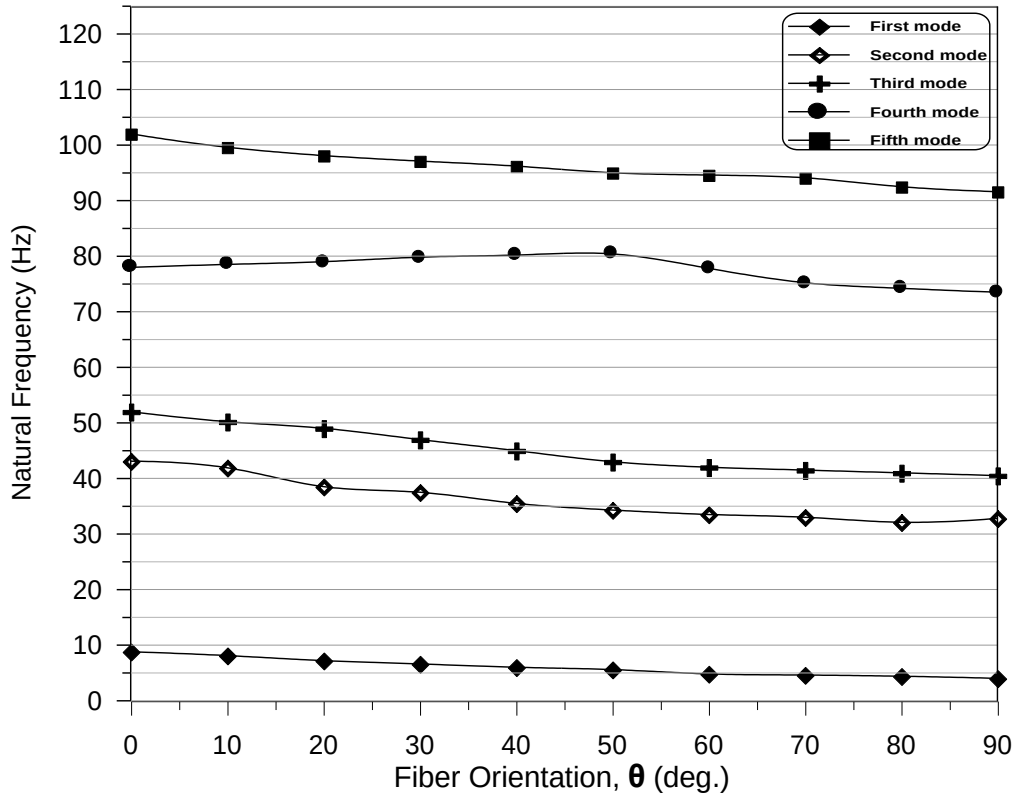


**Fig.(٤.١٦):** Variation of natural frequency with orientation angles of Spar٥**f**.

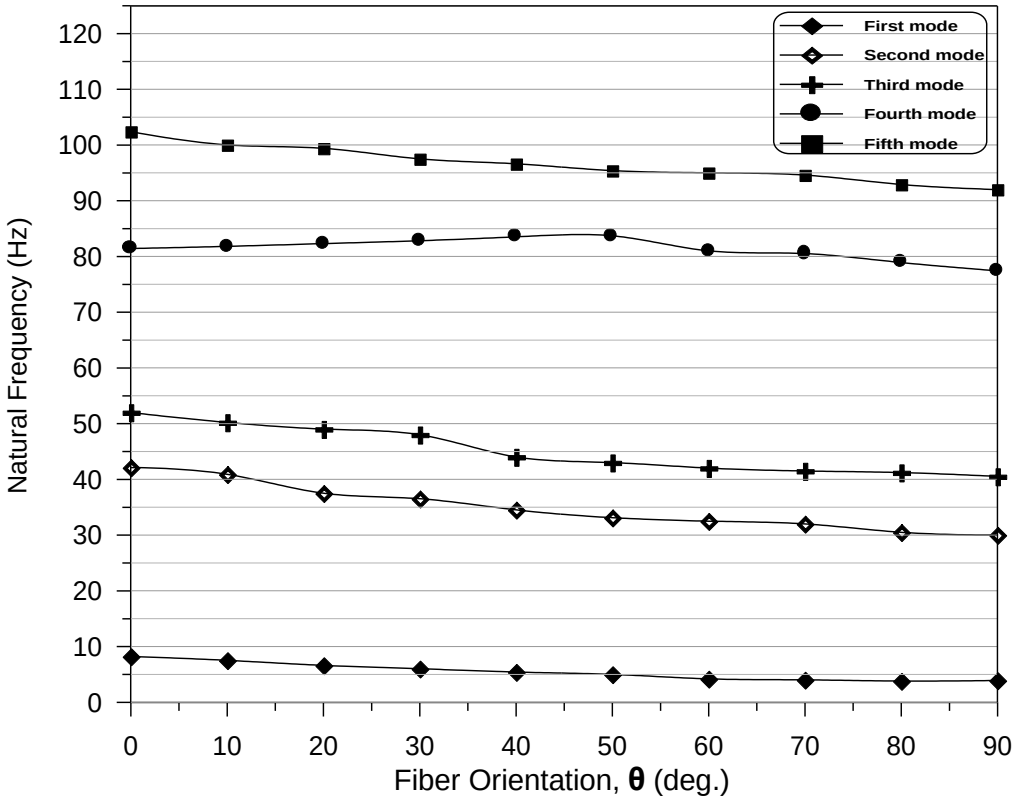


**Fig.(٤.١٧):** Variation of natural frequency with orientation angles of Spar٦**f**.

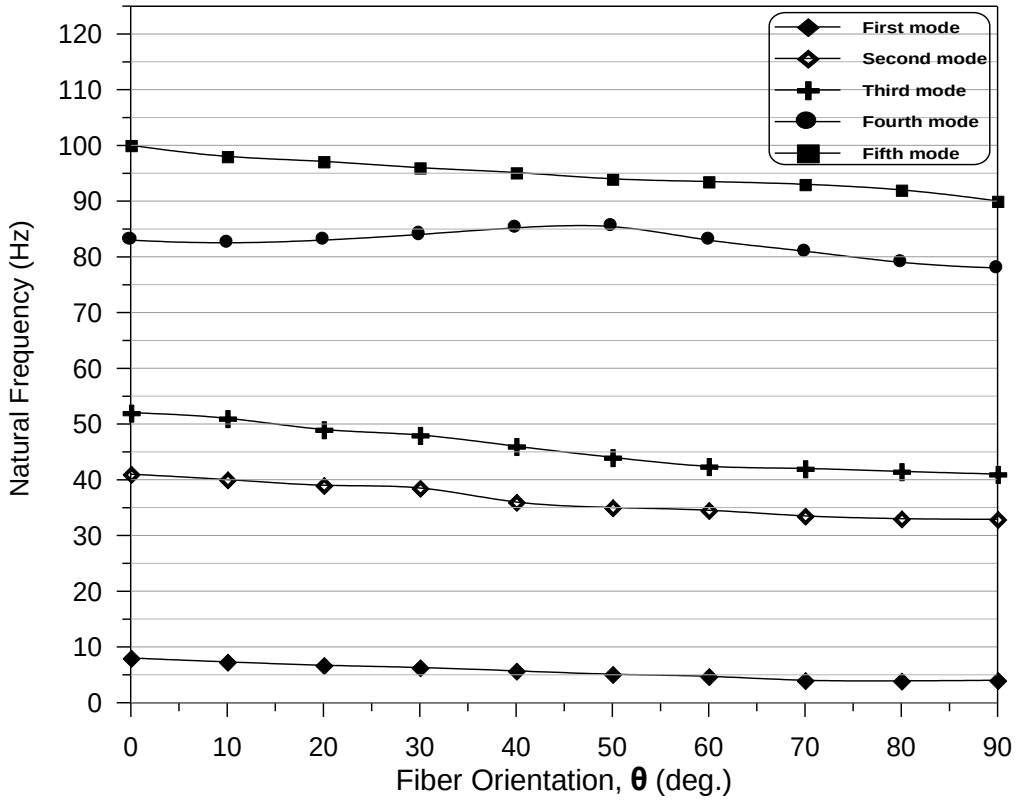


**Fig.(٤.١٨):** Variation of natural frequency with orientation angles of Spar٧**f**.

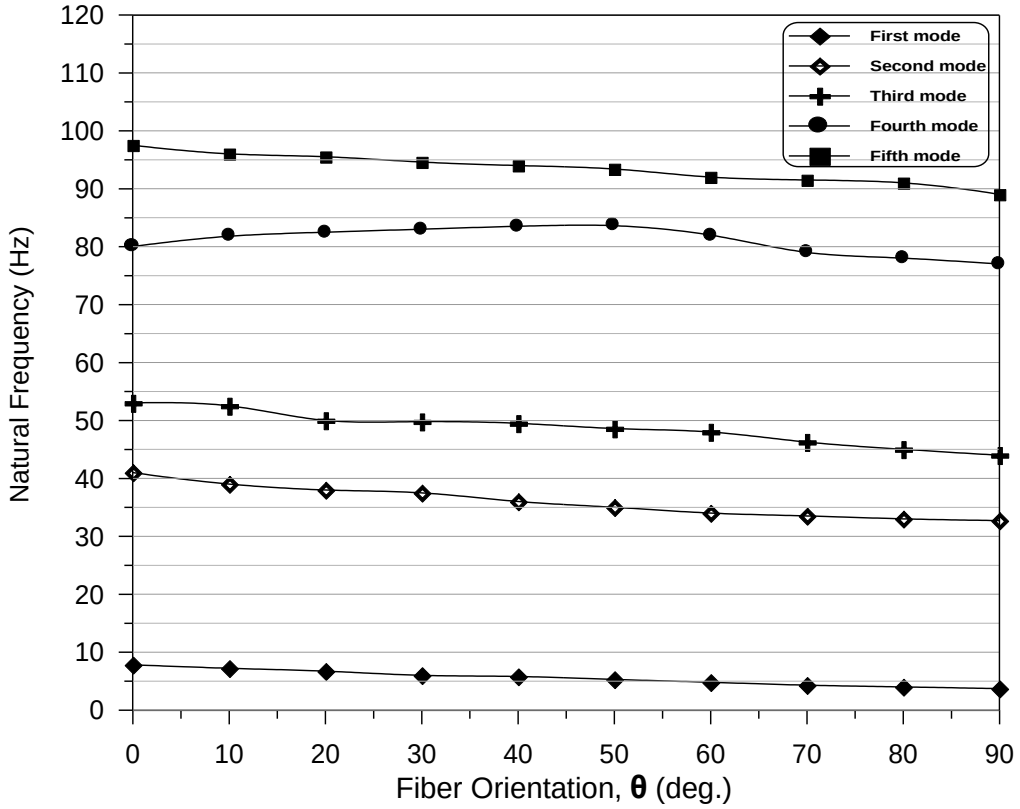


**Fig.(٤.١٩):** Variation of natural frequency with orientation angles of Spar٨**f**.

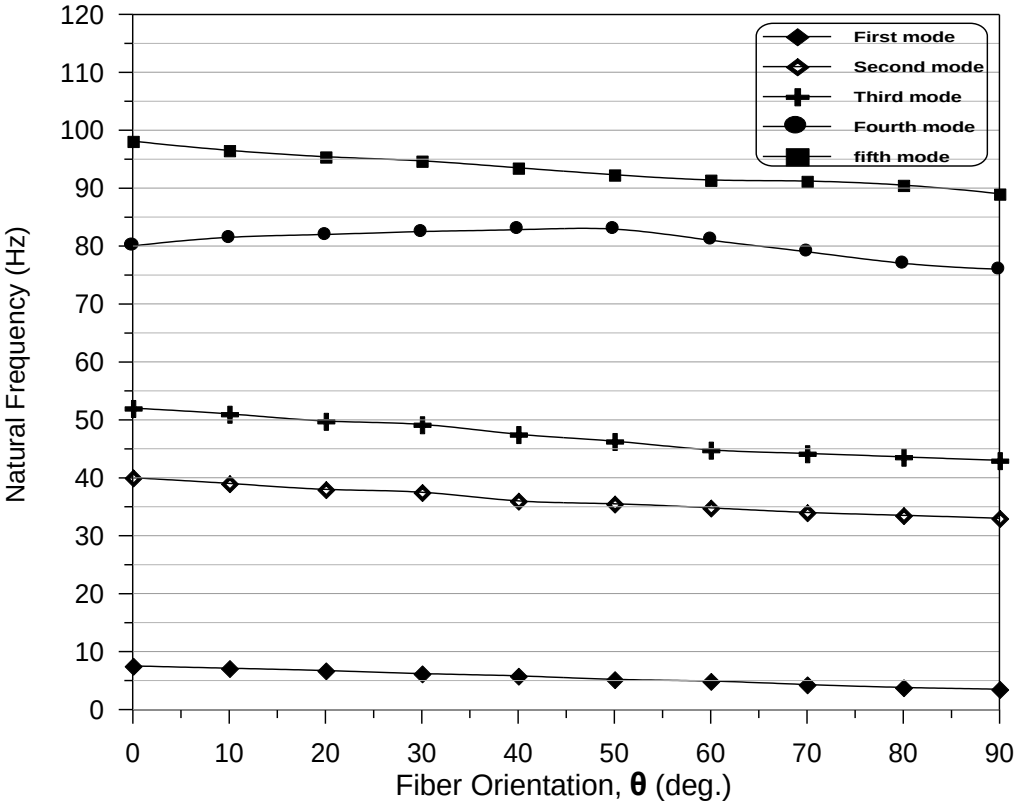


**Fig.(٤.٢٠):** Variation of natural frequency with orientation angles of Spar٩**f**.

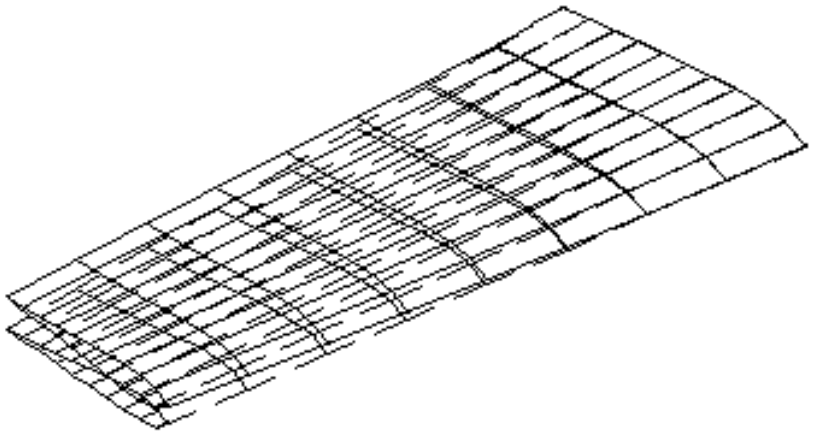

**Fig.(٤.٢١):** The first mode shape of the Rib١**f** in term of deformed and undeformed shapes.

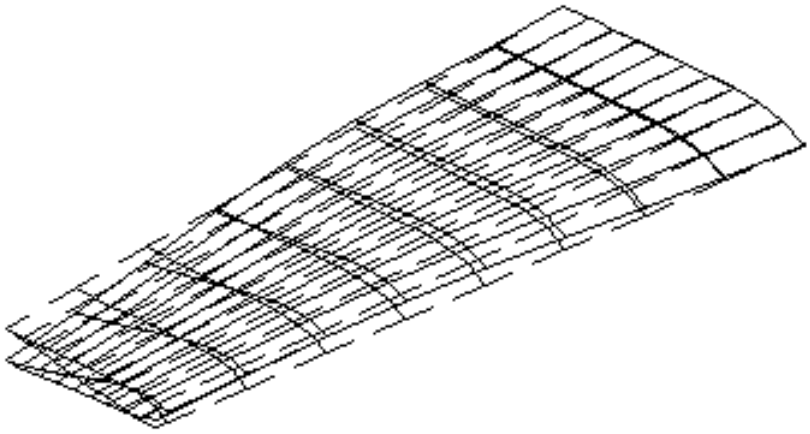

**Fig.(٤.٢٢):** The second mode shape of the Rib١**f** in term of deformed and undeformed shapes.

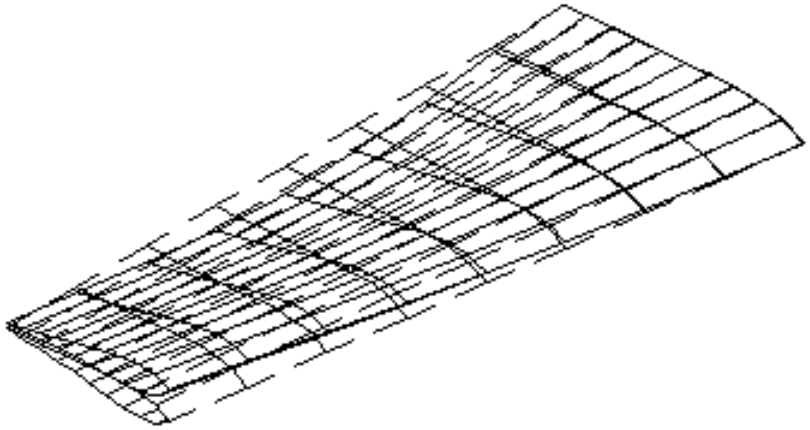

**Fig.(٤.٢٣):** The third mode shape of the Rib١**f** in term of deformed and undeformed shapes.

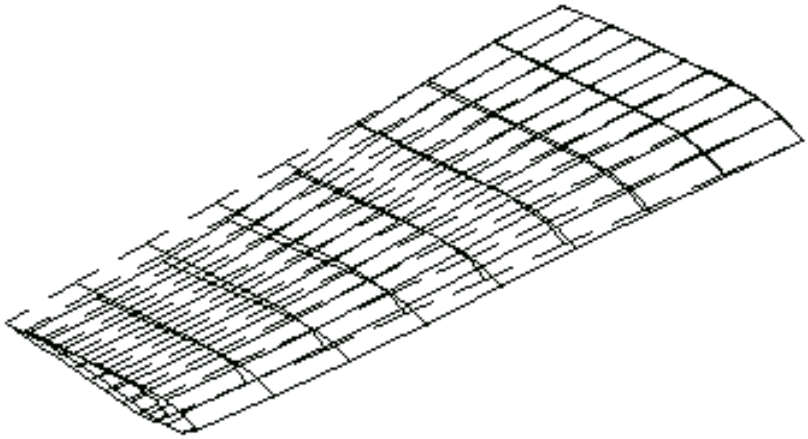

**Fig.(٤.٢٤):** The fourth mode shape of the Rib١**f** in term of deformed and undeformed shapes.

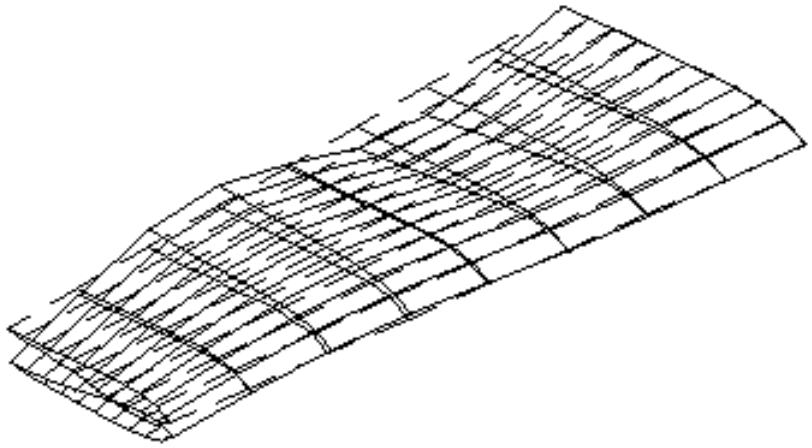

**Fig.(٤.٢٥):** The fifth mode shape of the Rib١**f** in term of deformed and undeformed shapes.

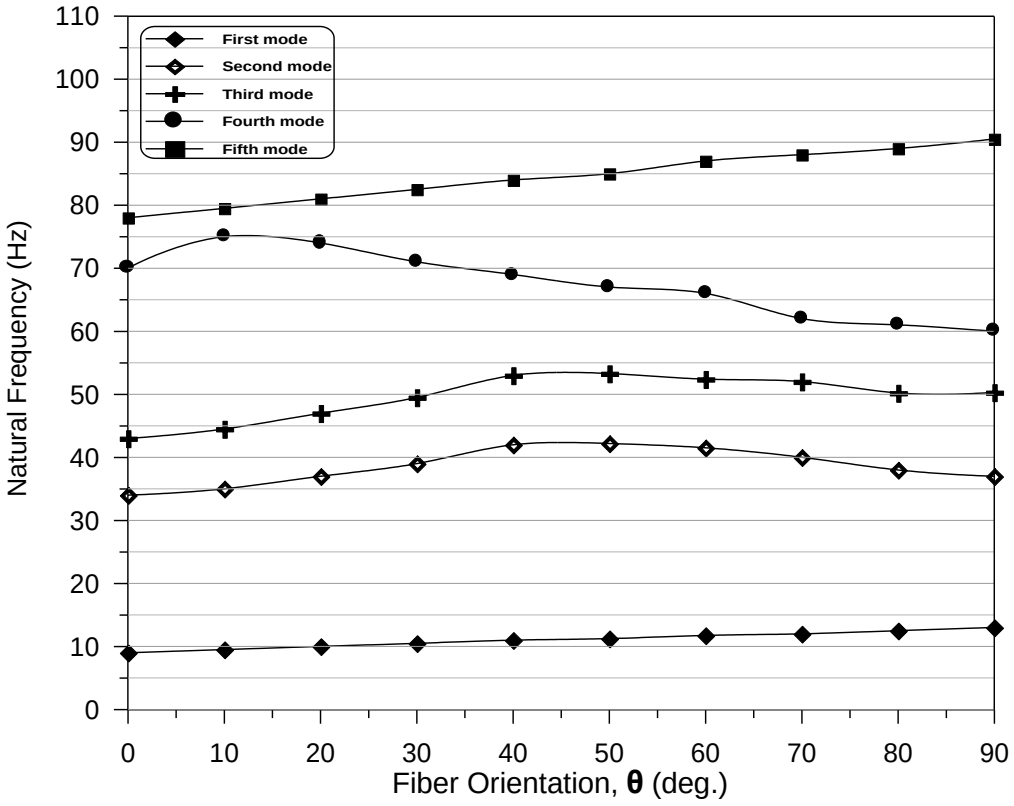


**Fig.(٤.٢٦):** Variation of natural frequency with orientation angles of Rib١**f**.

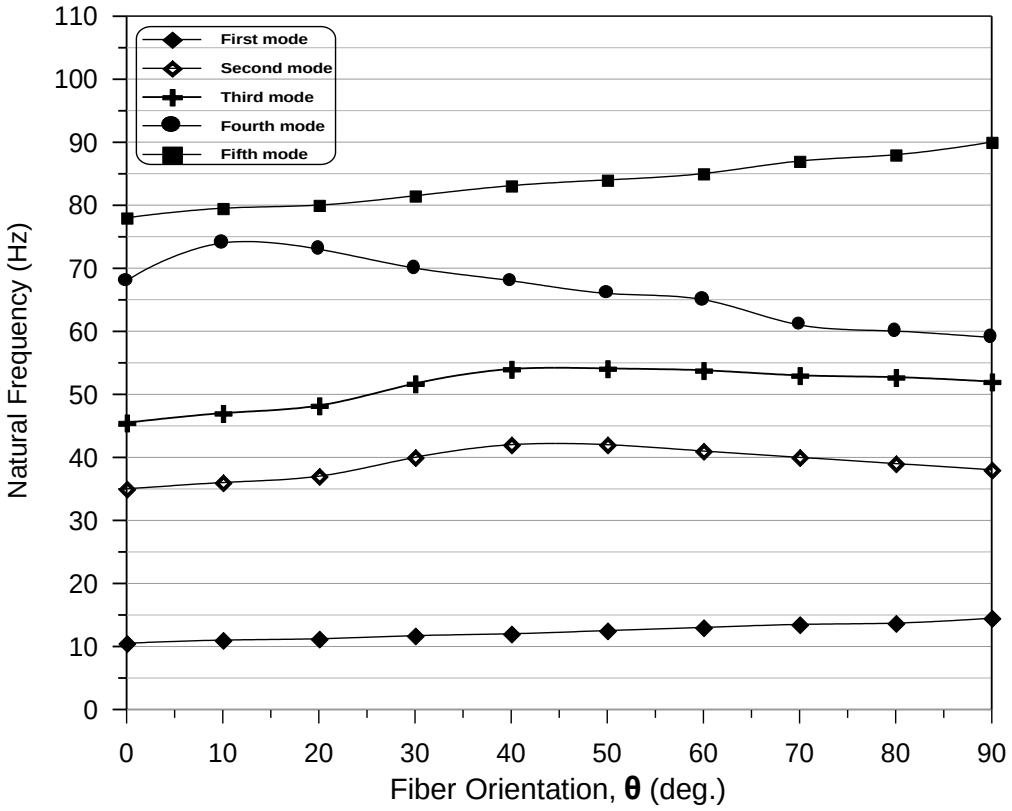


**Fig.(٤.٢٧):** Variation of natural frequency with orientation angles of Rib٢**f**.

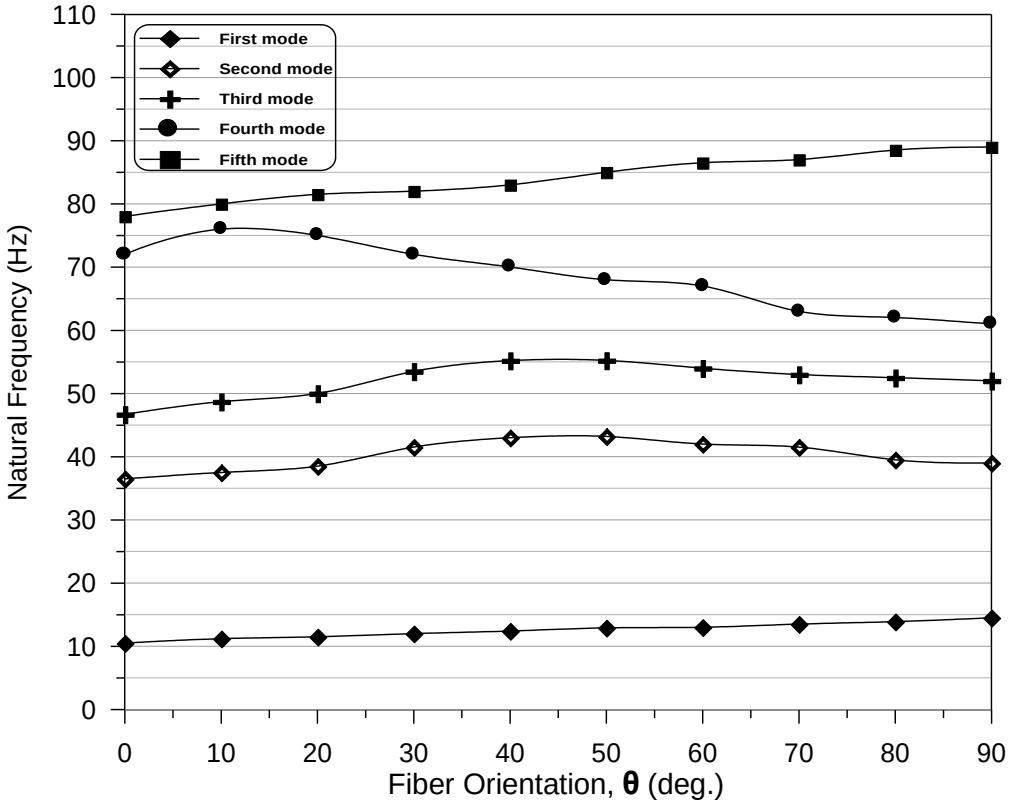


**Fig.(٤.٢٨):** Variation of natural frequency with orientation angles of Rib٣**f**.

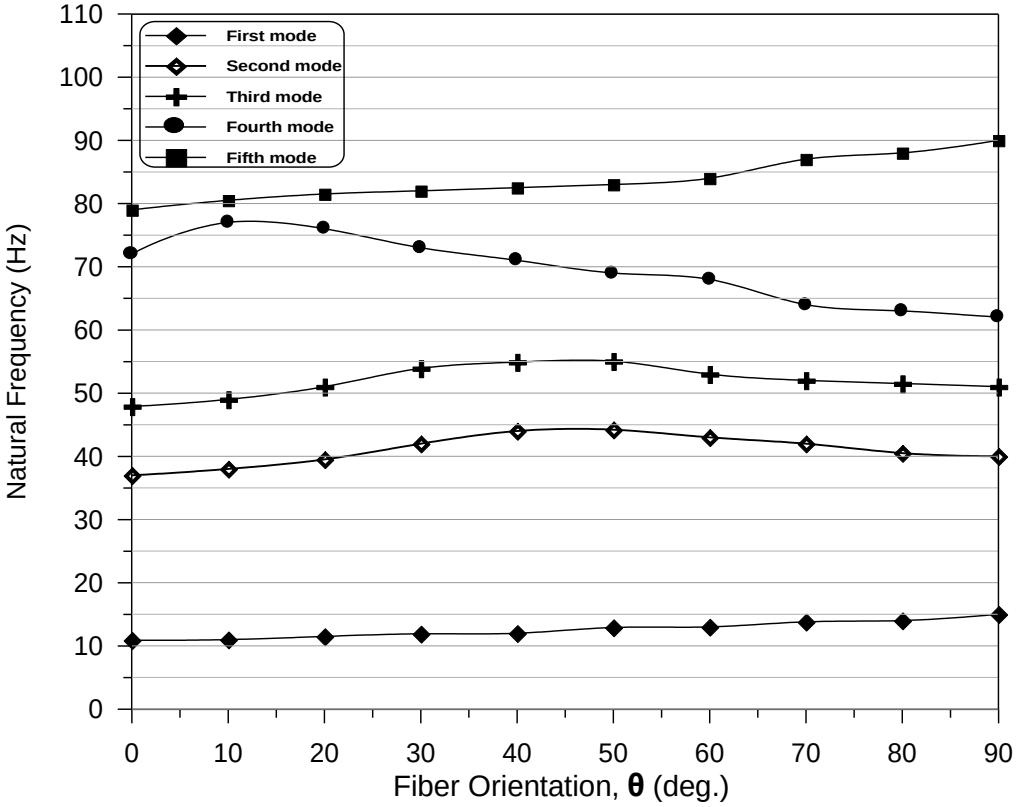


**Fig.(٤.٢٩):** Variation of natural frequency with orientation angles of Rib٤**f**.

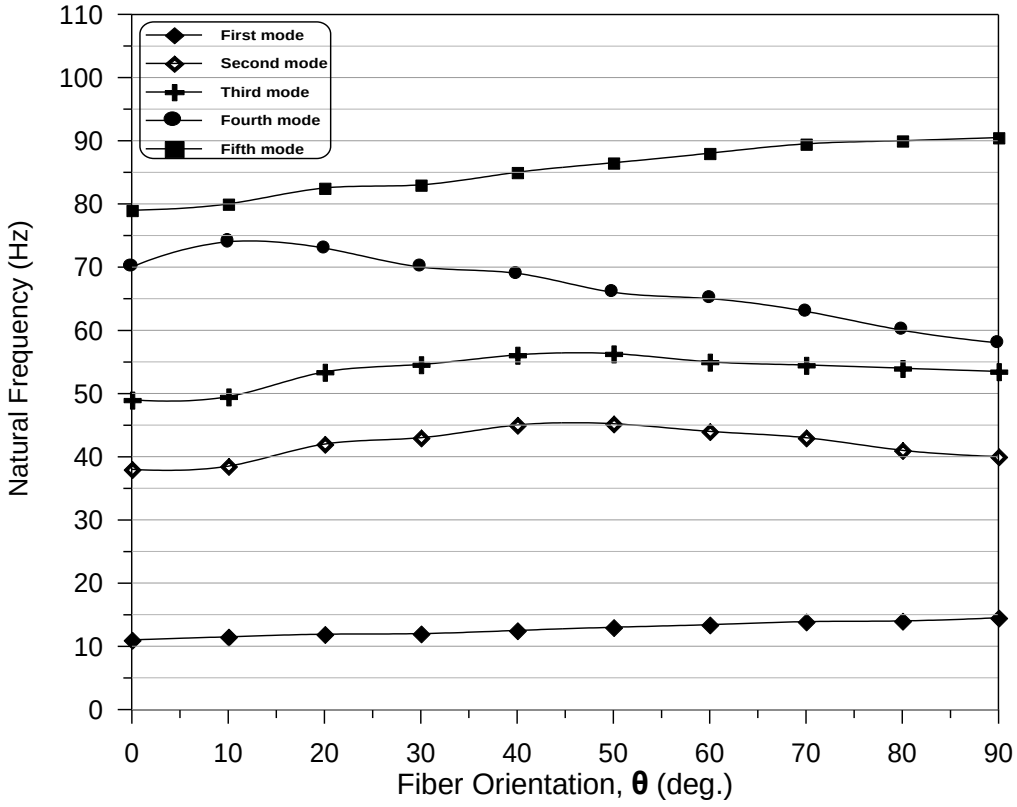


**Fig.(٤.٣٠):** Variation of natural frequency with orientation angles of Rib٥**f.**

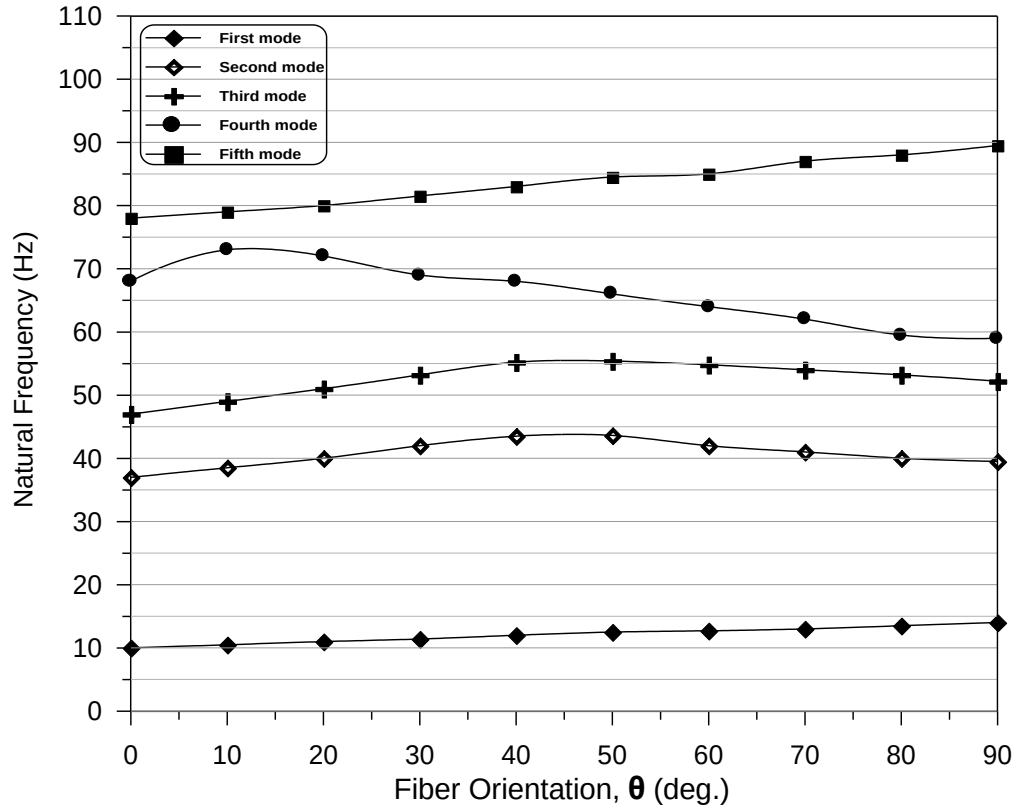


**Fig.(٤.٣١):** Variation of natural frequency with orientation angles of Rib٦**f**.

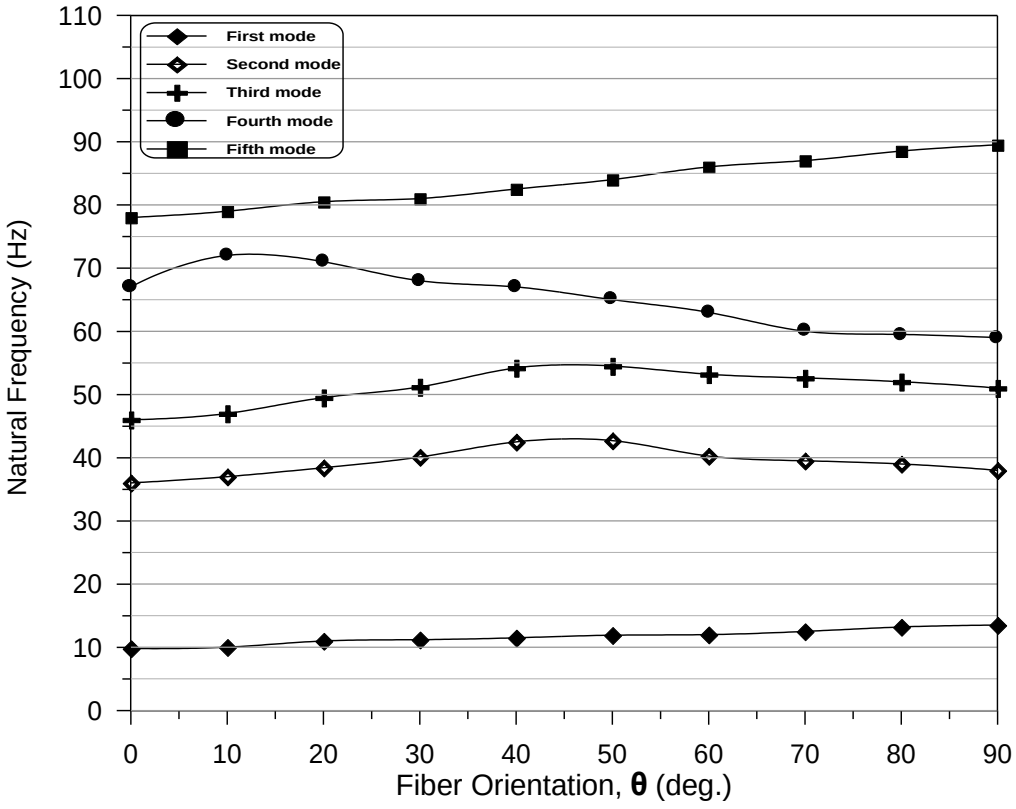


**Fig.(٤.٣٢):** Variation of natural frequency with orientation angles of Rib٧**f**.

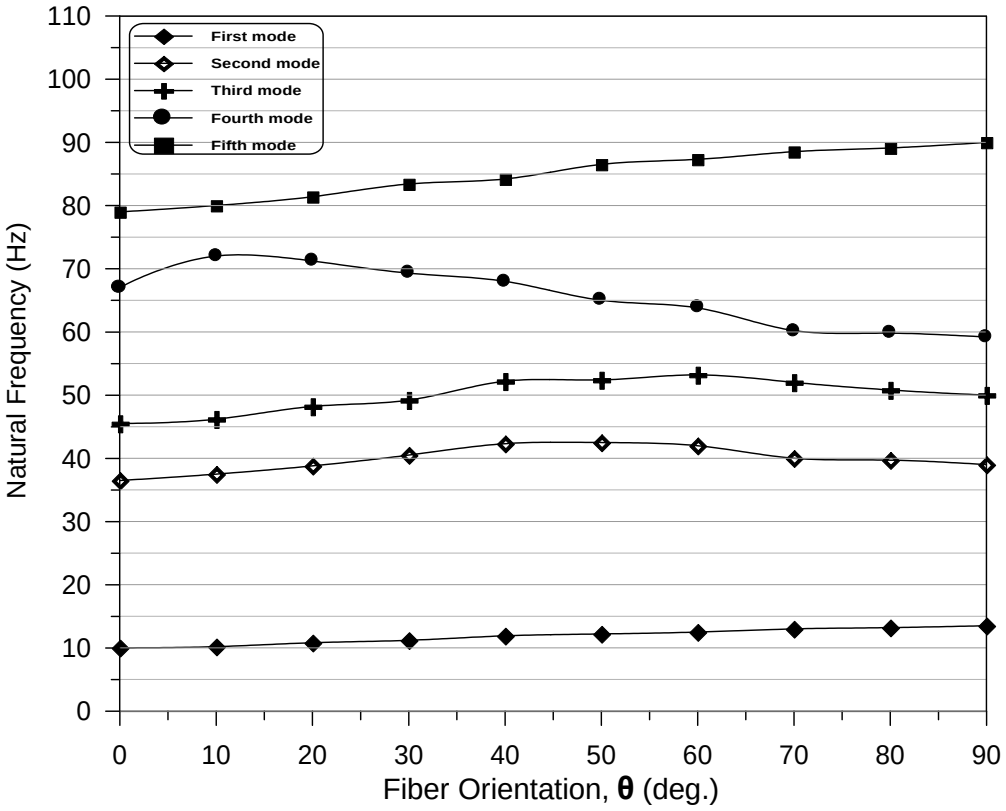


**Fig.(٤.٣٣):** Variation of natural frequency with orientation angles of Rib٨**f**.

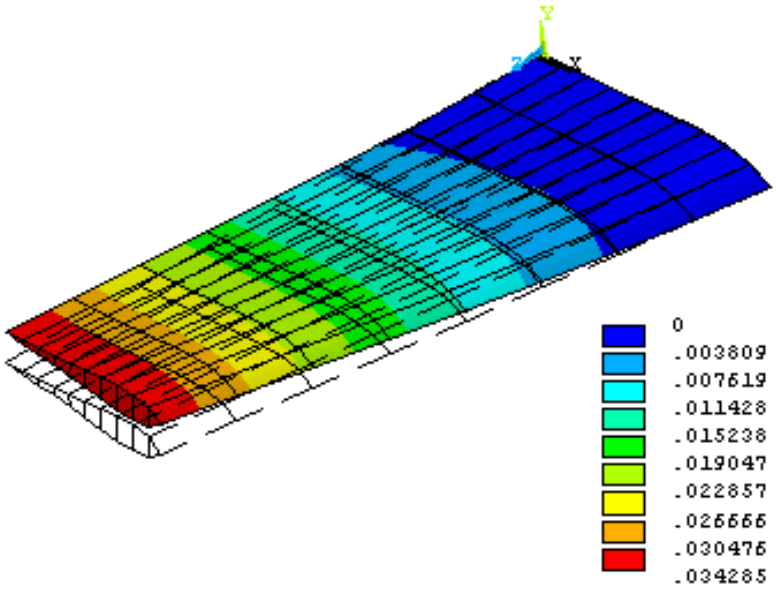


**Fig.(٤.٣٤):** Vertical displacement ($u_y$) of the first model (Rst١***OO***) in meter.

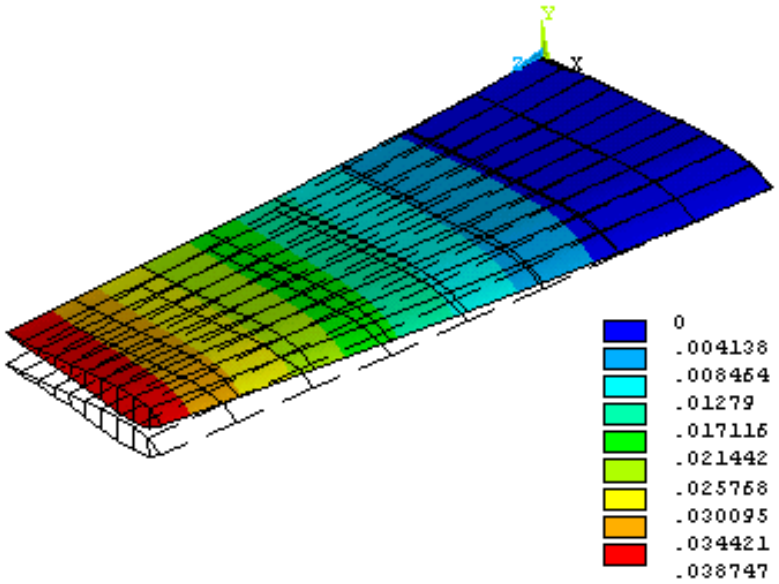


**Fig.(٤.٣٥):** Vertical displacement ($u_y$) of the second model (Rst٢***OO***) in meter.

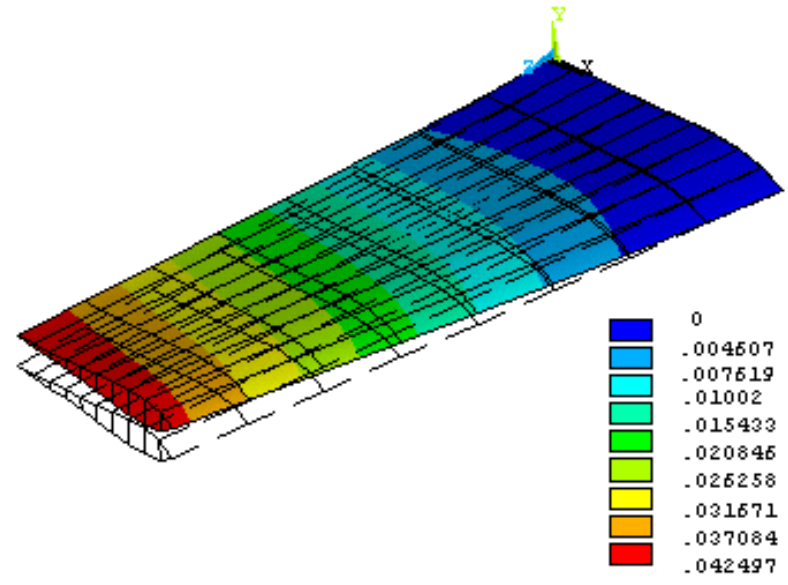


**Fig.(٤.٣٦):** Vertical displacement ($u_y$) of the third model (Rst٣***OO***) in meter.

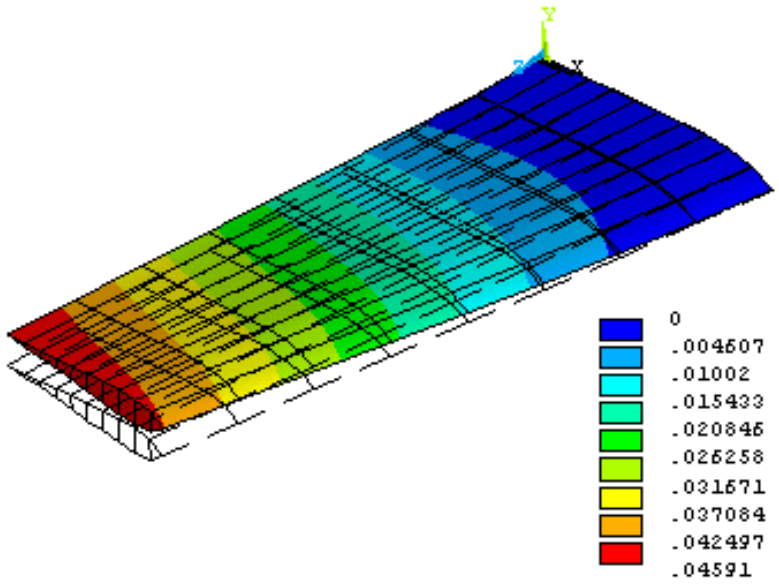


**Fig.(٤.٣٧):** Vertical displacement ($u_y$) of the fourth model (Rst٤***OO***) in meter.

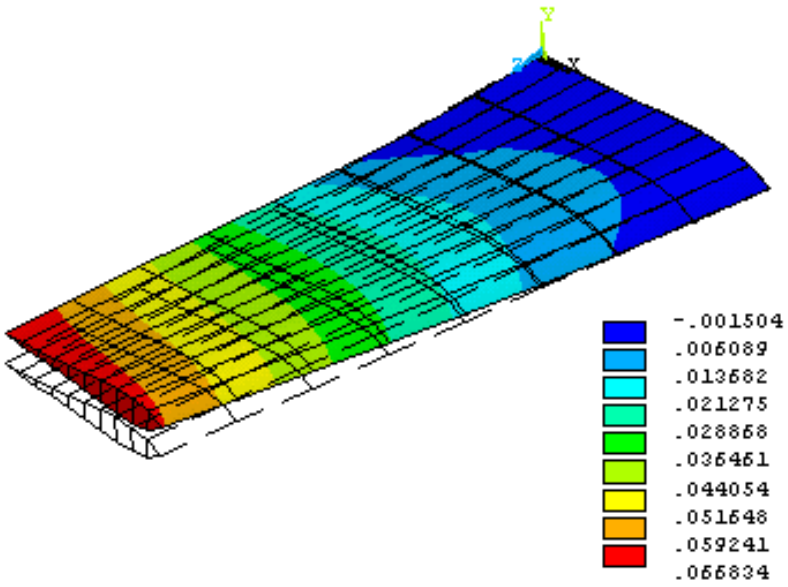


**Fig.(٤.٣٨):** Vertical displacement ($u_y$) of the fifth model (Rst١***AO***) in meter.

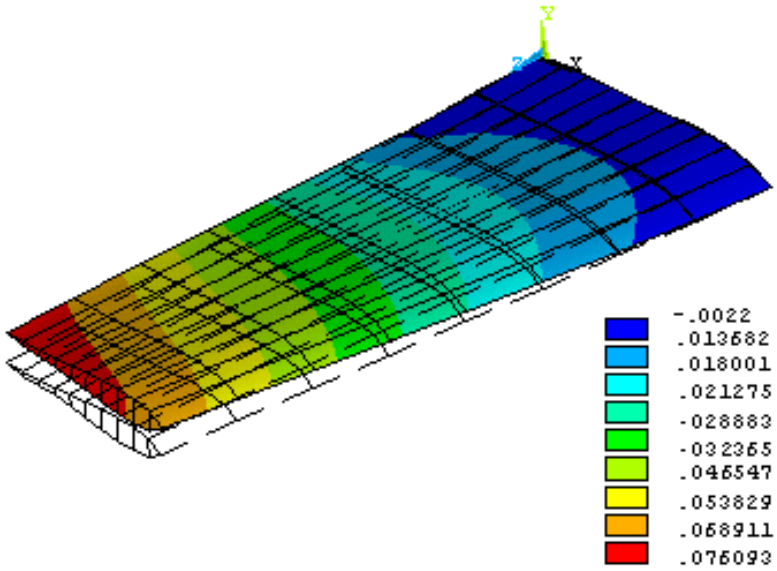


**Fig.(٤.٣٩):** Vertical displacement ($u_y$) of the sixth model (Rst٢***AO***) in meter.

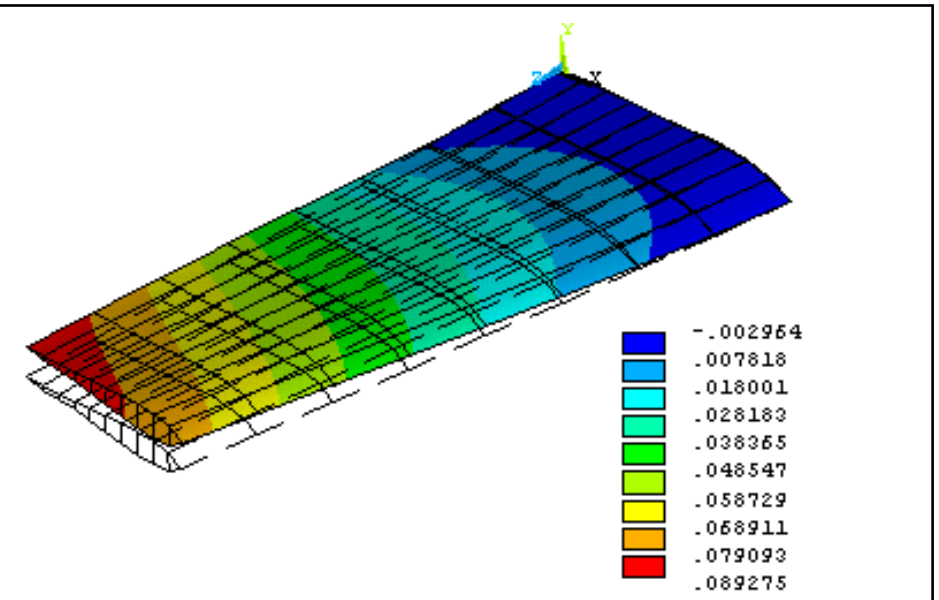


**Fig.(٤.٤٠):** Vertical displacement ($u_y$) of the seventh model (Rst٣***AO***) in mete

| | |
|---|---|
| ٣rd layer , θ = ٠, $t_i$ =٢.٩١٦ | |
| ٢nd layer, θ = ٤٥, $t_i$ =٢.٣٥٢ | |
| ١st layer, θ = ٠, $t_i$ =٢.٥١٢ | |
| Stiffeners (Spars and Ribs) | |
| ١st layer, θ = ٠, $t_i$ =٢.٨٢٦ | |
| ٢nd layer, θ = ٤٥, $t_i$ =٣.٠ | |
| ٣rd layer , θ = ٠, $t_i$ =٣.١٦ | |

a) Thickness of upper and lower skin in mm

| | |
|---|---|
| ٣rd layer , θ = ٠, $t_i$ =٢.٩٦ | |
| ٢nd layer, θ = ٤٥, $t_i$ =٣.٢١ | |
| ١st layer, θ = ٠, $t_i$ =٢.٨١ | |

b) Spar layers thickness in mm

| | |
|---|---|
| ٣rd layer , θ = ٩٠, $t_i$ =٣.٠٩ | |
| ٢nd layer, θ = ٤٥, $t_i$ =٣.٠٣ | |
| ١st layer, θ = ٩٠, $t_i$ =٢.٨٥ | |

c) Rib layers thickness in mm

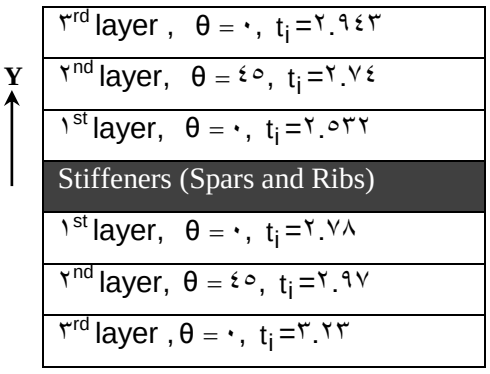


a) Thickness of upper and lower skin in mm

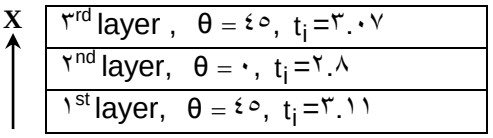


b) Spar layers thickness in mm

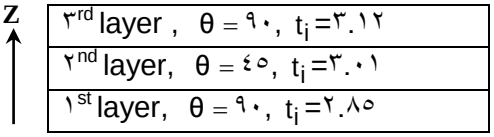


c) Rib layers thickness in mm

**Fig.(٤.٤٢):** Optimum layers thicknesses and its arrangements for composite wing structure of Rst٢***OO***.

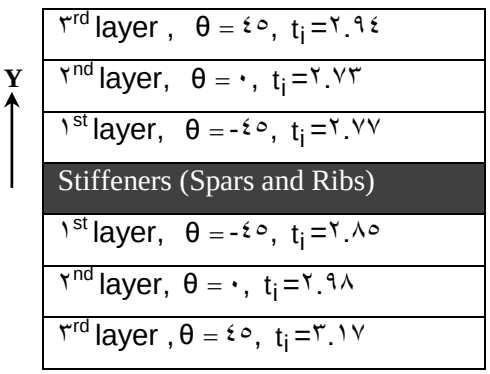


a) Thickness of upper and

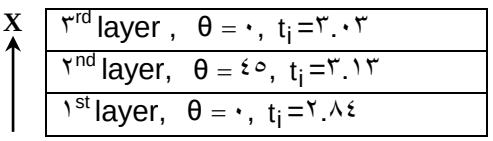


b) Spar layers thickness in mm

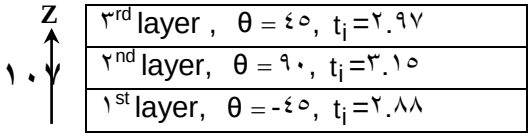


c) Rib layers thickness

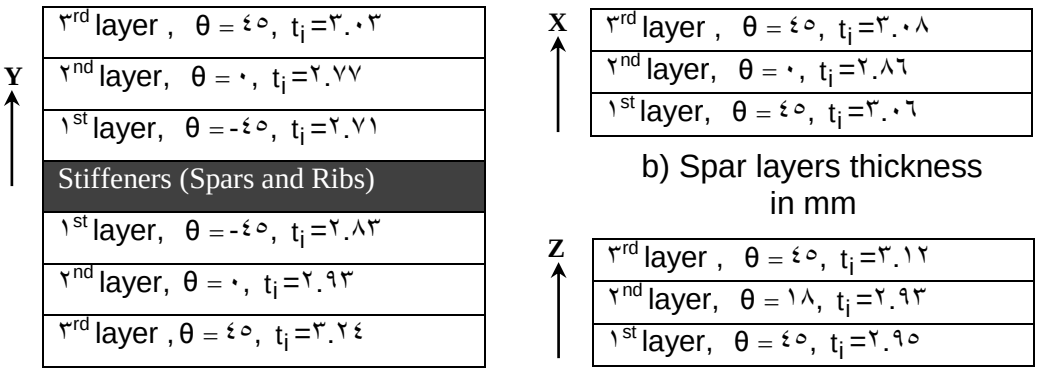


a) Thickness of upper and lower skin in mm

b) Spar layers thickness in mm

c) Rib layers thickness in mm

**Fig.(٤.٤٤ ):** Optimum layers thicknesses and its arrangements for composite wing structure of Rst٤***OO***.

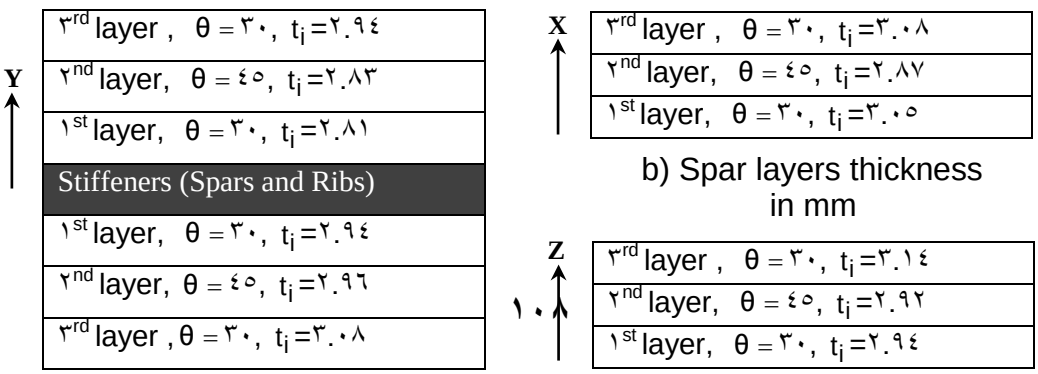


a) Thickness of upper and

b) Spar layers thickness in mm

c) Rib layers thickness

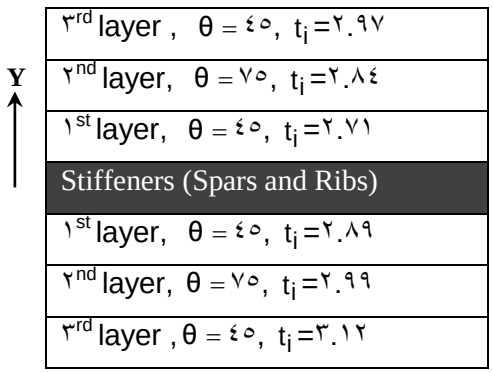


a) Thickness of upper and lower skin in mm

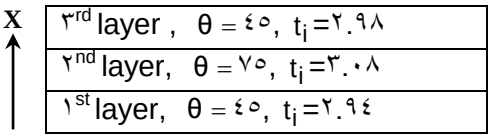


b) Spar layers thickness in mm

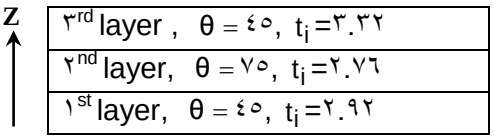


c) Rib layers thickness in mm

**Fig.(٤.٤٦):** Optimum layers thicknesses and its arrangements for composite wing structure of Rst٢***AO***.

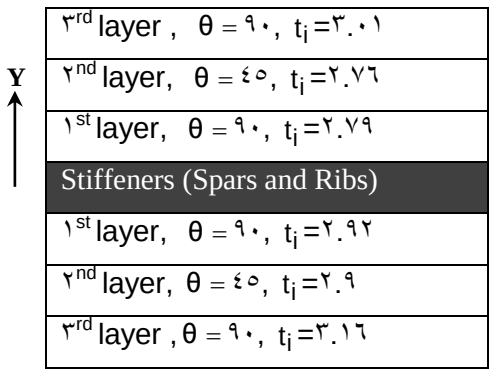


a) Thickness of upper and lower skin in mm

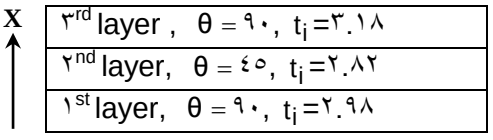


b) Spar layers thickness in mm

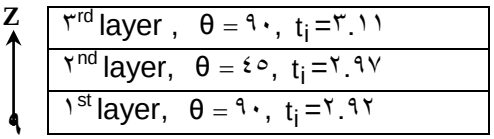


c) Rib layers thickness in mm

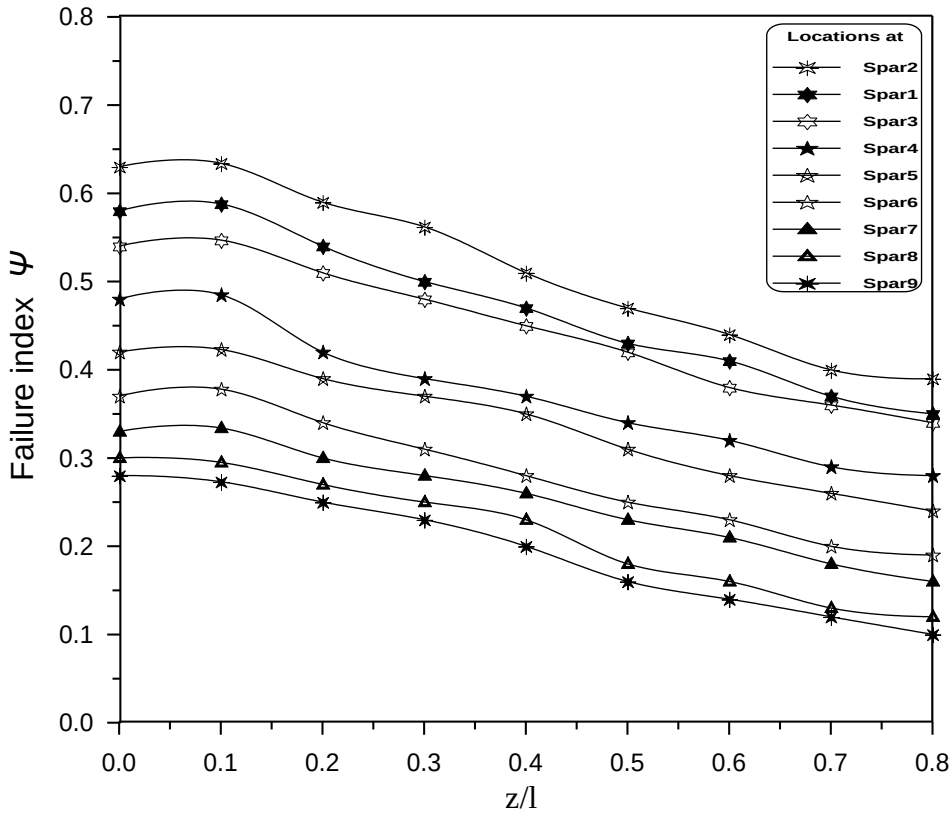


**Fig.(٤.٤٨):** Distribution of maximum Tsai-Wu failure index on the lower skin of Rst١١***OO***.

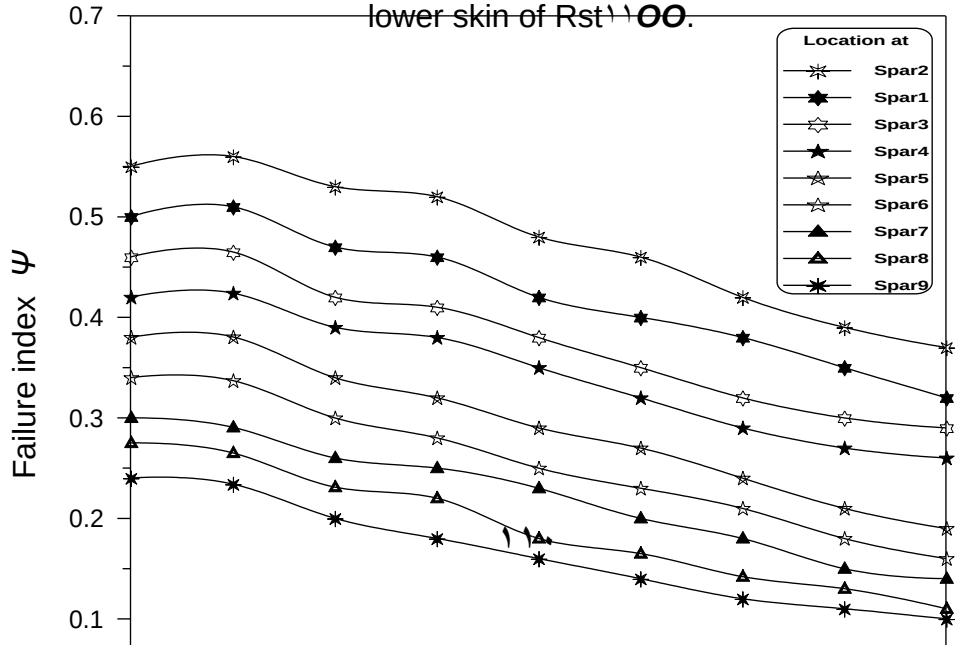

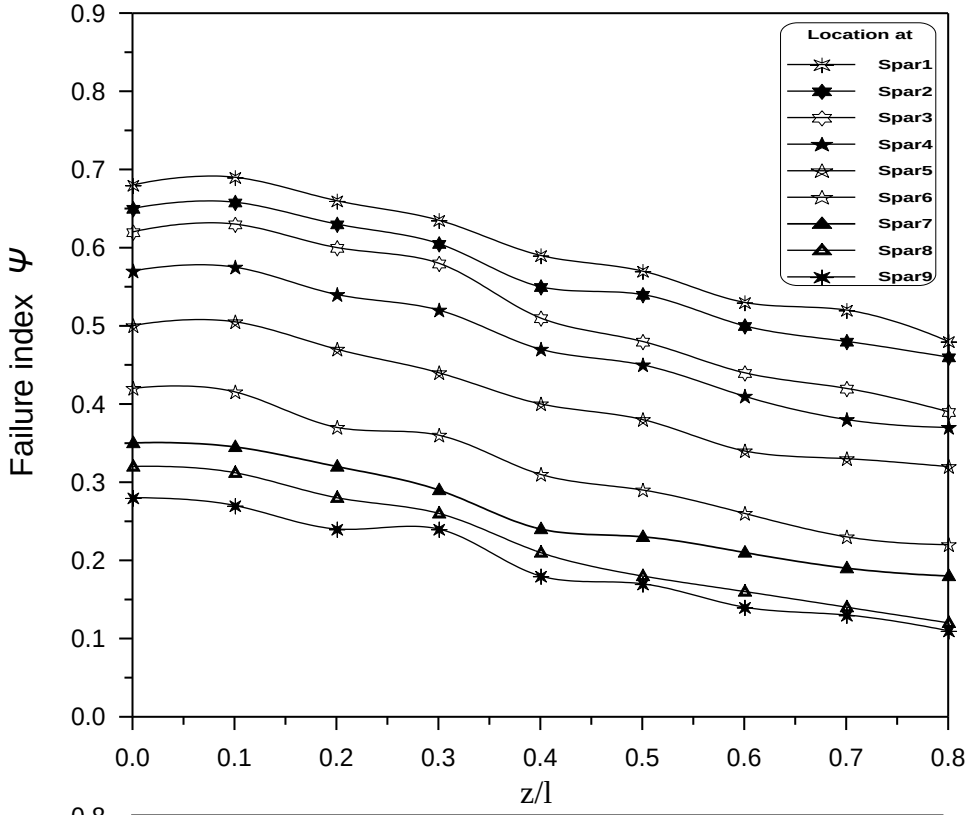


**Fig.(٤.٥٠):** Distribution of maximum Tsai-Wu failure index on the lower skin of Rst٢٢***OO***.

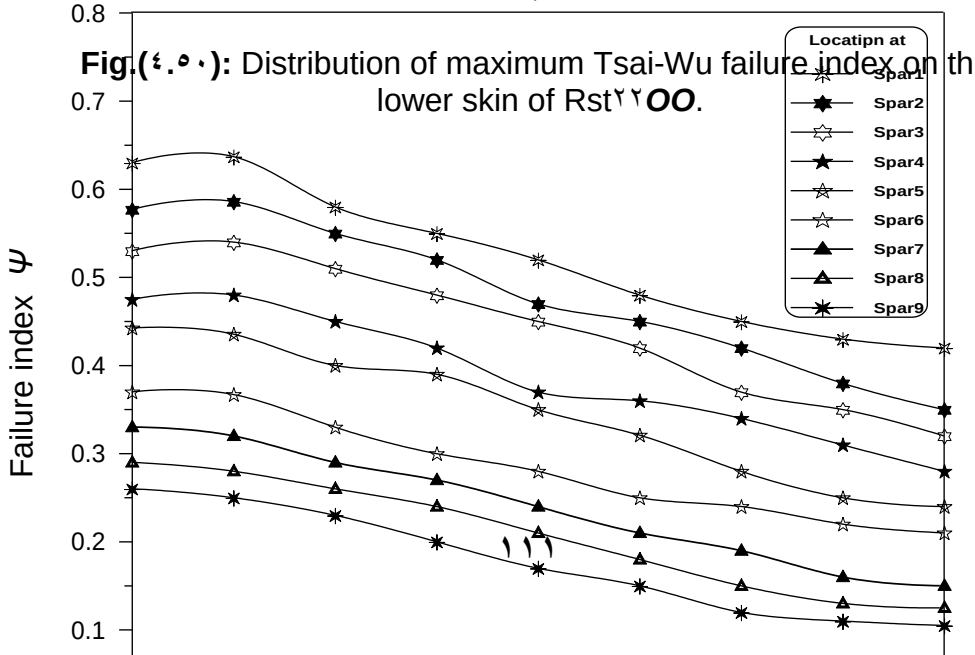

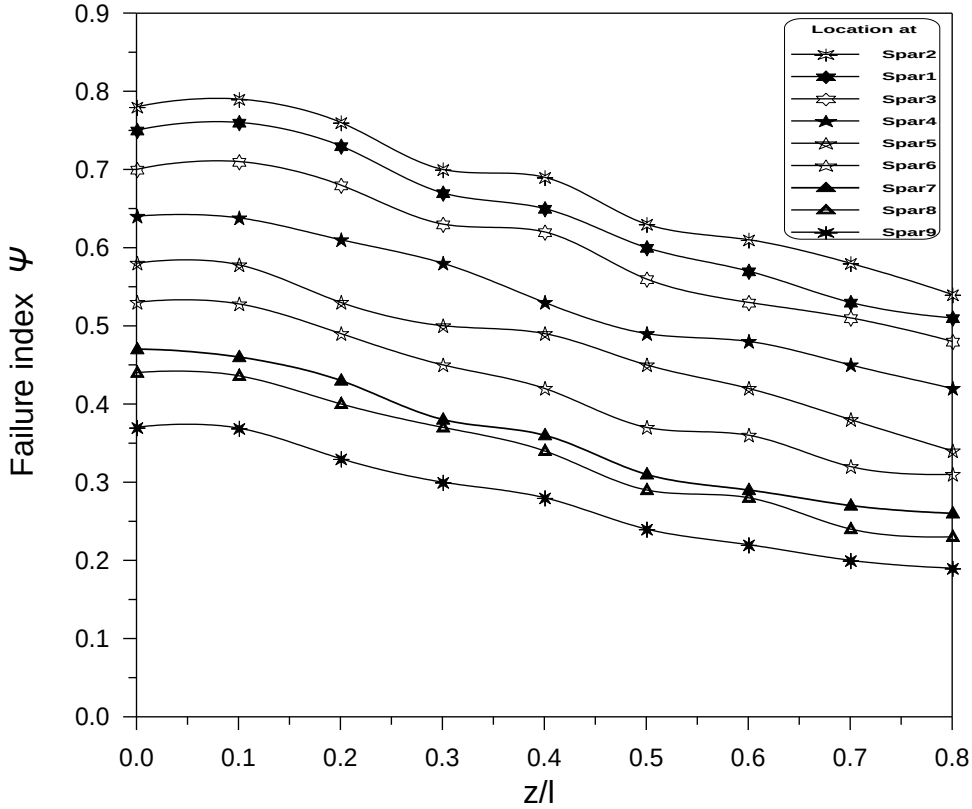
Location at
Spar2
Spar1
Spar3
Spar4
Spar5
Spar6
Spar7
Spar8
Spar9
Failure index ψ
z/l
0.0
0.1
0.2
0.3
0.4
0.5
0.6
0.7
0.8
0.9

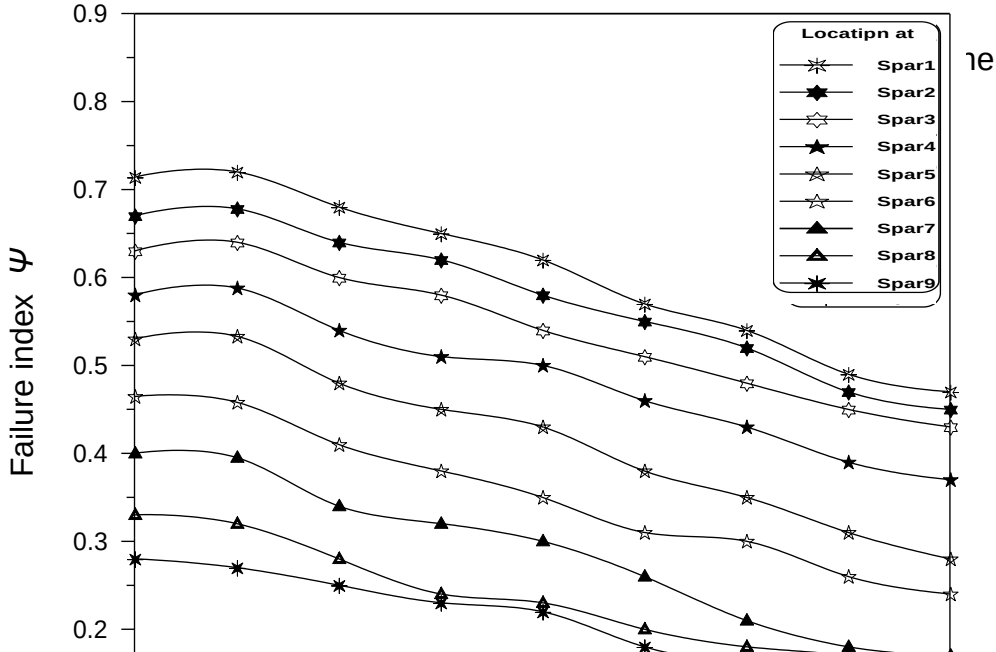
Locatipn at
Spar1
Spar2
Spar3
Spar4
Spar5
Spar6
Spar7
Spar8
Spar9
Failure index ψ
0.2
0.3
0.4
0.5
0.6
0.7
0.8
0.9

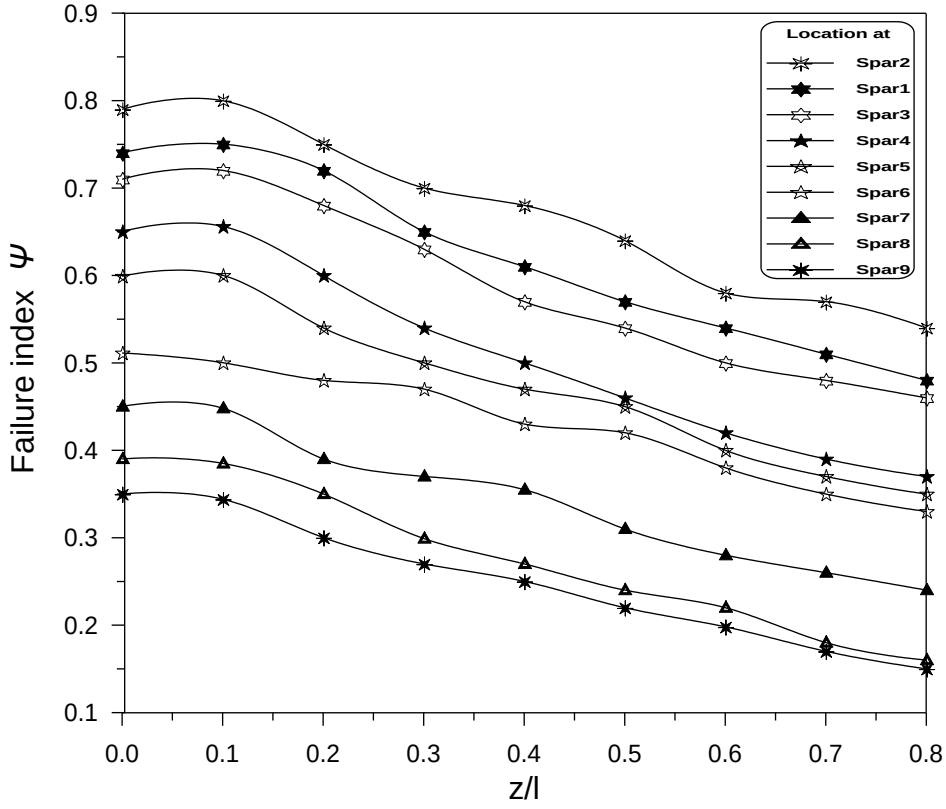


**Fig.(٤.٥٤):** Distribution of maximum Tsai-Wu failure index on the lower skin of Rst٤٤***OO***.

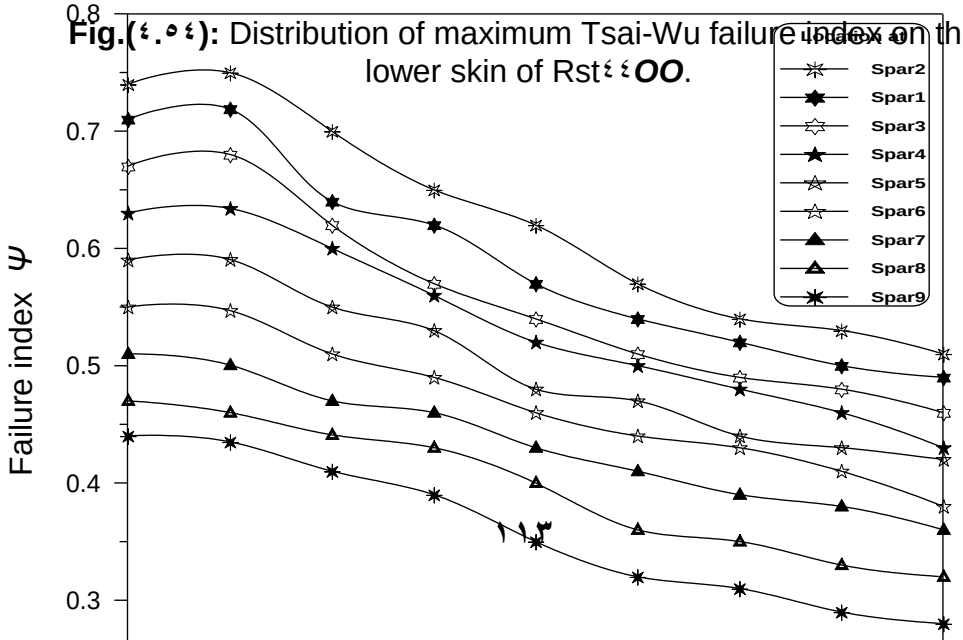

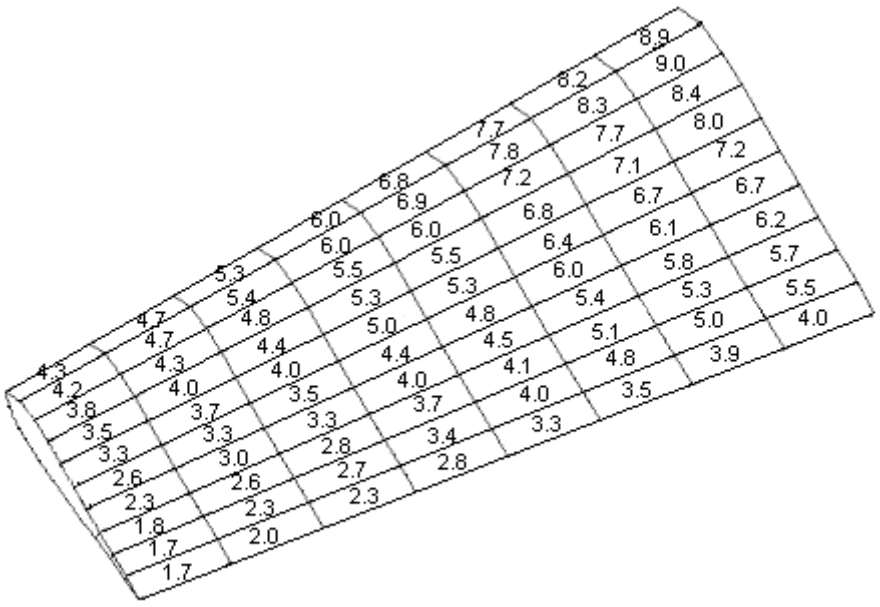


**Fig.(٤.٥٦):**Global tapered thickness distribution at the lower surface of Rst١١***OOtap***.

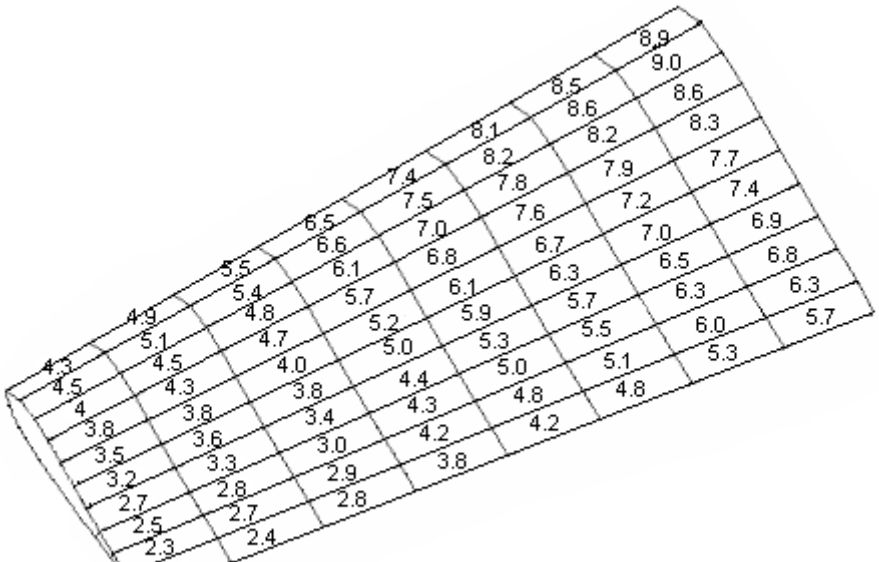

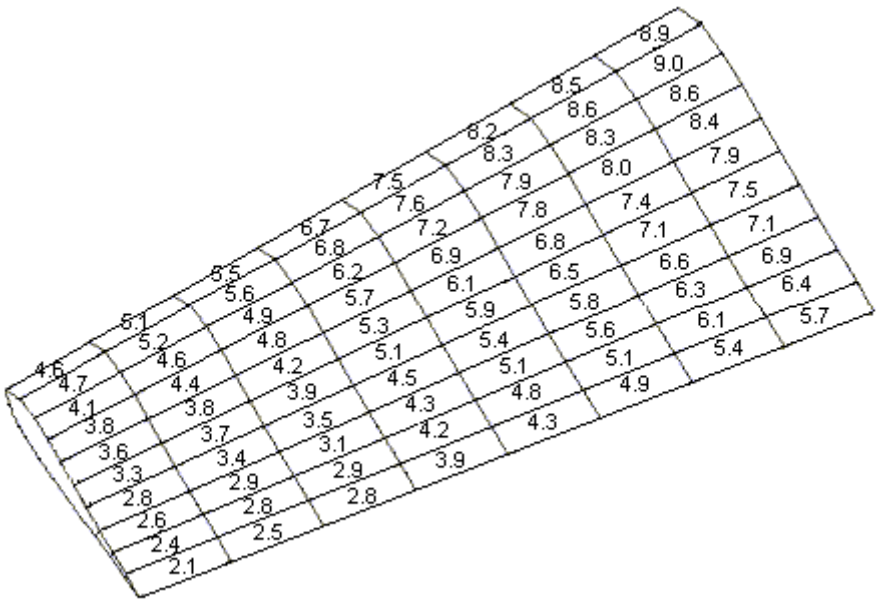


**Fig.(٤.٥٨):**Global tapered thickness distribution at the lower surface of Rst٣٣***OOtap***.

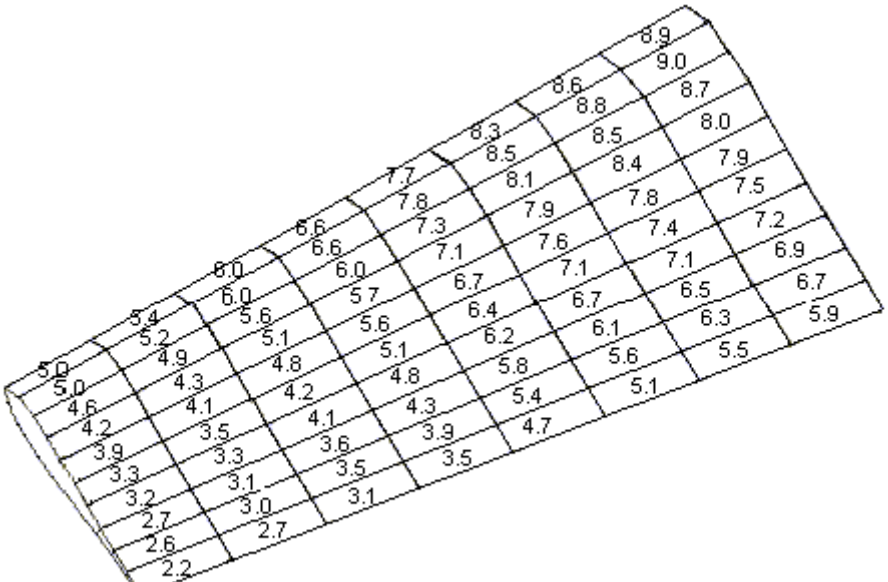

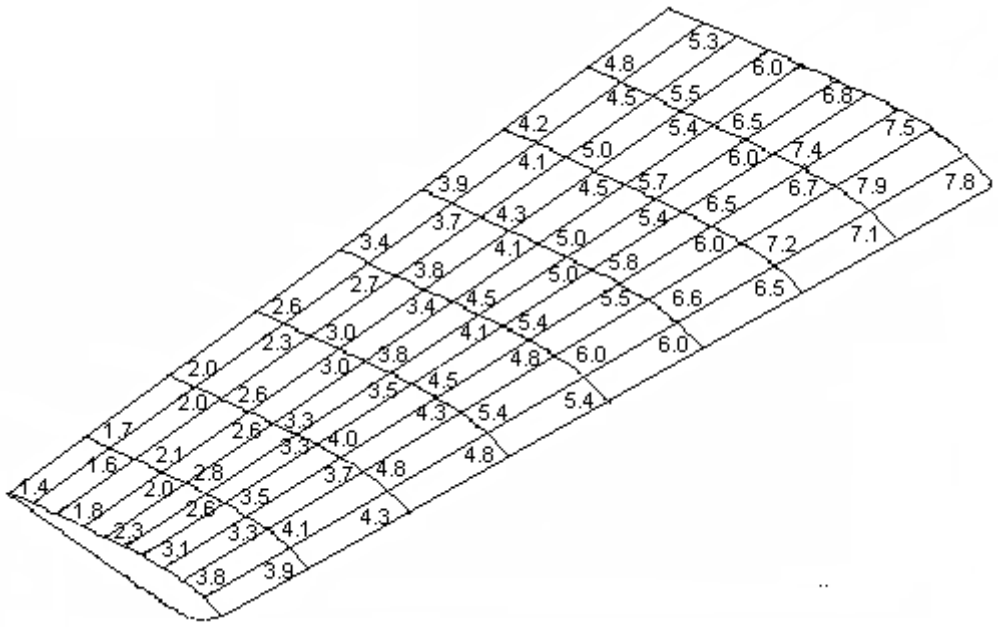

**Fig.(٤.٦٠):**Global tapered thickness distribution at the upper surface of Rst١١***OOtap***.

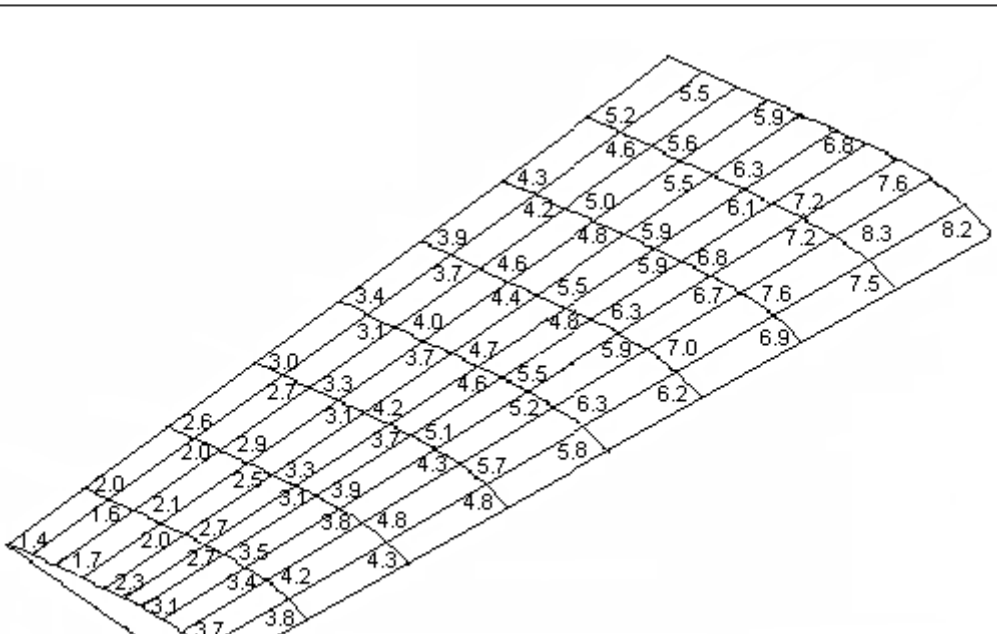

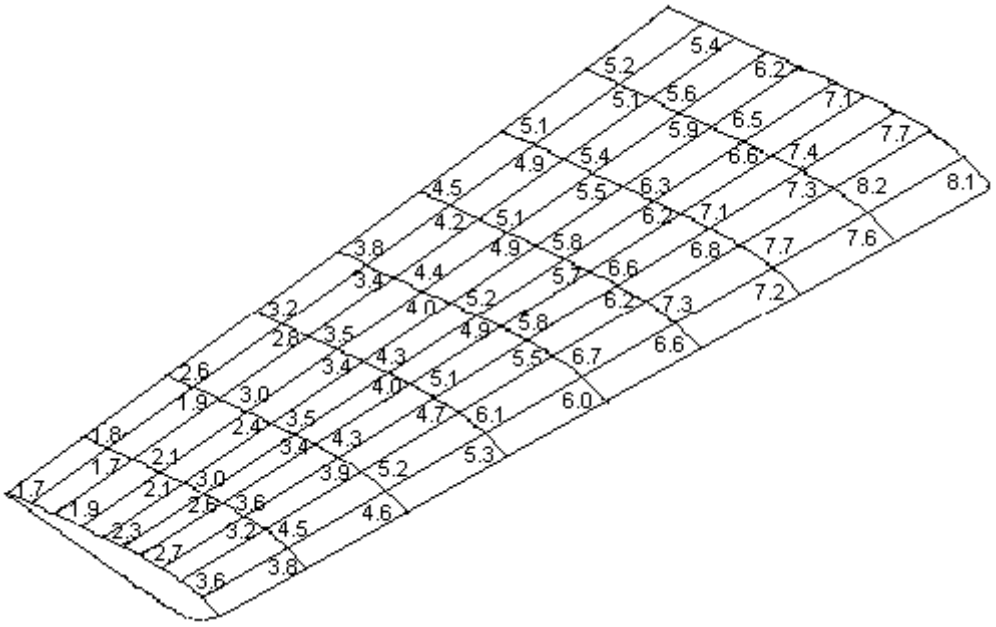


**Fig.(٤.٦٢ ):**Global tapered thickness distribution at the upper surface of Rst٣٣***OOtap***.

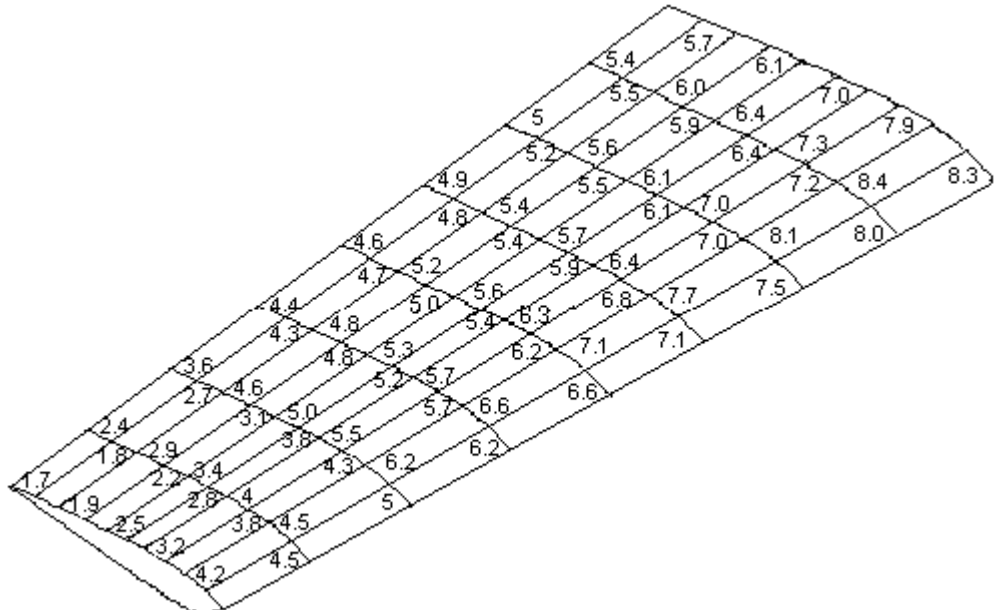

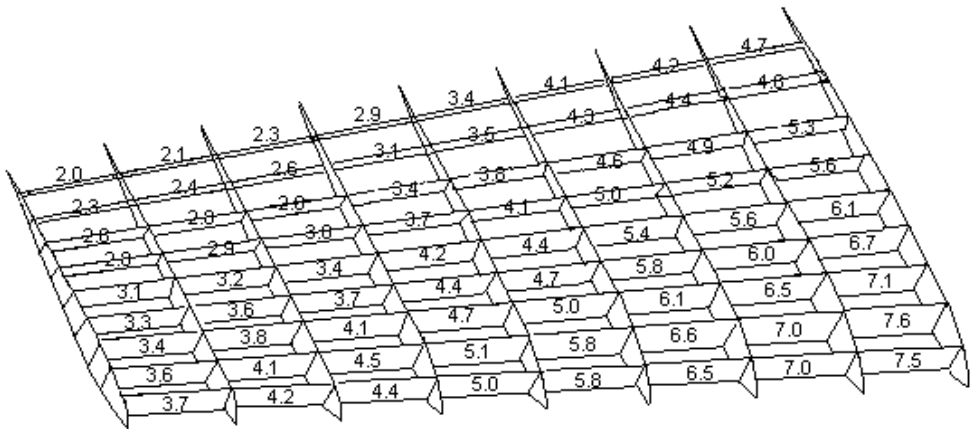


**Fig.(٤.٦٤):** Tapered thickness distribution of spars element of Rst١١***OOtap***.

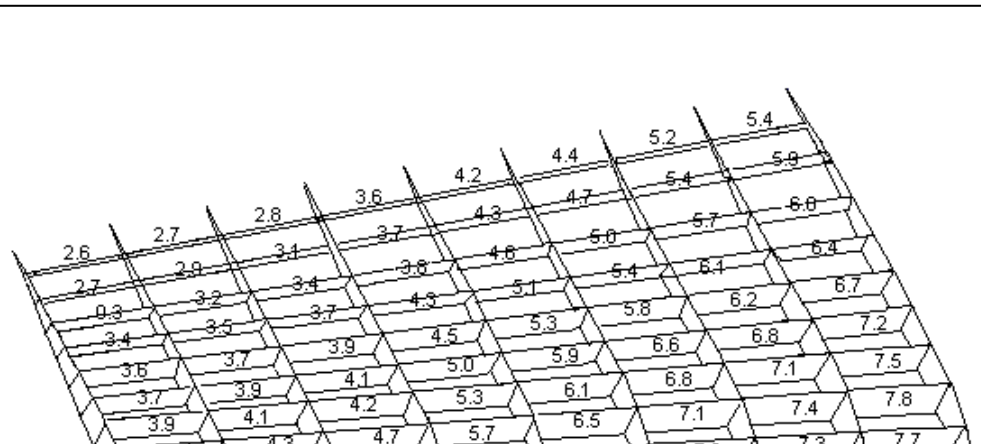

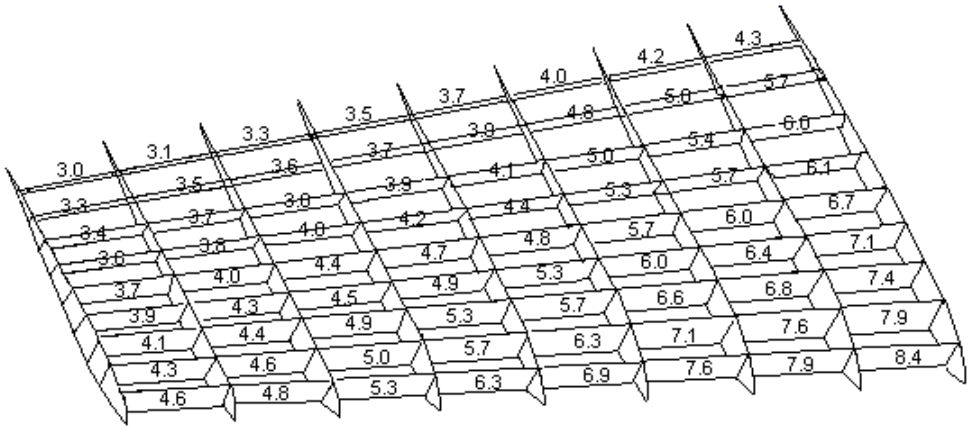


**Fig.(٤.٦٦):** Tapered thickness distribution of spars element of Rst٣٣***OOtap***.

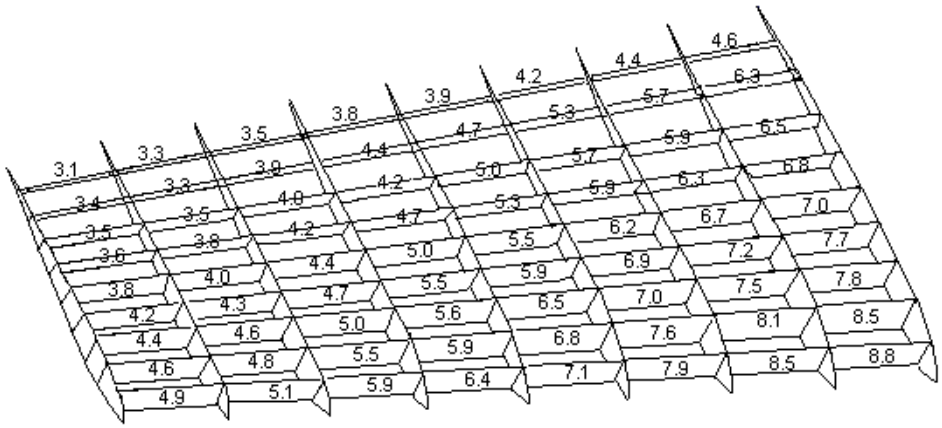




**Fig.(٤.٦٧):** Tapered thickness distribution of spars element of Rst٤٤***OOtap***.

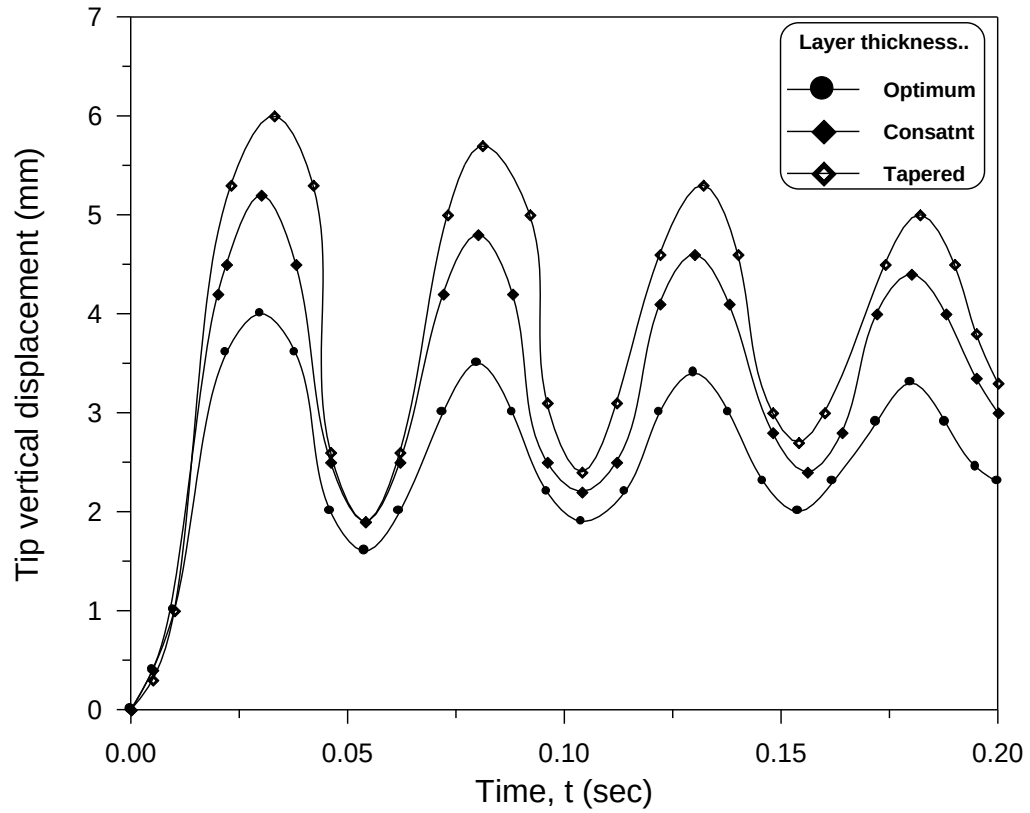


**Fig.(٤.٦٨):**The vertical displacement of Rst١**OO**,Rst١١**OO** , and Rst١١***OOtap***.

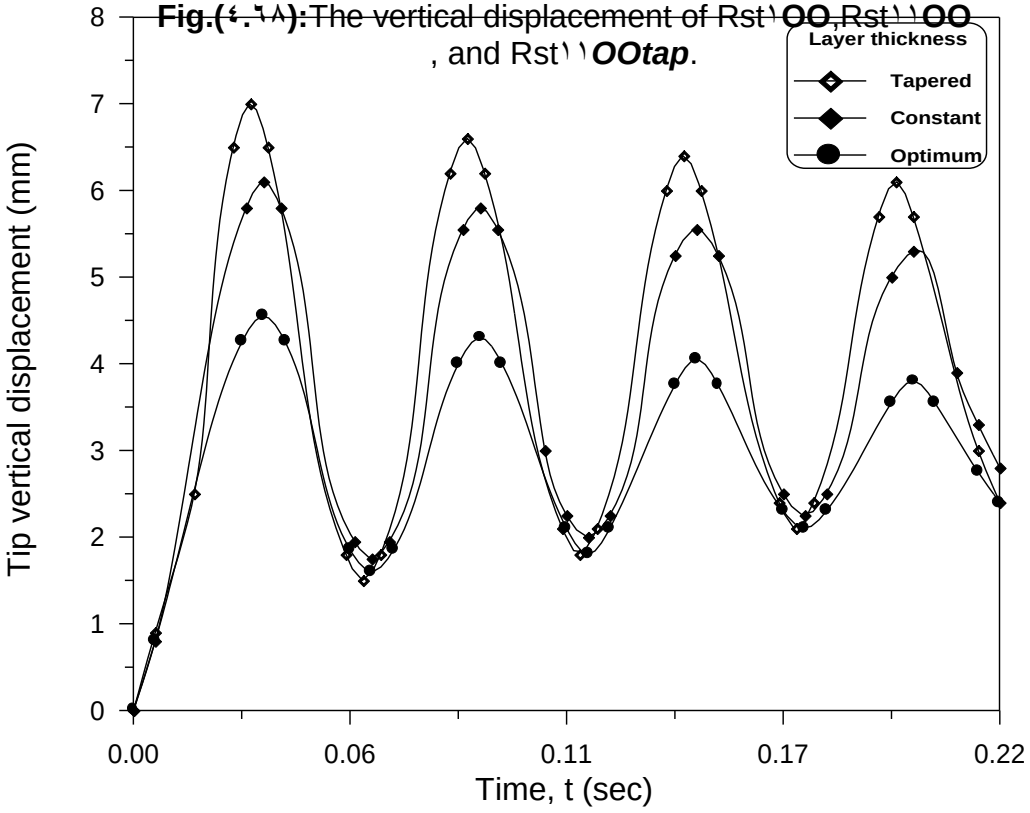


**Fig.(٤.٦٩):**The vertical displacement of Rst٢**OO**,Rst٢٢**OO** , and Rst٢٠٢***OOtap***.

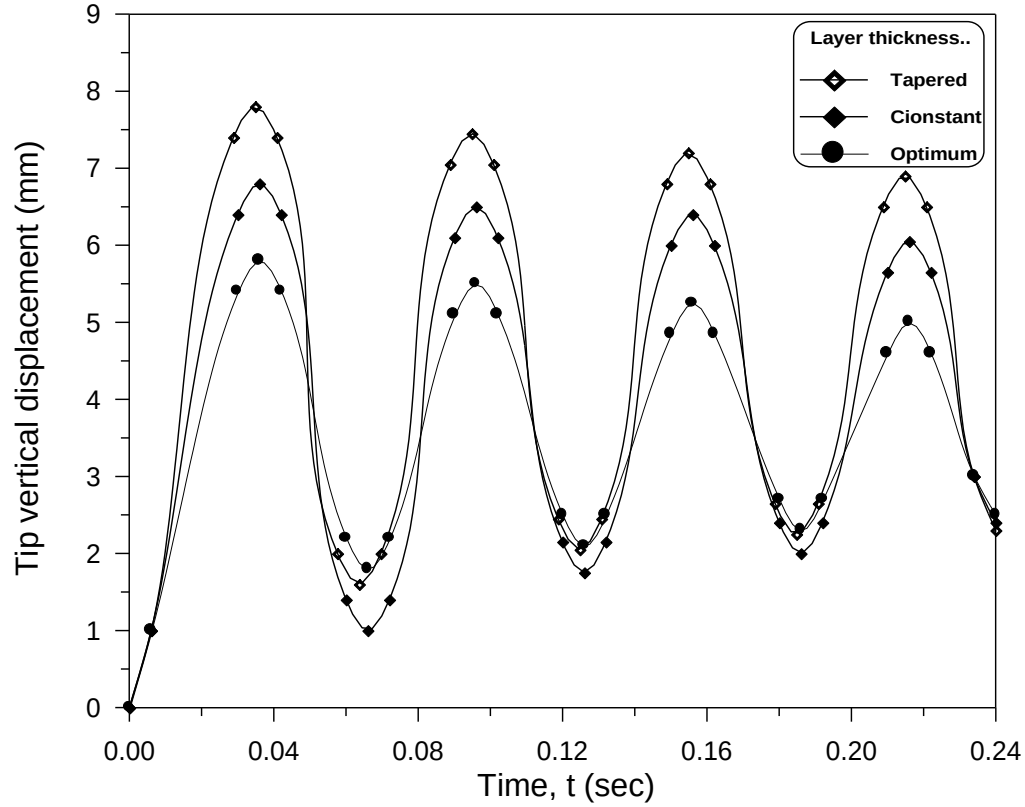


**Fig.(٤.٧٠):**The vertical displacement of Rst٣**OO**,Rst٣٣**OO** , and Rst٣٣***OOtap***.

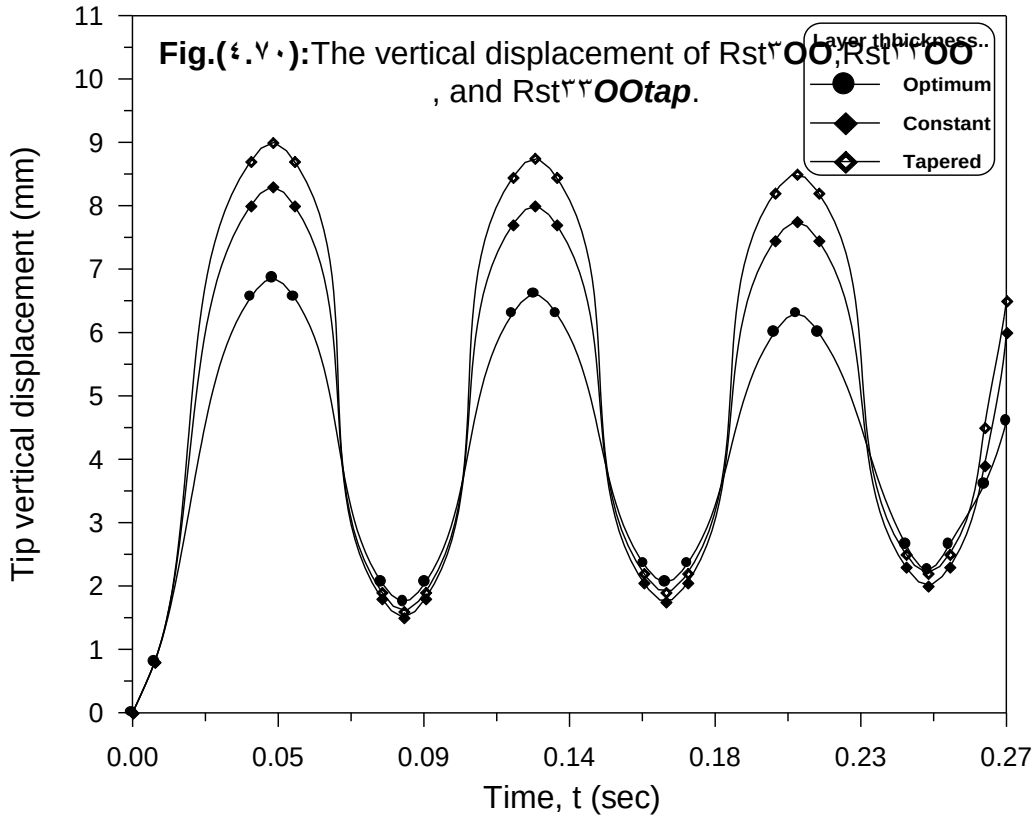


**Fig.(٤.٧١):**The vertical displacement of Rst٤**OO**,Rst٤٤**OO** , and Rst٤٤***OOtap***.

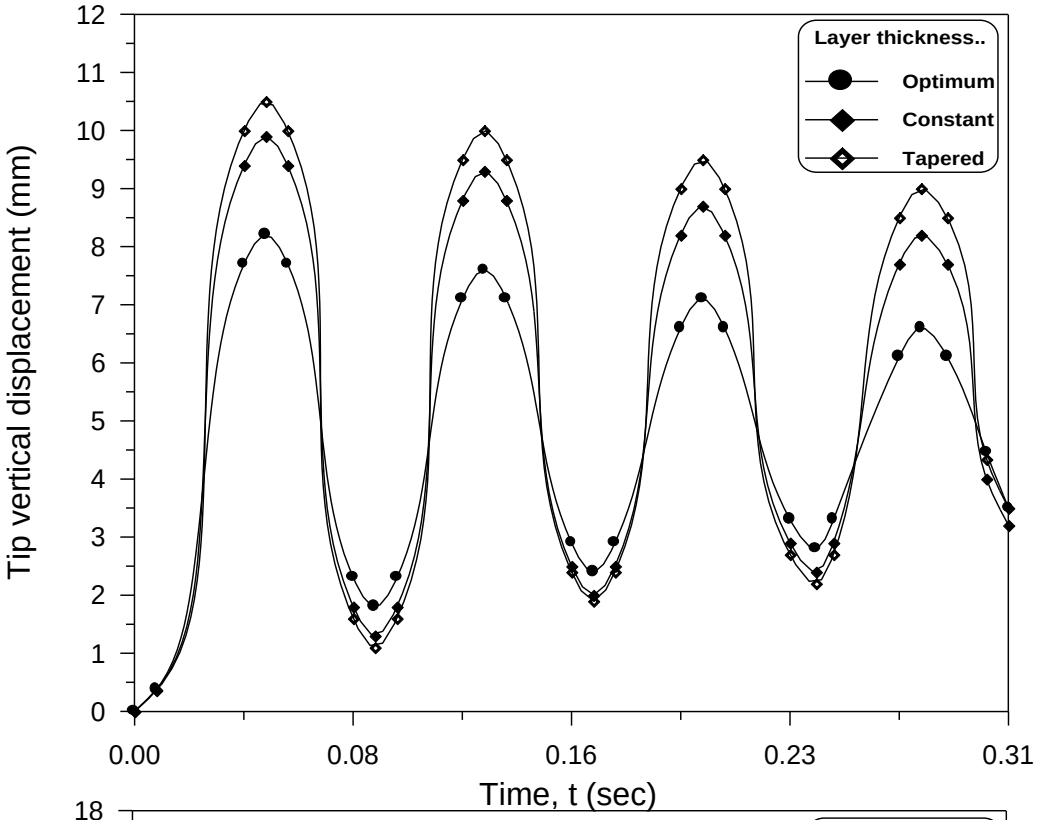


**Fig.(٤.٧٢):**The vertical displacement of Rst**AO**,Rst١١**AO** , and Rst١١***AOtap***.

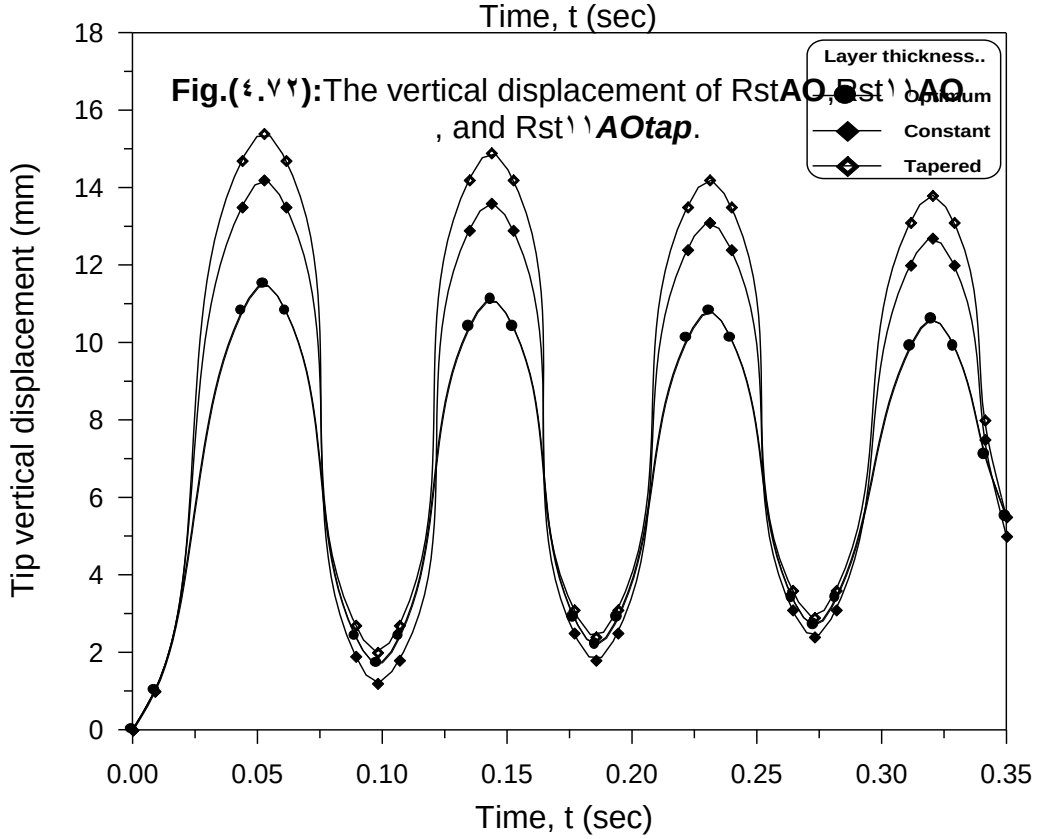


**Fig.(٤.٧٣):**The vertical displacement of Rst٢**AO**,Rst٢٢**AO** , and Rst٢٢***AOtap***.

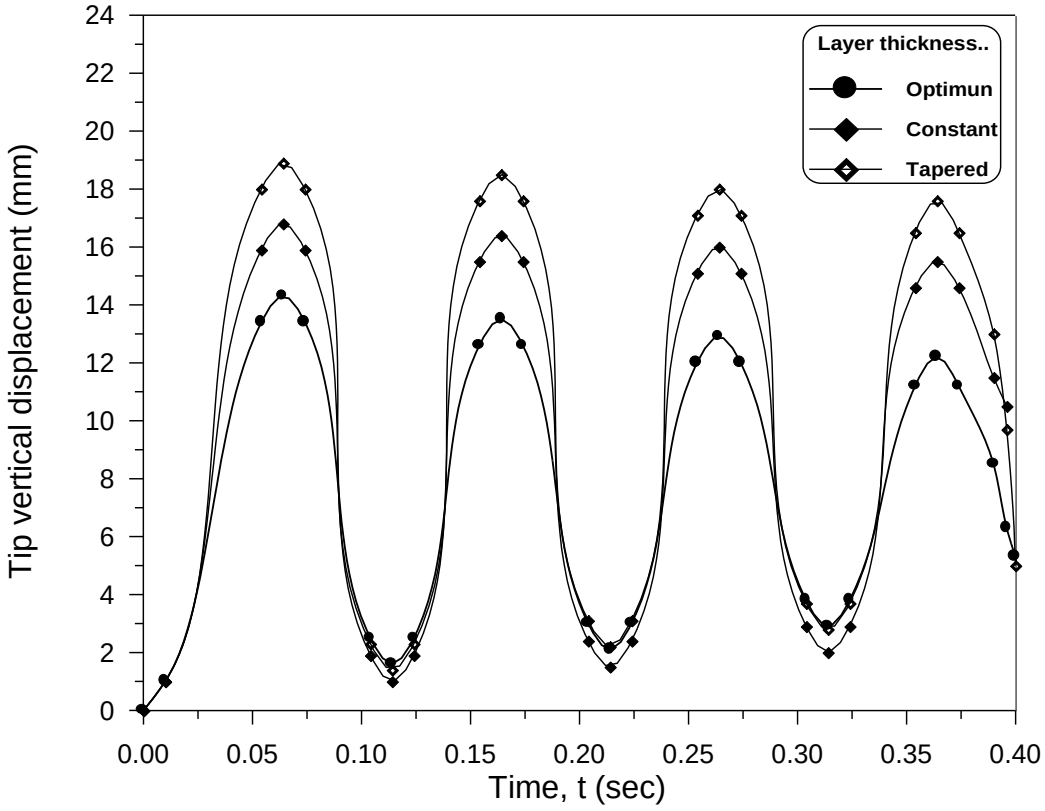


**Fig.(٤.٧٤):** The vertical displacement of Rst٣**AO**,Rst٣٣**AO** , and Rst٣٣***AOtap***.

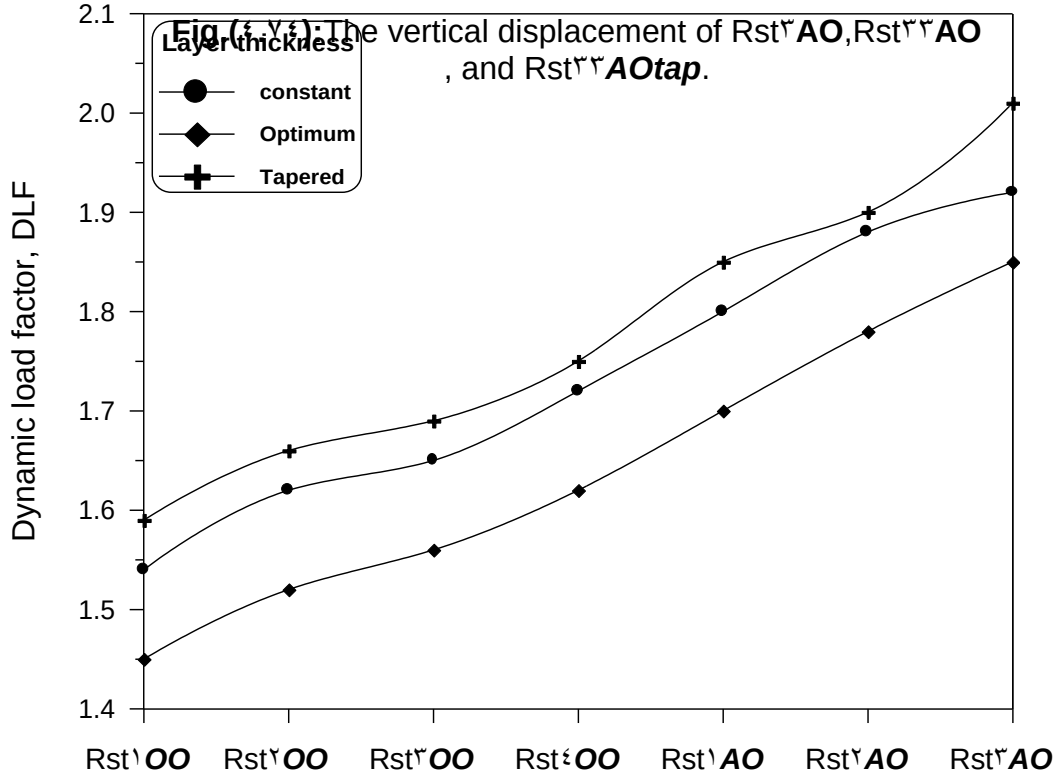


**Fig.(٤.٧٥):** Dynamic load factor of the models for different layer thicknesses

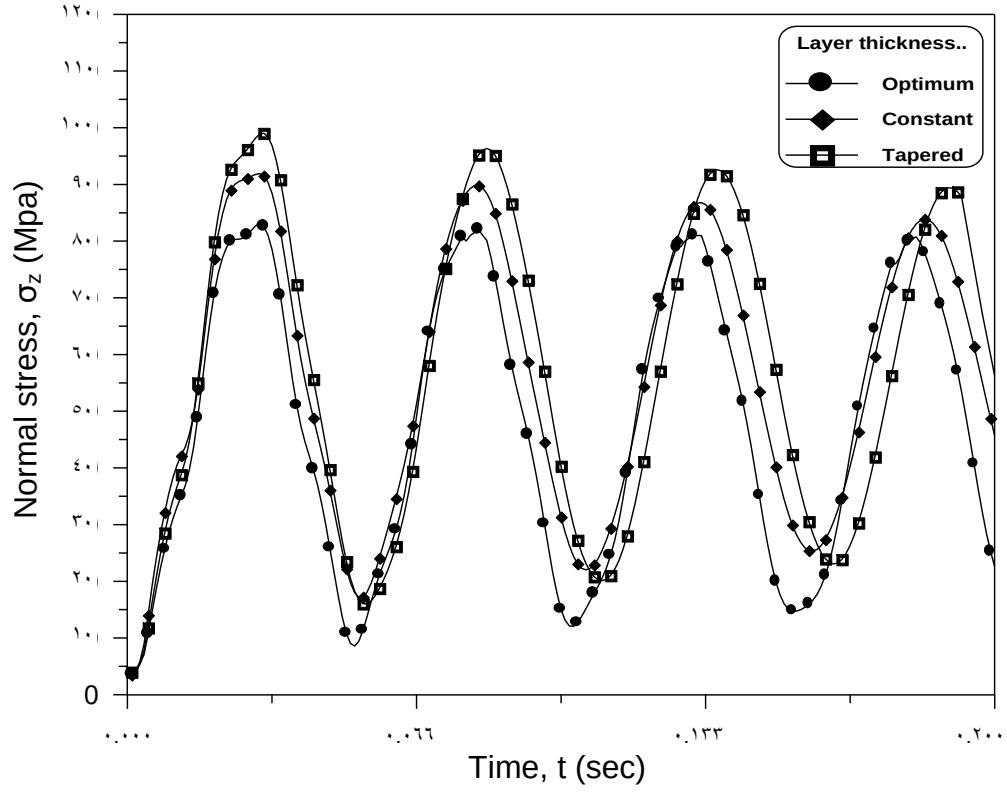


**Fig.(٤.٧٦)**: Dynamic response of maximum normal stress at different layer thicknesses for the first model.

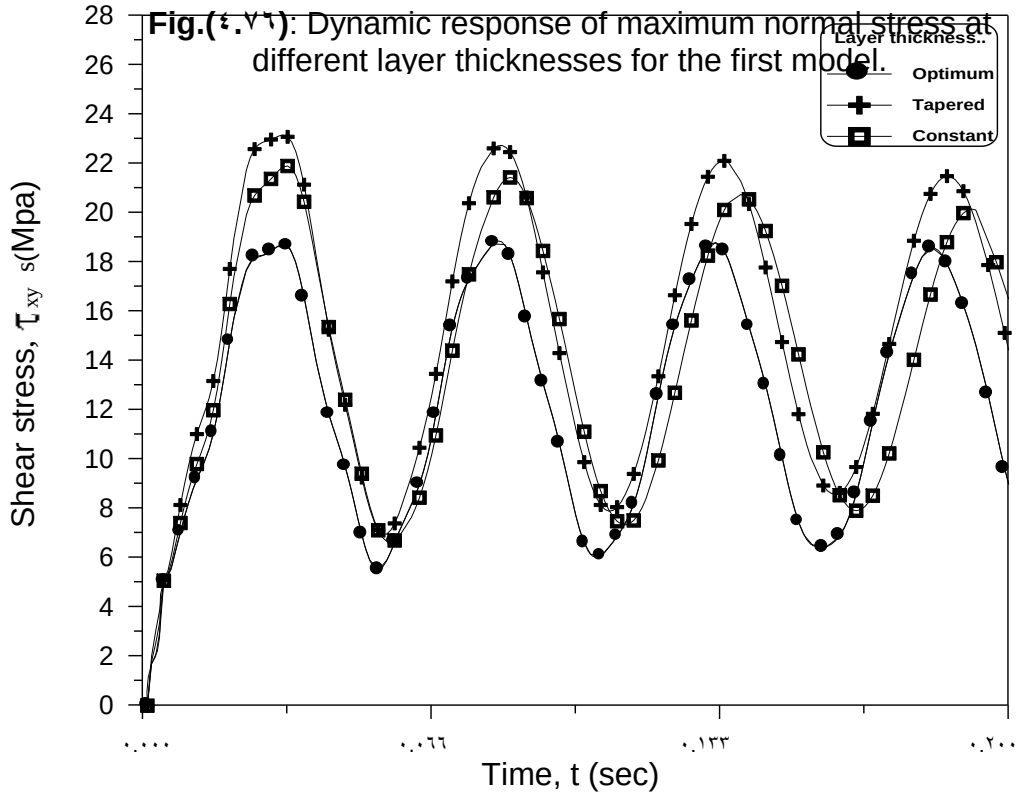


**Fig.(٤.٧٧):**Dynamic response of maximum shear stress at different layer thickness for the first model.

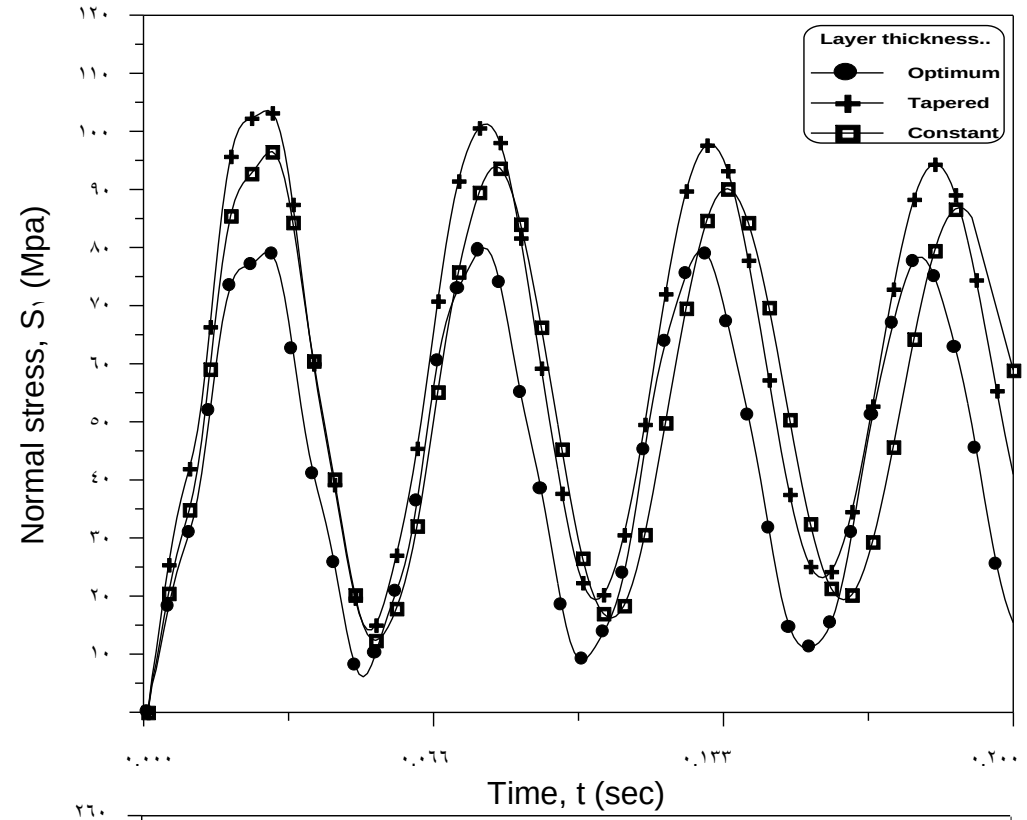


**Fig.(٤.٧٨):** Dynamic response of maximum principal stress at different layer thickness for the first model.

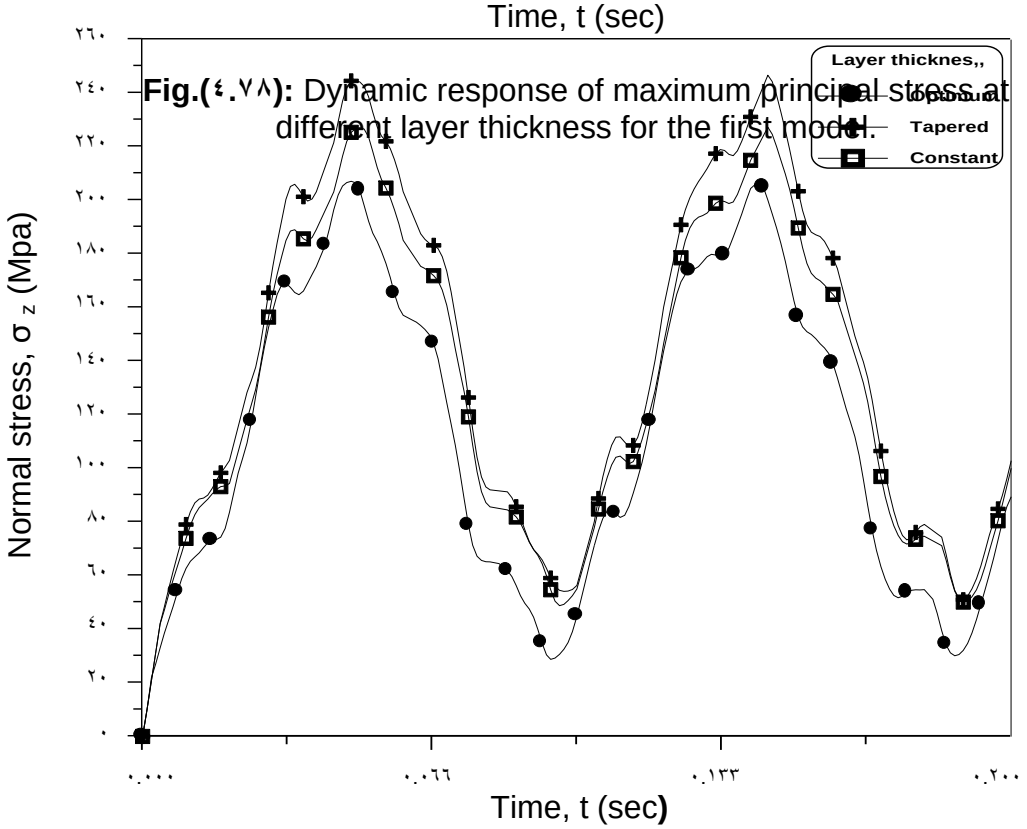


**Fig.(٤.٧٩)**: Dynamic response of maximum normal stress at different layer thicknesses for the seventh model.

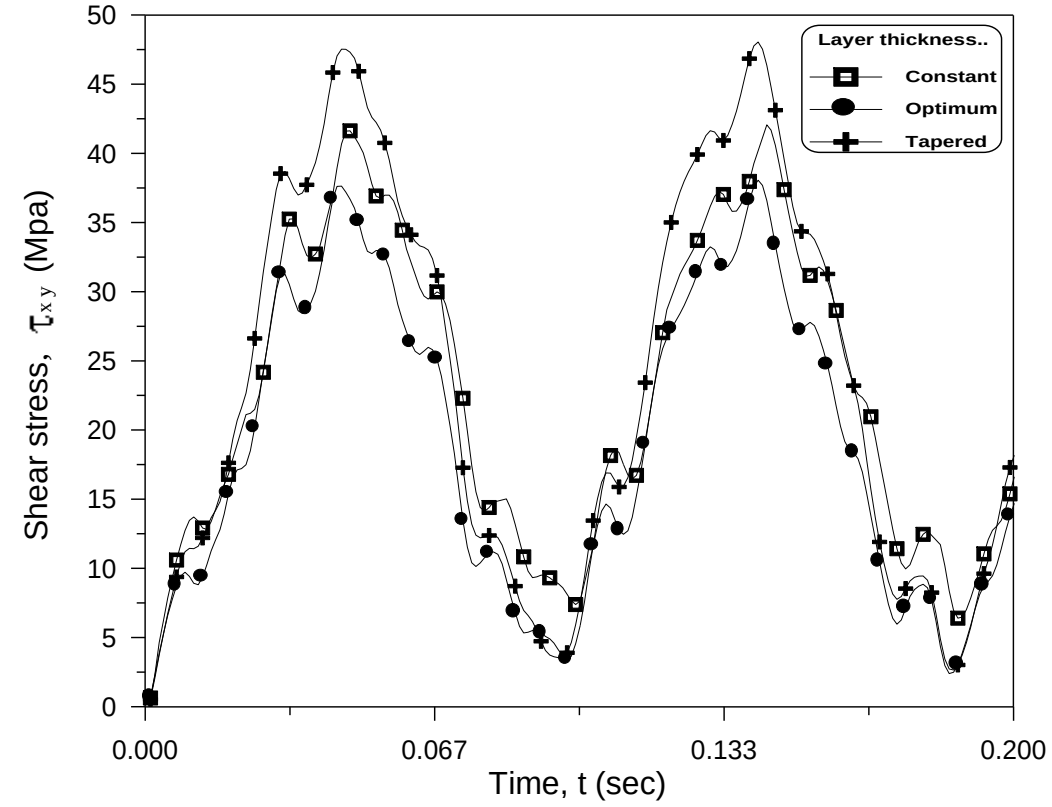


**Fig.(٤.٨٠)**: Dynamic response of maximum shear stress at different layer thicknesses for the seventh model.

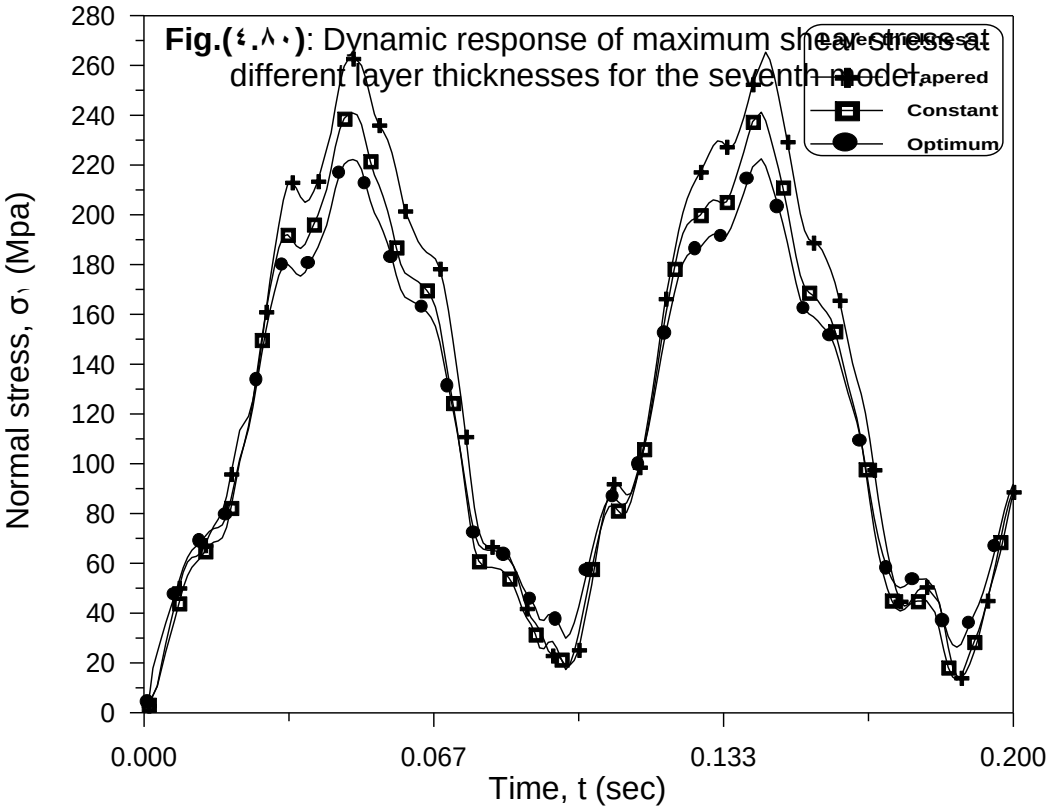


**Fig.(٤.٨١):**Dynamic response of maximum shear stress at different layer thickness for the seventh model.

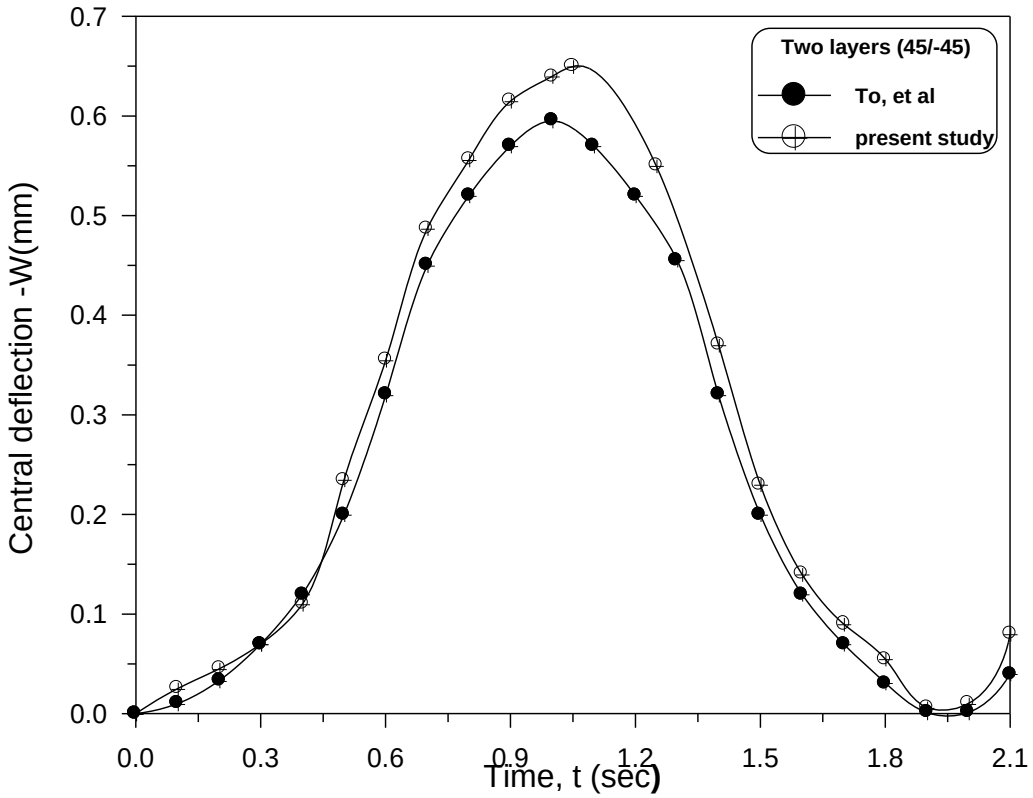


**Fig.(٤.٨٥):** Apex transient response.

# *CHAPTER FOUR*

# *RESULTS AND DISCUSSION*

## ٤.١ Introduction

The static and dynamic behavior of composite material is very affected by the stiffness properties. Since the stiffness properties of composite materials depend on the fiber orientation, lamina stacking sequence, lamina thickness, and allocations, thus studying of these variables is of significant importance. Based on this idea, a procedure to find the optimum design ( fiber orientation, layers thicknesses, and thickness distribution and allocation) became excessively necessary to be presented. Therefore, the results of this chapter are circulated in three parts: (١) Free vibration analysis (٢) Static analysis and (٣) Dynamic analysis.

Optimum orientations are obtained from the first part of the suggested technique, in addition seven models are constructed, each different to other in its orientation angle only. To verify the results of free vibration (authenticity of the suggested technique), the previously created models are analyzed statically and a comparison is made between their failure indices. In addition, optimum layer thickness and tapered thickness distribution are also performed. At last, the

dynamic analysis is done on the above models to study their dynamic effects and responses.

## ٤.٢ Structural Analysis

Structural analysis includes the free vibration analysis, static analysis, and dynamic analysis. In free vibration analysis, frequencies of five modes are obtained. Failure indices of the models are obtained by static analysis. Finally, time responses of displacements and stresses are executed by dynamic analysis.

### ٤.٢.١ Free Vibration Analysis

Free vibration analysis is the first step in the suggested technique. At first, the wing model is divided into three parts: spars (longitudinal stiffeners), ribs (transverse stiffeners) and the skins (upper and lower surfaces). These parts are defined previously in section (٣.٢).

Here, the effect of these parts will be studied separately on the structure by obtaining the relationship between the fiber orientations and frequencies that correspond to five mode shapes only. This accomplished by creating a substructural models named under different indices. As an example, if the substructural model has a name of Spar١**f**, then this model consists of the skins and the spar١ only, and other spars and ribs are neglected. Rib١**f** refers to a substructural model consisting of skins and Rib١ only; the other spars and ribs are neglected. The index of the substructural skins model is Skins**f**. The last letter **f** in the indices of the substructural models refers to the **f**ree vibration analysis. Therefore, nine substructural models for the spars, seven for the ribs, and one for the skins are created, they are: (Spar١**f**, Sapr٢**f**, Spar٣**f**, Spar٤**f**, Spar٥**f**, Spar٦**f**, Spar٧**f**, Spar٨**f**, and Spar٩**f**) and (Rib١**f**, Rib٢**f**, Rib٣**f**, Rib٤**f**, Rib٥**f**, Rib٦**f**, Rib٧**f**, and Rib٨**f** ) and (Skins**f)**, respectively.

#### ٤.٢.١.١ The Substructural Skins Model

The free vibration analysis is done on the substructural skins model to define the values of maximum natural frequency of each one of its five modes. Figures from (٤.١) to (٤.٥) present the first, second, third, fourth, and the fifth mode shapes while Figure (٤.٦) presents the variation of natural frequency values with the orientation angles of Skins**f**. The increments in the natural frequency with the number of mode mean that there is an increase in the stiffness of the corresponding modes itself. In other words, the minimum natural frequency corresponds the minimum stiffness and the maximum natural frequency corresponds the maximum stiffness. Dependency of natural frequency values on the stiffness and mass matrix for the same mass of the skins in each mode represents the main reason in the previous increment. The maximum natural frequency in the first mode occurs at ٠°. For the other mode shapes, the maximum natural frequency occurs at ٤٥°.

At last, the first mode shape of the minimum natural frequency value is more dangerous than the other modes because of its minimum stiffness.

### ٤.٢.١.٢ The Substructural Spars Models

The free vibration analysis is done on the substructural spars model to define the values of maximum natural frequency of each one of its five modes. Figures from (٤.٧) to (٤.١١) present the first, second, third, fourth, and the fifth mode shapes. Figures from (٤.١٢) to (٤.٢٠) present the variation of natural frequency values with orientation angles of Spar١**f**, Spar٢**f**, ..., and Spar٩**f,** respectively. It can be seen that for most substructural spars models, the locations of the spars have an apparent effect on the natural frequency values; thereby on the stiffness, so that the last is decreasing with the increase of the substructural spar index. It is noted that the minimum natural frequency that corresponds to the five modes is occurring at the substructural spars of indices of Spar٨ and Spar٩ which may lead to conclude that these substructural models have the smallest stiffness and

may not affect on the whole wing geometry. In other hand, the difference between the natural frequency values for each one of their modes are less than that corresponding of the substructural spars models. This mean that because of the little stiffness, the change in the fiber orientation gives less effect on the natural frequency as compared to the other substructural spars models.

For the first mode, the maximum natural frequency occurs at ٠° in which the fiber direction is in the direction of the wing span itself. The second mode of substructural spars models is a special case of bending which have a behavior similar to the first mode, ٠° is the angle of maximum natural frequency. Plane horizontal motion is presented in the third mode shapes. Torsion is the address of the fourth mode. It can be seen that the maximum natural frequency occurs between ٤٠° and ٥٠° (٤٥.٢), hence, maximum stiffness to resist the torsion. There are a slight difference in the natural frequency values according to the location of the spars ( substructural spars models).

At last, the fifth mode is the wave case which presents a complex bending. From the Figures, it can be seen that the maximum natural frequency occurs at ٠°.

### ٤.٢.١.٣ The Substructural Ribs Models

The free vibration analysis is done on the substructural ribs model to define the values of maximum natural frequency of each one of its five modes. Figures from (٤.٢١) to (٤.٢٥) present the first, second, third, fourth, and the fifth mode shapes. Figures from (٤.٢٦) to (٤.٣٣) present the variation of natural frequency values with the orientation angles of Rib١**f,** Rib٢**f, ...,** and Rib٨**f** respectively. The same, it can be seen that the first mode, bending; represents the mode of the lowest value of frequency. The locations of the ribs have a slight difference on the natural frequency value because the main benefit of the ribs is the torsion resistance which represents the second mode. Therefore, there is no large difference in the frequency values that is corresponding of the first mode shapes

of the substructural ribs models. It is noted that all the substructural ribs have a maximum frequency value at a value closing to ٤٥° and decreases at ٠° and ٩٠°, respectively.

The locations of the ribs have an apparent effect on the frequency values which increase gradually when the substructural ribs index increases also. In general, the more main reason that causes this effect is the mass of the selective ribs that decreasing due to the decreases in its volume; thereby an increase in the frequency values occurs. The third mode is the common mode between the first and the second. From the above figures, it is clear that the maximum frequency occurs at ٤٥° and decreases at ٠° and ٩٠°, respectively. However, the behavior is also common between the first and the second modes. The locations of the ribs (substructural ribs models) have an affect similar to that corresponding of the first and the second modes. Motion in the (x-z) plane of the model occurs in the fourth mode. The maximum frequency occurs between ١٠° and ٢٠°. For the fifth mode in which the substructural ribs models move in a wave form in the y-direction, it is noted that the maximum frequency occurs at ٩٠°. As mentioned previously, there are slight differences of the natural frequency values according to the ribs locations.

From the above figures, there are three values of the orientations in which the natural frequency is maximum for each one of the five modes which are ٠°,٩٠°,٤٥° and between ١٠° and ٢٠° , and ٩٠° for the first , second, third, fourth, and fifth modes, respectively.

It is important to refer that the natural frequency of the torsional mode in substructural spars model is greater than that corresponding in the substructural ribs models. Therefore, it can be concluded that the spars play an important role in increasing the torsion resistance in addition to increasing the bending one.

At last, as a general view for all figures above of the substructural models it is noted that firstly, the natural frequency is largely depends on the fiber orientation. Secondly, the natural frequency values of the substructural spars

models have a frequency approximately equal to that corresponding of the substructural ribs models. In other words, mass of the skins in the above models is the same for substructural spars and ribs models, mass of the spars is greater than of the ribs then the stiffness of the spars is greater than of ribs.

## ٤.٢.٢ Static Analysis

The main goal of the static analysis is to obtain the failure indices of each available tested models to define and decide the optimum one (optimum orientations and optimum thicknesses for a minimum failure index).

Depending on the results (optimum orientations of the substructural analysis) that are obtained from free vibration analysis, new four models consisting of all spars and ribs in addition to the skins (whole models) of indices named as Rst١***OO***, Rst٢***OO***, Rst٣***OO***, and Rst٤***OO*** are created. The last two letters (***OO***) represent the first letters of "***Optimum Orientation***" term. Each one of its elements consists of three layers. At first, each layer has the same thickness and orientations extracted from the free vibration outcomes (suggested technique). In addition to other three models of arbitrary orientations (their orientations are self-governing; independent on the free vibration optimization) of indices of Rst١***AO***, Rst٢***AO***, and Rst٣***AO*** for comparison purposes with those models based on the free vibration suggested technique and for studying the effect of fiber orientation on structure response in the same time. The last two letters (***AO***) represent the first letters of "***Arbitrary Orientation***". Table (٤.١) presents these models, their indices, and orientations. Static analysis is done on the above models, shown in Table (٤.١), in primary total thickness of ٧mm until the desired failure index (٠.٦٨) occurs. Table (٤.١) presents failure indices for

different thicknesses (٧,٨, and ٩mm) for all models. From the previous Table, it

| Model Index | Parts | Orien-tation (Deg.) | Failure indices of layers for different thicknesses | | | | | | | | |
|---|---|---|---|---|---|---|---|---|---|---|---|
| | | | Thickness=٧mm | | | Thickness=٨mm | | | Thickness=٩mm | | |
| | | | Layer ١ | Layer ٢ | Layer ٣ | Layer ١ | Layer ٢ | Layer ٣ | Layer ١ | Layer ٢ | Layer ٣ |
| Rst١***OO*** | Spar | ٠/٤٥/٠ | ٠.٧١ | ٠.٨٢ | ٠.٧٥ | ٠.٦٢ | ٠.٧٧ | ٠.٦٦ | ٠.٥٦ | ٠.٦٤ | ٠.٥٩ |
| | Rib | ٩٠/٤٥/٩٠ | ٠.٦٨ | ٠.٧٤ | ٠.٧٥ | ٠.٥٩ | ٠.٦٥ | ٠.٦٧ | ٠.٥٤ | ٠.٥٧ | ٠.٥٨ |
| | Skins | ٠/٤٥/٠ | ٠.٧٧ | ٠.٨٢ | ٠.٨٩ | ٠.٦٥ | ٠.٧١ | ٠.٧٦ | ٠.٦١ | ٠.٦٥ | ٠.٦٨ |
| Rst٢***OO*** | Spar | ٤٥/٠/٤٥ | ٠.٧٩ | ٠.٧٢ | ٠.٧٨ | ٠.٦٩ | ٠.٦٣ | ٠.٦٩ | ٠.٦٢ | ٠.٥٦ | ٠.٦١ |
| | Rib | ٩٠/٤٥/٩٠ | ٠.٦٧ | ٠.٧٣ | ٠.٧٥ | ٠.٥٨ | ٠.٦٤ | ٠.٦٤ | ٠.٥٤ | ٠.٥٧ | ٠.٥٩ |
| | Skins | ٠/٤٥/٠ | ٠.٨٣ | ٠.٨٨ | ٠.٩٥ | ٠.٧٢ | ٠.٧٧ | ٠.٨١ | ٠.٦٣ | ٠.٦٨ | ٠.٧٤ |
| Rst٣***OO*** | Spar | ٠/٤٥/٠ | ٠.٨٣ | ٠.٩٢ | ٠.٨٩ | ٠.٧٣ | ٠.٨١ | ٠.٧٧ | ٠.٦٥ | ٠.٧٢ | ٠.٦٩ |
| | Rib | ٤٥/٩٠/٤٥ | ٠.٧٧ | ٠.٨٧ | ٠.٧٩ | ٠.٦٧ | ٠.٧٣ | ٠.٦٨ | ٠.٦١ | ٠.٦٧ | ٠.٦٣ |
| | Skins | ٤٥/٠/-٤٥ | ٠.٩٥ | ٠.٩٩ | ١.٠٧ | ٠.٨٣ | ٠.٨٥ | ٠.٩٤ | ٠.٧٤ | ٠.٧٧ | ٠.٨٢ |
| Rst٤***OO*** | Spar | ٤٥/٠/٤٥ | ١.٠٤ | ٠.٩٧ | ١.٠٧ | ٠.٩٢ | ٠.٨٣ | ٠.٩٣ | ٠.٨١ | ٠.٧٦ | ٠.٨٢ |
| | Rib | ٤٥/١٨/٤٥ | ٠.٩٤ | ٠.٩٧ | ١.٠١ | ٠.٨٢ | ٠.٨٥ | ٠.٨٩ | ٠.٧٥ | ٠.٧٤ | ٠.٧٩٣ |
| | Skins | ٤٥/٠/-٤٥ | ٠.٩٦ | ١.٠١ | ١.٢١ | ٠.٨٤ | ٠.٨٩ | ١.٠١ | ٠.٧٦ | ٠.٧٩ | ٠.٨٧ |
| Rst١***AO*** | Spar | ٣٠/٤٥/٣٠ | ٢.٢١ | ٢.٢٨ | ٢.٢٣ | ١.٩٥ | ١.٩٩ | ١.٩٥ | ١.٧٢ | ١.٧٨ | ١.٧٤ |
| | Rib | ٣٠/٤٥/٣٠ | ٢.١٤ | ٢.١٧ | ٢.٢١ | ١.٨٧ | ١.٨٩ | ١.٩٣ | ١.٧١ | ١.٦٩ | ١.٧٢ |
| | Skins | ٣٠/٤٥/٣٠ | ٢.٢٣ | ٢.٢٥ | ٢.٣٤ | ١.٩٥ | ١.٩٦ | ٢.٠٣ | ١.٧٤ | ١.٧٥ | ١.٨٢ |
| Rst٢***AO*** | Spar | ٤٥/٧٥/٤٥ | ٣.٣٤ | ٣.٥٣ | ٣.٣٨ | ٢.٩٢ | ٣.٠٨ | ٢.٩٧ | ٢.٦ | ٢.٧٢ | ٢.٦٣ |
| | Rib | ٤٥/٧٥/٤٥ | ٢.٦٣ | ٢.٥٩ | ٣.١٣ | ٢.٣٥ | ٢.٢٩ | ٢.٧٥ | ٢.١٤ | ٢.٠١ | ٢.٤٣ |
| | Skins | ٤٥/٧٥/٤٥ | ٣.٤٢ | ٣.٥٢ | ٣.٥١ | ٢.٩٧ | ٣.٠٩ | ٣.٠٦ | ٢.٦٥ | ٢.٧٣ | ٢.٨٥ |
| Rst٣***AO*** | Spar | ٩٠/٤٥/٩٠ | ٤.١٠ | ٣.٧٩ | ٤.٣١ | ٣.٥٨ | ٣.٣٤ | ٣.٧٩ | ٣.١١ | ٢.٩٤ | ٣.٣٢ |
| | Rib | ٩٠/٤٥/٩٠ | ٣.٦٧ | ٣.٧١ | ٣.٨٢ | ٣.٢١ | ٣.٢٩ | ٣.٣٧ | ٢.٨٥ | ٢.٩ | ٣.٠١ |
| | Skins | ٩٠/٤٥/٩٠ | ٤.٢٤ | ٤.٠٢ | ٤.٤٥ | ٣.٧١ | ٣.٥٢ | ٣.٩٢ | ٣.٢١ | ٣.١٩ | ٣.٤٨ |

can be seen that failure indices of each layer are inversely proportional with the total thickness of each composite lamina, i.e., failure indices are decreasing with increasing the total thickness. The model reached firstly to the required failure index at ٩mm is Rst١***OO***. In addition, to verify a reality of the present suggested technique, it can be seen that the maximum failure indices occur at the arbitrary models (Rst١***AO***, Rst٢***AO***,and Rst٣***AO***) due to the arbitrary orientations, so that the required stiffness is not directed in the direction of load confrontation.

.

**Table (٤.١):** Failure indices for models under different thicknesses.

It can be seen that for most models, the fiber orientation has a great effect on the values of failure indices for each layer and model, so that for most results shown in the above Table, the failure index for the layer of optimum orientation is smaller than that corresponding of layers of arbitrary orientation. In addition, the difference between the failure indices of the first four models is smaller than that corresponding in the last three of arbitrary orientations. From the other hand, there are differences in failure index values for spars, ribs, and skins in the same model because of the stress state in them so that the maximum value occurs at the skins and minimum at ribs.

It is important to remember that the three layers of the above seven models have the same thickness, i.e., layer thickness is equal to the total composite thickness divided by ٣.

### ٤.٢.٢.١ Effect of Fiber Orientation on the Static Deflection

In this section, effect of fiber orientation on the static response is discussed in details. Figures from (٤.٣٤) to (٤.٤٠) present the normal deflection ($u_y$) of Rst١***OO***, Rst٢***OO***,... ,and Rst٣***AO***, respectively. it can be seen that the deflection values are different from model to other depending on the difference of their properties such as fiber orientation. From the above figures, it is clear that the deflection response (behavior) of the above models can be described as a combination response between the first and the second modes that resulted from free vibration view for most substructural models. Therefore the concentration of the discussion will be enlarged in the direction of the effect of fiber orientation on the static deflection response for these modes.

Firstly, a minimum deflection occurs at the first model and increases with increasing of the model index. However, it is reaching to the maximum value for the last three arbitrary orientations. Because of the differences in the deflection values for the same conditions of the applied static load firstly, and the inverse

proportionalities of the deflection with the stiffness values secondly, then these values are increasing with the decreasing of the stiffness properties. In other words, the model of the minimum deflection is of maximum stiffness.

In other hand, it is noted that the static responses are changed in clear form of the last three models, there are negative values of the vertical displacement that mean a material is displaced in opposite direction of Y-axis. These are clear signs on the inheritance of failure as buckling which represents a more dangerous case. To explain the above lines, each one of the models will be discussed alone as follows:

For the first model (Rst١***OO***) of a minimum deflection (maximum stiffness), each one of its orientations corresponds to the maximum natural frequency value (free vibration that means maximum frequency as verified previously) for each spars, ribs, and skins.

Skins and ribs of the second model (Rst٢***OO***) is the same for the first model. For the spars, two of the three layer orientations (٤٥°,٤٥°) increasing the stiffness of the fourth mode and the other one increase the first modes (bending). Therefore, the deflection is larger than that corresponding of the first model.

For the third model (Rst٣***OO***) spars orientations offer the same effect of the first model. Orientations of the ribs increase the stiffness of this model more than its increment in the first one. Skins orientations increase the stiffness of last four modes than the first mode. Therefore, the deflection value is larger than the first model.

For the fourth model (Rst٤***OO***) , effect of the spars orientations is the same as in third model. Ribs orientations increase the stiffness of the second, third, and the fourth modes. Skins orientations increase the stiffness of the last four modes larger than that of the first one.

For the last three models, it is noted that the deflection values are greater than the above four models. It is important to refer that the differences in the deflection values are greater than that corresponding of the previous four

models. The main reasons of these differences are the arbitrary orientations firstly, and the vanishing effect in building of the stiffness that required to resist the applied loads secondly, in other words, when a specific orientation increases the stiffness of the spars in a specific modes, it may vanished this stiffness in the skins or ribs; because of the difference in its optimum orientations. The main solution for the presented problem (interacted effect of enforcing and decaying the stiffness of the substructural models) is using of the substructural analysis to give each one of this substructural models its responsibilities to build a whole stiff structure.

Again, for the first arbitrary model (Rs١***AO***), fiber orientation of (٣٠°) gives good but not optimized stiffness for the spars, ribs, and the skins in different ratios. ٤٥° reduces the spars stiffness and increases the ribs stiffness in the second and third modes.

The second arbitrary model (Rst٢***AO***) has an orientations of (٤٥°,٧٥°, ٤٥°). The first and third orientations give a good stiffness for the last modes of the skins and less for the first mode. In addition it reduces the stiffness of the spars for all modes except the first one, at last increases the stiffness of the second and third modes of the skins only. The second orientation ( ٧٥°) decreases the stiffness of spars and skins for all modes, gives good efficiency for the ribs for all modes except the fourth one. For these reasons, the deflection of this model is greater than the above models.

At last, ( ٩٠°,٤٥°,٩٠°) are the orientations of the third arbitrary model (Rst٣***AO)***. The first and third orientations (٩٠°) offer good stiffness for the ribs in first and fifth modes and less in the second, third, fourth, respectively. In addition, it gives a minimum stiffness for the spars of all modes because minimum frequency occurs at this angles. Effect of ٤٥° is mentioned previously.

As a final point, depending on the different orientations of the above models in increasing or decreasing the stiffness of the first and the second modes, the deflections are also different.

### ٤.٢.٢.٢ Optimum Layer Thickness and Its Arrangement

Up to now, optimum orientations and failure indices for each layer are obtained. The main scope of this topic is to obtain the optimum layer thickness and its distribution across the composite lamina depending on the procedure mentioned in sec( ٣.١٠.١). Figures from (٤.٤١) to (٤.٤٧) show optimum layers thicknesses and its arrangement for skins, spars, and ribs of the first, second, and third layers at total layers thickness equal to ٩mm , respectively.

From the above figures, it is noted that the fiber orientation plays an essential role in limiting the layer thickness, so that the layer of optimum orientation has a small thickness as compared with those of not optimized (or in an arbitrary degree) in its orientations in which the thickness is of large value. These are logical results assure that when the fiber in a specific layer is oriented in the direction (or closed to the direction) of load resistance, the dependency on thickness of this layer is smaller than that corresponding to which the fiber not oriented in the direction (far from direction) of load resistance.

As an example, let me explain two cases of spars only, they are similar in all boundary and loading conditions (load in direction of longitudinal spar axis) except in orientations. The fiber orientation of the spars is ٠° in the first and ٩٠° in the second. The fiber in the first case will resist a greater value of the applied load than the matrix in the first case but in the second spar, the fiber will resist a very small value of the applied load and the other will be distributed in the matrix material. Because of the little strength of matrix material as compared with fiber material, the matrix will fall short under the applied load. Then, a need to increase the value of thickness is necessary to resist the applied load.

Up to now, the researcher agrees with **Eschenauer** [٥١] who said that "*It become possible to achieve a lower structural weight in the optimal design by doing a simultaneous optimization of thickness and fiber orientations compared to pure thickness optimization. In terms of physics the fibers are oriented in such*

*a direction, that the stiffness or strength requirements can be fulfilled by smaller layer thicknesses*" so that there is an accordance between the results and what he said.

It is important to refer that for all models above; the thicknesses in the upper skin layers are smaller than that in the lower skin layers, i.e., the total thickness in the upper skin is smaller than the lower skin. Here, the researcher doesn't agree with ***Boyang Liu*** [٥٢] who said that "*The upper skin panels are thicker than the lower skin panels*". In fact, this sentence is not absolutely true, because the strengths for most composite materials in tension are different than that corresponding in compression. Glass, boron, and graphite have strength in tension smaller than in compression. Due to the applied load, the upper skin will be in compression and the lower one will be in tension. Because the failure index is a function of strength for both tension and compression, failure index is smaller in compression than tension; thereby the thickness in the upper skin (compression) is smaller than the lower one (tension).

At last, due to non-equality in thickness values of the upper and lower skins as mentioned instantaneously; there is difference between them (equal to lower thickness - the upper thickness). The difference value is varying from model to another depending on the fiber orientations (stiffness). it can be seen that the maximum difference occurs at the first model and decreases with increasing the model index. Again, to verify the practicality of this distribution, a static analysis is done for the resulted models of optimized layers thicknesses. Indices of these models after the solution became Rst١١***OO***, Rst٢٢***OO***, Rst٣٣***OO***, Rst٤٤***OO***, Rst١١***AO***, Rst٢٢***AO***, and Rst٣٣***AO*** corresponding to Rst١***OO***, Rst٢***OO***, Rst٣***OO***, Rst٤***OO***, Rst١***AO***, Rst٢***AO***, and Rst٣*AO*, respectively for purposes of reformation only. Table (٤.٢) shows failure indices of the reformatted models at ٩mm only.

From this Table, it can be seen that still Rst١١***OO*** is more successful whenever presents a minimum failure index ( higher safety factor), maximum

failure indices of the models after optimum thickness distribution is smaller than that corresponding in case of constant layer thickness mentioned in Table (٤.١) previously . The main reason is that each one of layers has taken the required thickness to resist the supplied load. This is a strong guide on the veracity and the preeminence in the presented procedure. In general, it is noted that the decreasing and increasing in failure index values that resulted from the optimum

| | | | | | |
|---|---|---|---|---|---|
| Rst١١***OO*** | Spar | ٠/٤٥/٠ | ٠.٥٨ | ٠.٦١ | ٠.٦ |
| | Rib | ٩٠/٤٥/٩٠ | ٠.٥٥ | ٠.٥٦ | ٠.٥٨ |
| | Skins | ٠/٤٥/٠ | ٠.٦٣ | ٠.٦٢ | ٠.٥٦ |
| Rst٢٢***OO*** | Spar | ٤٥/٠/٤٥ | ٠.٥٧ | ٠.٥٩ | ٠.٦١ |
| | Rib | ٩٠/٤٥/٩٠ | ٠.٥٥ | ٠.٥٦ | ٠.٥٤ |
| | Skins | ٠/٤٥/٠ | ٠.٦٦ | ٠.٦٩ | ٠.٦٥ |
| Rst٣٣***OO*** | Spar | ٠/٤٥/٠ | ٠.٦٨ | ٠٦٦ | ٠.٦٨ |
| | Rib | ٤٥/٩٠/٤٥ | ٠.٦٤ | ٠.٦٠ | ٠.٥٨ |
| | Skins | ٤٥/٠/-٤٥ | ٠.٧٧ | ٠.٧٨ | ٠.٧١ |
| Rst٤٤***OO*** | Spar | ٤٥/٠/٤٥ | ٠.٨ | ٠.٧٨ | ٠.٧٦ |
| | Rib | ٤٥/١٨/٤٥ | ٠.٧٦ | ٠.٧٧ | ٠.٧٣ |
| | Skins | ٤٥/٠/-٤٥ | ٠.٧٩ | ٠.٨١ | ٠.٧٧ |
| Rst١١***AO*** | Spar | ٣٠/٤٥/٣٠ | ١.٧٩ | ١.٦٥ | ١.٨٤ |
| | Rib | ٣٠/٤٥/٣٠ | ١.٧٢ | ١.٧١ | ١.٦٣ |
| | Skins | ٣٠/٤٥/٣٠ | ١.٧٥ | ١.٧٨ | ١.٦٨ |
| Rst٢٢***AO*** | Spar | ٤٥/٧٥/٤٥ | ٢.٦٢ | ٢.٥٥ | ٢.٦٥ |
| | Rib | ٤٥/٧٥/٤٥ | ٢.٢٣ | ٢.٣١ | ٢.٢٣ |
| | Skins | ٤٥/٧٥/٤٥ | ٢.٦٨ | ٢.٧٦ | ٢.٧٧ |
| Rst٣٣***AO*** | Spar | ٩٠/٤٥/٩٠ | ٣.١٨ | ٣.١١ | ٣.١٢ |
| | Rib | ٩٠/٤٥/٩٠ | ٢.٩٤ | ٢.٩٥ | ٢.٨٢ |
| | Skins | ٩٠/٤٥/٩٠ | ٣.٢٧ | ٣.٢٣ | ٣.٣٠ |

thickness for each layer are depending on the differences between old layer thickness (٣mm) and new optimized one.

**Table (٤.٢):** Maximum failure indices for models after optimum thickness distribution

| Model index | Parts | Orien-tation (Deg) | Failure indices of layers for different thicknesses | | |
|---|---|---|---|---|---|
| | | | Thickness=٩mm | | |
| | | | Layer ١ | Layer ٢ | Layer ٣ |

At last, in the same Table, it can be concluded that the optimized layer thickness technique has an excellent efficiency for models of optimum fiber orientation and less for those of arbitrary orientation. This is another guide adding to the previous models on the dependency of composite materials on the reinforced elements (fibers) and its orientations.

Failure indices distribution for upper and lower skins for the models is illustrated in Figures from(٤.٤٨) to (٤.٥٥). It is noted that all illustrated models have the same behavior in general but different in values and locations of maximum failure indices. In addition, these values in the upper skin are smaller than corresponding in the lower skin as mentioned previously. The maximum failure indices occur at a distance between ١٠-٠٪ from the wing root because of maximum bending moment.

The locations of maximum failure index for the above models are distributed between the first and second spar. Spar ٢ is the location of maximum failure for the first, third, and fourth model and spar ١ for the second model. These differences depended itself on the structural parameters such as stiffness that building from oriented fiber in such direction.

The main benefit from this distribution (failure index) not only to give an idea about the static response but to give another one about the values of tapered thickness distribution in a global structure as explained in the next section ,so the location of maximum failure index will be of maximum thickness values and the same for minimum failure index that occurs at the tip and attains a minimum thickness value.

### ٤.٢.٢.٣ Tapered Distribution in Global Thickness of The Structure

The final step in the suggested technique is the address of this section to obtain a "***Tapered distribution in global thickness of the structure***". The procedure of this distribution is mentioned previously in Sec (٣.١٠.٢). At first, the procedure is applied on Rst١١***OO***, Rst٢٢***OO***, Rst٣٣***OO***, and Rst٤٤***OO*** only in which the total thickness for each one of its elements is constant (٩mm), in other words if the element of number ١ has a total thickness of ٩mm then total thicknesses of the other elements are ٩mm also. For the other three models, there is no benefit of displaying the tapered distribution because it has originally failed. New models of indices named as: Rst١١***OOtap***, Rst٢٢***OOtap***, Rst٣٣***OOtap***, and Rst٤٤***OOtap*** corresponding to Rst١١***OO***, Rst٢٢***OO***, Rst٣٣***OO***, and Rst٤٤***OO***, respectively, are developed as a result of the procedure application. The last section of the developed indices refers to ***"Tapered"***. Figures from (٤.٥٦) to (٤.٦٧) present the tapered distribution of total thickness for all developed models in the upper and the lower skins in addition to the spars elements.

From the above figures, it is noted that maximum thickness occurs at the element closed to the wing root due to the maximum failure index (maximum

stress intensity), and decreases along the wing span in the direction of the tip in which a minimum thickness is attained.

## ٤.٣ Dynamic Analysis

To investigate the dynamic characteristics of all models, a dynamic analysis is applied. To achieve this, the time histories of responses are recorded after the models being perturbed from the steady state by different load sets. In the wing models, localized pattern of fluctuation are represented in term of impulsive input. The dynamic characteristics of the impulsive excitation is presented in **Appendix-B**. The total effective time represents the summation of all times steps size (٠.٠٠٢ sec), (***Ansys**R*, ١٩٩٨) [٥٦]. The dynamic response will be represented in two types: (١) displacements response and (٢) stresses response. Dynamic analysis is done on the models to study their dynamic effects.

### ٤.٣.١ Displacements Response

Figures from (٤.٦٨) to (٤.٧٤) present the more important, vertical displacement dynamic response ($U_y$) for the models under study. It can be seen that the model of optimum layer thickness gives a smaller dynamic displacement than the tapered and constant layer thickness for the same model, respectively. The main reason is the stiffness as shown previously.

Finally, from the previous figures, it is noted that the models of optimum layer thickness gives good results if they are compared with the constant and tapered layer thickness. While, the tapered thickness has an efficient performance in dynamic behavior less than that corresponding in static case. Depending on the displacements values, there is an important relationship between the dynamic displacement and the dynamic load factor.

### ٤.٣.٢ Dynamic Load Factor (DLF)

Dynamic load factor represents the maximum ratio of dynamic to static displacement for the structure. It is very important factor in the dynamic analysis

and gives a complete information about the structure stiffness and its natural frequency. Models of smaller dynamic load factor is more stiff than that of higher dynamic load factor. Figure (٤.٧٥) shows the dynamic load factor relationship with models mentioned previously. It is noted that this factor is different with both of models and type of layer thickness, and it is of minimum value for optimum layer thickness and greater value for constant and tapered layer thickness.

It can be seen that DLF largely depends on the applied load frequency and the structural parameters (natural frequency and damping ratio). It is noted that DLF is increasing gradually with increasing of model index, the main reason is its dependency on the natural frequency of these structures under the same conditions of applied load.

As mentioned previously, the first model has a maximum frequency, hence maximum stiffness. The stiffness of first model is greater than the second and the second is greater than the third, etc.. Therefore, natural frequency of the first is greater than the second and the second is greater than the third, etc., reaching to the last model of minimum natural frequency. In other words, the frequency ratio of the first model is smaller than the second and the second is smaller than the third reaching to the last model of maximum one. From the figures above, it can be concluded that DLF gives an idea about the required time for structure to reach to the steady state response case, so that the structure of minimum DLF need to a time smaller than corresponding of larger DLF.

Finally, it is important to refer that there is a reliance relationship between the deflection and DLF values, so that increasing in the dynamic deflection values leads to increasing in the corresponding DLF because of their connections with so called “stiffness” term.

### ٤.٣.٣ Stresses Response

The main goal from the previous study is to obtain the optimum design for fiber-reinforced composite wing structure depending on changing of specific

parameters such as: fiber orientation, layer thickness, and stacking sequence. As mentioned previously, is to study the dynamical effect and the behavior of composite structure, it is preferred to have superior properties in order to be more effective. Because of the large number of the models under study, the researcher will concentrate on the first model (best optimized one, higher safety factor) and the seventh model ( worst model, smaller safety factor). A comparison can be made between the results to understand the effect of fiber orientation on the dynamical behavior firstly and dynamical behavior itself secondly.

Figs.(٤.٧٦), (٤.٧٧), and (٤.٧٨) present the dynamic response of maximum normal , shear, and principal stresses for the first model, respectively. It can be seen that the values of response for the optimum model are smaller than that the constant and tapered models, respectively due to the changing in the layer thicknesses and the stiffness.

For the seventh model, Figs.(٤.٧٩), (٤.٨٠), and (٤.٨١) show the dynamic response of maximum normal, shear, and principal stresses. Also, it can be noted that differences exists in corresponding values of normal and shear stresses for the first and the seventh models, so there are large differences between them. The main reason is fiber orientations; thereby the stiffness.

## ٤.٤ Verification and Application

A several examples are studied and compared with the available research results for verification purpose. Three examples of static, free, and dynamic analysis, respectively, are presented. Another example is presented to verify the applicability of the optimization procedure (such as fiber-reinforced plate structure)

***Example No. ١: (Static Analysis)***

A ٠°/٩٠° cross ply laminated simply supported spherical square patch under uniform pressure load is analyzed. Because of the symmetry of the geometry

and loading, only one quadrant of the shell is modeled using ٤*٤ mesh. All above properties of the sphere geometry are listed in Figure (٤.٨٢). The problem had been solved by **(*Yunus and Khonke,* ١٩٨٩)**[٢٠], using a finite element method. The formulation of element was based on three-dimensional continuums mechanic theory. Table (٤.٣) shows the non-dimensional central deflection ($\bar{w}$) of the structure under verification. It can be seen that there is an excellent agreement with solution of **(*Yunus and Khonke,* ١٩٨٩)**[٢٠]. The non-dimensional central deflection is calculated as : $(\bar{w}) = (w\, t^{٣}\, E_{٢}/p\, a^{٤})*١٠^{٢}$, where w is central deflection of A

**Table (٤.٣):** Comparison of results with theoretical study **(Ex.١)**

| case | R/a | a/t | Yunus, et al | Present work |
|---|---|---|---|---|
| ١ | ٣ | ١٠٠ | ٠.٦٤٢٧E-٢ | ٠.٦٣٩٩E-٢ |

***Example No. ٢: (Free Vibration Analysis)***

A full circular cylindrical shell is modeled with eight element along its circumstance and four element along its length of ٠°/٩٠° laminate. All the details of the geometry are given in Figure (٤.٨٣). The problem had been solved by ***Kumar and Rao***[٤١] using the finite element method of a curved shell element of five degrees of freedom. Table (٤.٤) presents the non-dimensional frequency



**Geometrical parameters**

R/t=٥

L/R=٢

parameter $K_w$ which is defined as: $(K_w)^{٢} = \frac{\rho\omega^2 L^4}{D_{11}\pi^4}$ , $D_{١١}=\frac{(1+F)}{2} * Q_{11}t^2/12$ ,

$F = E_{٢}/E_{١}$. There are good agreement with the results shown in Table (٤.٤).

**Table (٤.٤):** Comparison of results with theoretical study **(Ex.٢)**

| R/t | L/R | Kumar, et al | Present work |
|---|---|---|---|
| ٥ | ٢ | ١.١٣٣ | ١.٢٢ |

***Example No. ٣: (Dynamic Analysis)***

Two layers of ٤٥°/-٤٥° ply-laminated simply supported spherical shell under uniformly distributed load is analyzed. A distributed step pressure is applied to the outer surface. It has intensity P=٢٠٠٠N/m$^{٢}$ with time step size of ٠.٠٣s. The details and specifications of the geometry are given in Fig.(٤.٨٤). The total thickness of the laminated composite shell is ٠.٠١m. **(*To and Wang*)** [٦٦] in ١٩٩٨ solved this example using the finite element method by employing the eight node hybrid strain based shell element with six degrees of freedom at each node.

**Sphere geometry**

R=١٠m

b=٠.٩٩٩m

**Material properties**

$E_{١}$=٢.٥E+١١ N/m$^{٢}$

$E_{٢}$=١.٠E+١٠ N/m$^{٢}$

$G_{١٢}=G_{١٣}$=٠.٥E+١٠ N/m$^{٢}$

$G_{٢٣}$=٠.٢E+١٠ N/m$^{٢}$

$\upsilon_{١٢}$= ٠.٢٥

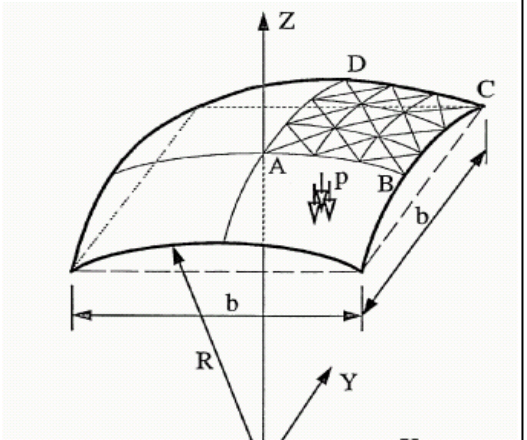

Fig.(٤.٨٥) shows Apex transient response (point A). It can be seen that there is good accordance between ***To and Wang*** [٦٦] solution and present work, so that the same behavior for the two responses was achieved.

***Example No. ٤ (Verification of the Suggested Technique)***

Two layers, simple supported, square and angle ply laminate plate is analyzed. The plate side length is ٠.٢٥m and thickness of ٠.٠٥m. The problem was solved by (***Nabeel, ٢٠٠٤***)[٦٧] for several times of different orientation angles. From his study, he concluded that the best angle to minimum deflection, minimum summation of normal stress and minimum shear stress in plate is ٤٥°. From the application of the optimum orientations procedure on the same problem, the results are extracted for free vibration analysis and the orientation angle that corresponds to the maximum natural frequency was ٤٤.٢٧°. This mean that there is good agreement between the results firstly, and the previously presented procedure can be executed on the composite plate structure secondly.

# CHAPTER FIVE

# CONCLUSIONS AND RECOMMENDATIONS

## ٥.١ Conclusions

shell structures. During execution of the suggested technique, and from obtained the results obtained from the static and dynamic analyses and their discussion in chapter four, the following conclusions can be drawn:

١- From free vibration analysis, the fiber orientations of laminas have a considerable effect on the natural frequencies of the structure in each one of their modes.

٢- The natural frequency of the structure in each mode depends on the stiffness of the mode itself. So, the maximum stiffness in the structure is corresponding to the maximum natural frequency. Therefore, the study must be focused on the first two or three modes of minimum natural frequencies because of their minimum stiffness.

٣- The substructural analysis represents an excellent tool in the study of the more complex structures such as wings. Therefore, the complex structure is divided into substructural models and studied it alone (separately). The substructural method must be used in complex fiber-reinforced composite structures to avoid the vanishing and the building interaction between their effects as mentioned previously, and in a less importance for complex isotropic materials.

٤- At studying of the substructural spars, ribs, and skins models, it is found that each one of these substructural models has different natural frequencies. These differences represent the main reason in using the substructural analysis. In other words, the optimum fiber orientation is a function to the structural configuration and boundary condition of constraint. Since, it was noted that optimum

orientation angles take different styles in each one of substructural models, then there is agreement in this conclusion with ***Shapana*** [٣٩] who concluded that the behaviors of composite structures are largely depending on the boundary conditions.

٥- The optimum arrangement of lamina through shell thickness is a function to the structural shape and applied load, so that the skins laminas are arranged symmetrically in its orientations about the stiffeners (spars and ribs). The skins laminas are arranged along skins thicknesses such that, a lamina of maximum stiffness against applied load is located on exterior surface (where the flexural deflections are maximum), and a lamina of minimum stiffness are located near the stiffeners (where the flexural deflections are minimum).

٦- The technique is suitable for both composite shells and plates structures.

٧- Maximum failure index occurs at a distance from ٠-١٠٪ of wing span measured from the root and decreases in the direction of the free end.

٨- From the dynamic analysis, it is noted that the model that give a good behavior in the static response gives a good behavior in dynamic also.

٩- The dynamic load factor represents an excellent factor from which one can more understand the dynamical behavior of structure. It is found that DLF for the composite materials is arranged between ١.٤٥ and ١.٨٥ in the safe case.

## ٥.٢ Recommendations and Suggestions

Many aspects may be concerned with the objectives of the current work, in addition to other which features are not considered in the current work. Thus it possible to suggest the following items as further objectives in future

١- The constituent materials of composite are assumed to behave as isotropic manner. Then it is required to study a material of other behavior such as hyper elastic and visco-elastic in matrix.

٢- Although unidirectional configuration is the most types of lamina that are used in the fabrication of composite structures, but other types such as multiple orientations fiber, woven fiber configurations and rounded fiber configurations are also present in the industry. Thus it is suggested to extend and use the suggested technique to cover these laminas types.

٣- For reality, the subject requires to be supplemented by experimental results to be obtained from high performance laboratory tests under static and dynamic loads.

٤- In the prediction of elastic failure of laminated composite materials, Tsai-Wu failure criteria theory is used, which doesn’t consider delamination failure. Thus there is need for to studying the effect of delaminating on the dynamic behavior of laminated composite shell.

٥- Macro and micromechanics could be integrated and adopted to enable the designers to instantly study the sensitivity of micromechanics variables on the final design.

# List of Contents

**Contents**

## Contents

# *Examination Committee Certification*

*We certify that we have read the thesis entitled "**DYNAMIC ANALYSIS OF FIBER-REINFORCED COMPOSITE SHELL STRUCTURE UNDER ACTION OF IMPULSIVE EXCITATION**" and as examining committee, examined the student **Salwan Obeed Waheed** in its contents and what is related to it, and that in our opinion, it meets the standard of a thesis for the degree of Master of Science in Mechanical Engineering.*

Signature:
Name: **Dr. Hatem H. Al-Taee**
(Supervisor)
Date: / / ٢٠٠٦

Signature:
Name: **Dr.Ala M. Hosain**
Assist. Professor
(Supervisor)
Date: / / ٢٠٠٦

Signature:
Name: **Dr. Ahmad A. Al - Rajihy**
Assist. Professor
(Member)
Date: / / ٢٠٠٦

Signature:
Name: **Dr. Haydar A. Hussain**
Assist. Professor
(Member)
Date: / / ٢٠٠٦

Signature:
Name: **Dr. Husain M. Husain**
Professor
(Chairman)
Date: / / ٢٠٠٦

Signature:
Name:
Dean of Engineering College
Date: / / ٢٠٠٦

Signature:
Name: **Assist. Prof. Dr. Ala M. Hosain**
Dean of Mechanical Engineering
Date: / / ٢٠٠٦

# REFERENCES


١. ***Stegman, J., and Lund, E.,*** "Notes on Structural Analysis of Composite Shell Structures", First Edition, publisher ٢٠٠٢.

٢. ***Lekhnitskii, S. G.,*** "Theory of Elasticity of Anisotropic Body", Second Edition, Moscow, ١٩٨١. [Mentioned in reference number ٧].

٣. ***Jones, R. M.,*** **"**Mechanics of Composite Materials", McGraw-Hill, New York, ١٩٧٥.

٤. ***Ferreira, A. J. M., and Fernandes, A. A., "*** A Review of Numerical Methods for the Analysis of Composite and Sandwich Structure", http:\www.google.com (key Words " Numerical + Composite +Laminated +Sandwich", ٢٠٠٣.[paper].

٥. ***Raj, R. G, Manocha, L. M., Bahl, O. P., and Verma, D. S., "*** Impact Strength on Fracture of Glass Fiber Reinforced Epoxy Composite", Fiber Science and Technology, Vol.١٧, ١٩٨٢, p.p. ١٤١-١٤٨.

٦. ***Ashby, M. F., and Jones, D. R. D.,*** "Engineering Materials ٢; An Introduction to Microstructures, Processing and Design", Pergamon Press, ١٩٨٨. [Mentioned in ***Abdul-Raheem*** (٢٠٠٠)].

٧. ***Abdul-Raheem, K. A.,*** "Stress Analysis of Laminated Fiber Reinforced Composite Cylinder", M.Sc. Thesis, University of Babylon, Hilla, Iraq. ٢٠٠٠.

٨. ***Paul, B.***, "Linear Bending Theory of Laminated Cylindrical Shells under Axi-Symmetric Load", ASME Journal of Applied Mechanics, March, ١٩٦٣, p.p. ٩٨-١٠٢.

٩. ***Hsu, T. M.,*** "A Theory of Laminated Cylindrical Shells Consisting of Layers of Orthotropic Lamina", AIAA Journal, Vol. ٨, No. ١٢, December, ١٩٧٠, p.p. ٢١٤١-٢١٥١.

١٠. ***Ahmed, I., and Zienkiewicz,, O.,*** "Analysis of Thick and Thin Shell Structure by Curved Finite Elements", International Journal for Numerical Method in Engineering, ١٩٧٠.

١١. ***Govil, A. K., Arora, J. S., and Haug, E. J.,*** " Optimal Design of Wing Structure With Substructuring", Computers and Structures, Vol.١٠, ١٩٧٩, p.p.٨٩٩-٩١٠.

١٢. ***Venkatesh, A., and Rao, S.*** **"**A Doubly Curved Quadrilateral Finite Element for The Analysis of Laminated Anisotropic Thin Shells of Revolution", Computers and structures, Vol. ١٢, ١٩٨٠, p.p. ٨٢٥-٨٣١.

١٣. ***Panda, S., and Nataragan, R.,*** "Analysis of Laminated Composite Shell Structures by Finite Element Method", Computers and Structures, Vol.٤, No.٣, ١٩٨١, p.p. ٢٢٥-٢٣٠.

١٤. ***Reddy, J. N.,*** "Exact Solutions of Moderately Thick Laminated Shells', Journal of Engineering Mechanic, Vol.١١٠, No. ٥, May ١٩٨٤, p.p. ٧٩٤-٨٠٧.

١٥. ***Ramana, P. V.,*** "Analysis of Laminated Composite Thin Shell of Revolution Using a Doubly Curved Quadrilateral Finite Element", International Journal for Numerical Methods in Engineering, Vol. ٢٧, ١٩٨٥, pp. ٢٨٥-٢٩٩.

١٦. ***Seide, P., and Chaudhuri, R. A.,*** "Triangular Finite Element for Analysis of Thick Laminated Shells", International Journal for Numerical Method in Engineering, Vol. ٢٤, ١٩٨٧, p.p. ١٥٦٣-١٥٧٩.

١٧. ***Reddy, J.N., and Pandy***, "A General Fiber-Reinforced Composite Shell Elements Based on a Refined Shear Deformation Theory", Computers and Structures, Vol. ٤٥, No. ٨, ١٩٨٩, p.p. ١٢٨-١٣٧

١٨. ***Yeom, C. H., and Lee, S. W.,*** **"**An Assumed Strain Finite Element Model for Large Deflection Composite Shells", International Journal for Numerical Methods in Engineering, vol. ٢٨, ١٩٨٩, p.p. ١٧٤٩-١٧٨٩.

١٩. ***Kant, T., and Menon, M. P.,*** "Higher Order Theories for Composite and Sandwich Cylindrical Shells with $C^o$ Finite Element", Computers and Structures, Vol. ٣٣, No.٥, ١٩٨٩, p.p. ١١٩١-١٢٠٤.

٢٠. ***Yunus, S. M., and Khonke, P. C.,*** "An Efficient Through-Thickness Integration Scheme in an Unlimited Layer Doubly Curved Isoparametric Composite Shell Element", International Journal for Numerical Methods in Engineering, Vol. ٢٨, ١٩٨٩, p.p. ٢٧٧٧-٢٧٩٣.

٢١. ***Liao, C. L., and Reddy, J. N.,*** "Analysis of Anisotropic Stiffened Composite Laminates Using A Continuum-Based Shell Element", Computers and Structural, Vol. ١٤, No. ٩, ١٩٩٠, p.p. ٣٠٥-٣١٥.

٢٢. ***Surana, S. S., and Sorem, R. M.,*** "Curved Shell Elements Based on Hierarchical p-Approximation in the Thickness Direction for Linear Static Analysis of Laminated Composite", International Journal for Numerical Method in Engineering, Vol. ٢٩, ١٩٩٠, p.p. ١٣٩٣-١٤٢٠.

٢٣. ***Mallikarjuna, T, and Kant, T.,*** "A General Fiber-Reinforced Composite Shell Element Based on a Refined Shear Deformation Theory", Computers and Structures, Vol. ٤٢, No. ٣, ١٩٩٢.

٢٤. ***Lee, C. Y., and Liu, D.,*** **"**Layer Reduction Technique for Composite Laminate Analysis"**,** Computers and Structures, Vol. ٤٤, No. ٦**,** ١٩٩٢, p.p. ١٣٠٥-١٣١٥.

٢٥. ***Kalamkarov, A. L., and Kolpakov, A. G.***, "On the Analysis and Design of Fiber-Reinforced Composite Shells", ASME Journal of Applied Mechanics, Vol. ٦٣, December ١٩٩٦, p.p. ٩٣٩-٩٤٥.

٢٦. ***Mohan, P.,*** "Development and Applications of a Flat Triangular Element for Thin Laminated Shells", Ph.D Thesis, Virginia Polytechnic Institute and State University, Virginia, U.S.A, ١٩٩٧.

٢٧. ***Masud, A., and Panahandeh, M.,*** **"**Finite Element Formulation for Analysis of Laminated Composite", Journal of Engineering Mechanics, Vol.١٢٥, No.١٠, October, ١٩٩٩, Paper No. ١٩٦٩٨.

٢٨. ***Davila, C. G., Ambur, D. R., and McGowan, D. M,*** "Analytical Prediction of Damage Growth in Notched Composite Panels Loaded in Axial Compression", American Institute of Aeronautics and Astronautics, paper AIAA-٩٩-١٤٣٥, April ١٢-١٥, ١٩٩٩, p.p. ١- ٦.

٢٩. ***Wu, C. P., and Lo, J. Y.,*** "Three-Dimensional Elasticity Solution of Laminated Annular Spherical Shells", Journal of Engineering Mechanics, Vol August, ٢٠٠٠, p.p. ٨٨٢-٩٠٤.

٣٠. ***Kessler, S. S., and Spearing, S, M.,*** **"** Design, Analysis and Testing of a High-g Composite Fuselage Structure", Massachusetts Institute of Technology, Cambridge, MA٠٢١٣٩, USA.

٣١. ***Langley, P. T.,*** **"**Finite Element Modeling of Tow-Placed Variable-Stiffness Composite Laminate", M.Sc. Thesis, Virginia Polytechnic Institute and State University, Virginia, ١٩٩٨, U.S.A.

٣٢. ***Whenbin, H. H., "***A Geometrically Non-Linear Shear Deformation Theory for Composite Shell", Journal of Applied Mechanics, Vol.٧١, January, ٢٠٠٤, p.p. ١-٩.

٣٣. ***Stavsky, Y., and Loewy, R.,*** **"**On Vibrations of Heterogeneous Orthotropic Cylindrical Shells", Journal of Sound and Vibration, Vol. ١٥, ١٩٧١, pp. ٢٣٥-٢٥٦.

٣٤. ***Patnaik, S. N., and Sankaran, G. V.,*** **"**Optimum Design of Stiffened Cylindrical Panels With Constraint on the Frequency in the Presence of Initial Stresses", International Journal for Numerical Methods in Engineering, Vol. ١٠, ١٩٧٦.

٣٥. ***Rao, S. S., and Raju, P. C.,*** "Vibration of Anti-Symmetrically Laminated Cylindrical Shells", Composite Materials-I, Applied Science Publishers, ١٩٧٧, Chap. ٣.

٣٦.***Reddy, J. N.,*** **"**Transient Response of Laminated, Bimodular-Material, Composite Rectangular Plate", Journal of Composite Materials, Vol. ١٦, March, ١٩٨٢, p.p. ١٣٩-١٤٩.

٣٧. ***Greenberg, J. B., and Stavsky, Y.,*** "Vibrations of Laminated Filament-Wound Cylindrical Shells", AIAA Journal, Vol. ١٩, No. ٨, August, ١٩٨١.

٣٨. ***Rao, S. S.***, **"**Vibrations of Layered Shells with Transverse Shear and Rotatory Inertia Effect, Journal of Sound and Vibration, Vol. ٨٧, ١٩٨٣, pp. ١٤٧-١٥٠.

٣٩. ***Shapana, A. A.,*** **"**Effect of Using Composite on the Dynamic Response of Multi-Body Systems", Journal of Sound and Vibration, Vol. ١٠٨, No.٣, ١٩٨٦, p.p. ٤٨٧-٥١٢.

٤٠. ***Mustafa, B. A. J., and Ali, R.,*** "Free Vibration Analysis of Multi-Symmetric Stiffened Shells", Journal of Computers and Structures, Vol. ٢٧, No. ٦, ١٩٨٧, p.p. ٨٠٣-٨١٠.

٤١. ***Kumar, R. R., and Rao, S. S.,*** " Free Vibrations of Multi-layered Thick Composite Shells" Journal of Computers and Structures, Vol. ٢٨, No. ٦, ١٩٨٨, p.p. ٧١٧- ٧٢٢.

٤٢. ***Malhotra, S. K.,*** "Effect of Fiber Orientation on the Vibration Behavior of Orthotropic Shells", Journal of Composite Materials, Vol. ٢٢, November, ١٩٨٨.

٤٣. ***Attaf, A., and Hollaway, L.,*** "Vibrational Analysis of Stiffened and Unstiffened Composite Structures Subjected to In-Plane Loads", Journal of Composite Materials, Vol. ٣١, No. ٢, ١٩٩٠.

٤٤. ***Suzuki, K., Shikanai, G., and Leissa, A. W.,*** "Free Vibrations of Laminated Composite Non-Circular Thin Cylindrical Shells", ASME Journal of Applied Mechanics, Vol. ٦١, December, ١٩٩٤.

٤٥. ***Chakravorty, D, P. K., and Bandyopadhyay, J. N.,*** "Application of FEM on Free and Forced Vibration of Laminated Shells", Journal of Engineering Mechanics, Vol. ١٢٤, No.١, January, ١٩٩٨, p.p. ١-٥.

٤٦. ***Yen, C. F., and Cassin, T.,*** **"**Progressive Failure Analysis of Thin Walled Composite Tubes under Low Energy Impact".

٤٧. ***Nayfeh, J. F., and Rivieccio, N, J.,*** "Nonlinear Vibration of Composite Shell Subjected to Resonant Excitation" Journal of Aerospace Engineering, April ٢٠٠٠, p.p. ٥٩-٦٥.

٤٨. ***Liew, K. M., Ng, T. Y., and Zaho, X.,"*** Vibration of Axially Loaded Rotating Cross-Ply Cylindrical Shells via Ritz Method", Journal of Engineering Mechanic, September, ٢٠٠٢, p.p. ١٠٠١-١٠٠٧.

٤٩. ***Nawras, H. M.,*** "Elastic-Plastic Waves Propagation in Prismatic and Non-Prismatic Systems", M.Sc. Thesis, University of Babylon, Hilla, Iraq. ٢٠٠٥.

٥٠. ***Reddy, J. N., and Wang, C. M.,*** "Deflection Relationships between Classical and Third-Order Plate Theories", Acta Mechanica ١٣٠, ١٩٩٨, p.p. ١٩٩-٢٠٨.

٥١. ***Eschenauer, H. A.,*** "Multidisciplinary Design of Composite Aircraft Structure Using LAGRANGE", Multicriteria Design Optimization, Springer, Berlin, ١٩٩٢.

٥٢. ***Liu, B., and Haftka, R. T.,*** "Composite Wing Structural Design with Continuity Constraints", AIAA, ٢٠٠١, Paper no. A٠١-٢٥٠٢١, p.p. ١-١٢.

٥٣. ***Warburton, G. B.,*** **"**The Dynamical Behaviour of Structures", Pergamon Press Ltd., Oxford Ox٣٠BW, England, ١٩٧٦.

٥٤. ***Calcote, L. R.***, "The Analysis of Laminated Composite Structures", Van-Nostrand Reinhold, New York, ١٩٦٩.

٥٥. ***Hate , H. O.***, "Investigation of Performance and Optimum Design of Fiber-Reinforced Composite Shell of Aircraft Structure", ", Ph.D. Thesis, The Military College of Engineering , Baghdad, Iraq. ٢٠٠٢.

٥٦. ***ANSYS$^{R}$***, Engineering Analysis System Theoretical Manual, "Http:\\ www. Ansys. Com", Ansys Version ٥.٤, ١٩٩٨.

٥٧. ***Timosheinko, S.P., Young, D.H., and Weaver, W. J. R.,*** "Vibration Problems in Engineering", Fourth Edition, ١٩٧٤.

٥٨. ***Weaver, W. J. R., and Johnston, P. R***, "Introduction to Structural Dynamic", Prentice-Hall, Inc., USA, ١٩٨٧.

٥٩. ***Bathe, K. J.***, "Finite Element Processing in Engineering Analysis", Printce Hall, Englewood Cliffs, N.T., ١٩٩٦.

٦٠. ***Pytet, M.,*** "Introduction to Finite Element Vibration Analysis", ١٩٩٠. [Mentioned in ***Hayder***, ٢٠٠٠].

٦١. ***Subbaraj, K., and Dokainish, M.A.,*** "A Survey of Direct Time Integration Methods in Computational Structural Dynamics-II. Implicit Method", Computers and Structures, Vol.٣٢, No.٦, P.P.١٣٨٧-١٤١٠, ١٩٨٩.

٦٢. ***Zienkiewics, O.C.,*** "The Finite Element Method", Third Edition, McGraw-Hill Book Company, London, ١٩٧٧.

٦٣. ***Al-Sarraf, S .Z., Alwash, N.A.A, and Al-Bidairie, S. H***., "Elastic Stability and Large Displacement Analysis of Beam-Like Lattice Structure Under Static and Dynamic Loads", Accepted for Publications in Journal of Babylon University in ٢٠٠٣, Vol.٩, No.٥.

٦٤. ***Hayder, M.K.,*** "Large Displacement and Post-Buckling Analysis of Non-Prismatic Members in Plane Under Static and Dynamic loads", M.Sc. Thesis, University of Babylon, Hilla, Iraq, ٢٠٠٠.

٦٥. ***Hussain, H.M, Al-Daami., H., and Amash, H.K.,*** "Buckling Behavior of Rectangular Plate with Variable Thickness", Engineering and Technology (Baghdad), Vol.٢١. No.١٠, ٢٠٠٢, p.p. ٧٣٦-٧٤٥.

٦٦. ***To, C.W.S, and Wang, B.*****, "**Transient Response of Geometrically Laminated Composite Shell Structure**",** Finite Elements in Analyses and Resign, Vol. ٢١, (١٩٩٨), p.p. ١١٧-١٣٤.

٦٧. ***Ali, N. H.,*** "Finite Element Dynamic Analysis of Laminated Composite Plates Including Damping Effect", M.Sc. Thesis, University of Babylon, Hilla, Iraq. ٢٠٠٤.

Republic of Iraq
Ministry of Higher Education
and Scientific Research
Babylon University

# DYNAMIC ANALYSIS OF FIBER - REINFORCED COMPOSITE SHELL STRUCTURE UNDER ACTION OF IMPULSIVE EXCITATION

*A Thesis*

**Submitted to the College of Engineering of the University of Babylon in Partial Fulfillment of Requirements for the Degree of Master of Science in Mechanical Engineering (Applied Mechanics)**

***By***

**SALWAN OBEED W. AL-KHAFAJI**

**(B.Sc.)**

**٢٠٠٥**

# *CERTIFICATION*

*We certify that this thesis entitled* ***" DYNAMIC ANALYSIS OF FIBER-REINFORCED COMPOSITE SHELL STRUCTURE UNDER ACTION OF IMPULSIVE EXCITATION"*** *was prepared by* ***Salwan Obeed Waheed*** *under our supervision at the University of Babylon in partial fulfillment of the requirements for the degree of Master of Science in Mechanical Engineering (Applied Mechanics).*

Signature:
Name: **Dr. Hatem H. Al-Taee**
(Supervisor)
Date: / / ٢٠٠٦

Signature:
Name: **Dr.Ala M. Hosain**
Assist. Professor
(Supervisor)
Date: / / ٢٠٠٦